Finanziato dall'Unione europea NextGenerationEU
Ministero dell'Università e della Ricerca
Italiadomani
UNIVERSITÀ DI SIENA 1240
GIOVANISÌ
Regione Toscana
Consiglio Nazionale delle Ricerche
UNIVERSITÀ DI PISA
UNIVERSITÀ DEGLI STUDI FIRENZE
Da un secolo, oltre.
UNIVERSITÀ DI SIENA 1240

Dipartimento di Scienze della Vita

Dottorato in Scienze della Vita-Life Sciences

38° Ciclo

Coordinatrice: Prof.ssa Simona Maccherini

Advanced *in vitro* Human Immune Profiling of GMMA-based vaccines

Settore scientifico disciplinare: BIOS-08/A Biologia Molecolare

Candidata

Mariateresa Marrocco

Sede di attività

GlaxoSmithKline, Siena

Università degli Studi di Siena

Firma digitale del/della candidato/a

Firmato il 16/12/2025 11:37
Mariateresa Marrocco (m.marrocco1@student.unisi.it)

Mariateresa Marrocco

Certificato da yousign

Supervisore

Cristina Ulivieri

Università degli Studi di Siena

Co-supervisori

Francesca Schiavetti

Bruna Clemente

GlaxoSmithKline, Siena

Anno accademico di conseguimento del titolo di Dottore di ricerca

2024/25

Table of Contents

ACKNOWLEDGEMENTS

A mamma e papà che mi hanno dato la possibilità di fare tutto ciò che volevo, sostenendomi

A mio fratello che mi ha sempre strappato un sorrido nei momenti più bui

A Bruna e Simona che mi hanno supportato e sopportato tutti i giorni, infondendomi la loro passione e la loro carica

A Francesca e Cristina, sempre pronte ad ascoltarmi ed aiutarmi

Al mio Lab, che tra risate e scienza, mi ha fatto sentire a casa

Ai miei amici, vicini e lontani, che sono rimasti … nonostante tutto

Grazie , grazie di cuore perchè mi avete fatto crescere da ogni punto di vista e per questo, felice di dedicarvi questo grande traguardo.

ABSTRACT

Generalized Modules for Membrane Antigens (GMMA) are outer membrane vesicles derived from engineered Gram-negative bacteria. GMMA, resembling bacterial surface, present antigens in their native conformation and provide self-adjuvanticity, establishing them as a flexible vaccine platform. Despite previous studies demonstrated that GMMA-based vaccines, administered intramuscularly in healthy subjects, elicited a strong specific antibody response, our understanding of how GMMA-based vaccines influence immune cell function and development, as well as activation of other cell subsets at the injection-site remains limited. Using multi-parametric flow cytometry combined with cytokine detection assays, we define the Mode of Action (MoA) of *Shigella* and *N. gonorrhoeae* (Ng) GMMA-based vaccines on immune cells. Specifically, we developed *in vitro* models which recapitulate the peripheral blood, hPBMCs and a specific subpopulation of innate immune cells, the dendritic cells (DCs) which are known to drive T cell differentiation and function. Moreover, to gain insight into the role of GMMA on the cellular crosstalk occurring at the site of injection, which is instrumental for the priming of adaptive immunity, a primary muscle cell model (PMCM), which combines immune cells with myotubes, was developed. Both GMMA-based vaccines activated immune cells, including hPBMCs and Mo-DCs, eliciting a strong innate pro-inflammatory response. Furthermore, Mo-DCs internalized GMMA and secreted factors that skewed naïve CD4+ T cells toward a Th1 phenotype. GMMA-based vaccines also activated non-immune muscle cells, revealing, in the PMCM cultures, a distinct cytokine milieu compared to hPBMCs *in vitro* model. In conclusion, our data demonstrated that GMMA-based vaccines are internalized by both

professional antigen presenting cells and muscle cells and promoted the secretion of pro-inflammatory mediators, thereby shaping the development and function of T cells independently of the bacterial origin.

LIST OF ABBREVATIONS

Abbreviation	Meaning
AMR	Antimicrobial Resistance
OMV	Outer Membrane Vescicles
GMMA	Generalized modules for Membrane Antigens
PAMPs	Pathogen-associated Molecular Patterns
PRRs	Pathogen-recognition receptors
TLRs	Toll-like Receptors
LPS	Lipopolysaccharide
PLs	phospholipids
OMPs	Outer Membrane proteins
APCs	Antigen-presenting Cells
DAMPs	Damage-associated Molecular Patterns
DCs	Dendritic Cells
nOMV	native Outer Membrane Vesicles
dOMV	detergent-extracted Outer Membrane Vesicles
mdOMV	mutant-derived Outer Membrane Vesicles
AH	Alum Hydroxide
PBMCs	Peripheral Blood Mononuclear Cells
Mo-DCs	Monocyte-derived DCs
EXPEC	extraintestinal pathogenic *E. coli*
MHC	major histocompatibility complexes
Spp.	species
OAg	O-antigen
pDCs	Plasmacytoid Dendritic Cells
CDC	Centers for Disease Control and Prevention
Ng	*Neisseria gonorrhoeae*
hSBA	human serum bactericidal assay
BAI	bacterial adhesion inhibition
LOS	lipo-oligosaccharides
Opa	opacity-associated protein
MoA	Mode of Action
mDCs	myeloid Dendritic Cells
iMo-DCs	immature monocyte-derived dendritic cells
mMo-DCs	mature monocyte-derived dendritic cells
O/N	overnight
Th	T helper
FSC	forward scatter

SSC	side scatter
SN	supernatants
TFs	transcription factors
RT	Room Temperature
NK	Natural killer
T-bet	T-box expressed in T cells
RORγt	retinoic acid receptor-related orphan receptor gamma t
GATA-3	GATA-binding protein-3
iMFI	integrated Mean Fluorescence Intensity
geoMFI	geometric Mean Fluorescence Intensity
PMCM	Primary Muscle Cells Model
OPG	Osteoprotegerin
LIF	Leukemia Inhibitory Factor
MIP-1α	Macrophage Inflammatory Protein α
MIP-1β	Macrophage Inflammatory Protein β
SkGM	Skeletal Muscle growth medium
hEGF	human Epidermal Growth Factor
FBS	Fetal Bovine Serum
GA	Gentamicin/Amphotericin-B

1. INTRODUCTION

1.1 Towards OMV as Vaccine platform against bacterial infectious diseases

Vaccines are one of the most effective tools in modern medicine, designed to prevent infectious diseases by training the immune system to recognize and respond to specific pathogens without causing illness. Despite their long-standing success, the development of new and effective vaccines against emerging infectious diseases remains a major challenge (1). The growing demand for prophylactic vaccines is driven by several factors among which, the Antimicrobial Resistance (AMR) is the most predominant (2). Indeed, the global rise of antimicrobial-resistant pathogens (3-9) and limited efficacy of antibiotic treatments for certain infections pose a serious threat to healthcare systems (5). In this scenario, vaccination would be an effective intervention against bacterial infections due to the induction of immunity before bacterial propagation and dissemination, reducing the use of antibiotics and, consequently, decreasing the evolutionary pressures that aid resistant strains. Furthermore, the possibility to design vaccine against multiple targets not only reduce potential resistance episodes in the vaccinated population (10), but also provide multivalent vaccines able to target several infectious diseases (11). Vaccination can also provide indirect protection (herd-immunity) to non-vaccinated people, minimizing the spread of the pathogens and, therefore, the development of infections (10, 12-14).

Additionally, the development of multivalent vaccines is of pivotal importance for life quality improvement in low- and middle-income

countries, in which infectious disease are responsible for 91% of deaths due to the inadequate socio-economic conditions (15).

Over the years, a variety of vaccine platforms have been developed and/or refined, ranging from traditional inactivated and live-attenuated vaccines to more advanced technologies as protein/polysaccharide subunit vaccines, conjugate vaccines, outer membrane vesicles (OMV)-based vaccines, Virus-like particles (VLPs) and Viral vector, DNA and mRNA based vaccines (1, 16, 17).

Each vaccine technology offers distinct advantages but also presents limitations. For example, live-attenuated vaccines elicit robust and long-lasting immunity but carry the risk of reversion to virulence (18). Subunit vaccines are safer but often require complex production processes and adjuvants to enhance immunogenicity (19). mRNA vaccines allow rapid and scalable production, yet their stability and cold-chain requirements remain significant hurdles (20). In this scenario, the OMV platform offers a solution to the majority to these drawbacks, resulting in a promising and innovative approach for bacterial vaccines. Indeed, OMV, being vesicles naturally released from gram-negative bacteria and thus, mimicking the bacterial outer membrane, have innate immunostimulatory properties (21). Moreover, OMV production is low cost and can be exploited as carriers for several antigens, giving the possibility for multivalent vaccines development (22, 23). However, this platform also has some limitations, as many bacterial strains release low levels of OMV. In the last decades, this drawback has been addressed by the development of particular OMV derived from engineered gram-negative bacteria, known as Generalized Modules for Membrane Antigens (GMMA).

1.2 Outer Membrane Vesicles (OMV)

1.2.1 OMV biogenesis, structure and composition

During growth, many Gram-negative bacteria naturally release outer membrane vesicles (OMV), likely because of an imbalance between cellular expansion and outer membrane synthesis. This imbalance results in the extrusion of excess membrane material in the form of vesicles (24). OMV play a multifaceted role in bacterial physiology and pathogenesis: they contribute to survival under stress conditions, facilitate the delivery of virulence factors and genetic material to host cells, and are implicated in biofilm formation as well as in the persistence both within host organisms and in environmental niches such as soil. Additionally, OMV enhance bacterial defence mechanisms against antibiotics and participate in the horizontal transfer of antibiotic resistance genes (24-29). Naturally secreted OMV resemble the bacterial outer membrane, carrying several molecules in their native conformation. These include phospholipids (PLs), Outer Membrane proteins (OMPs), and lipopolysaccharides (LPS), but also periplasmic proteins and cell wall components. However, OMV can also contain periplasmic and cytoplasmic proteins, DNA, RNA, ions, metabolites and signalling molecules (30-32) (**Figure 1**).

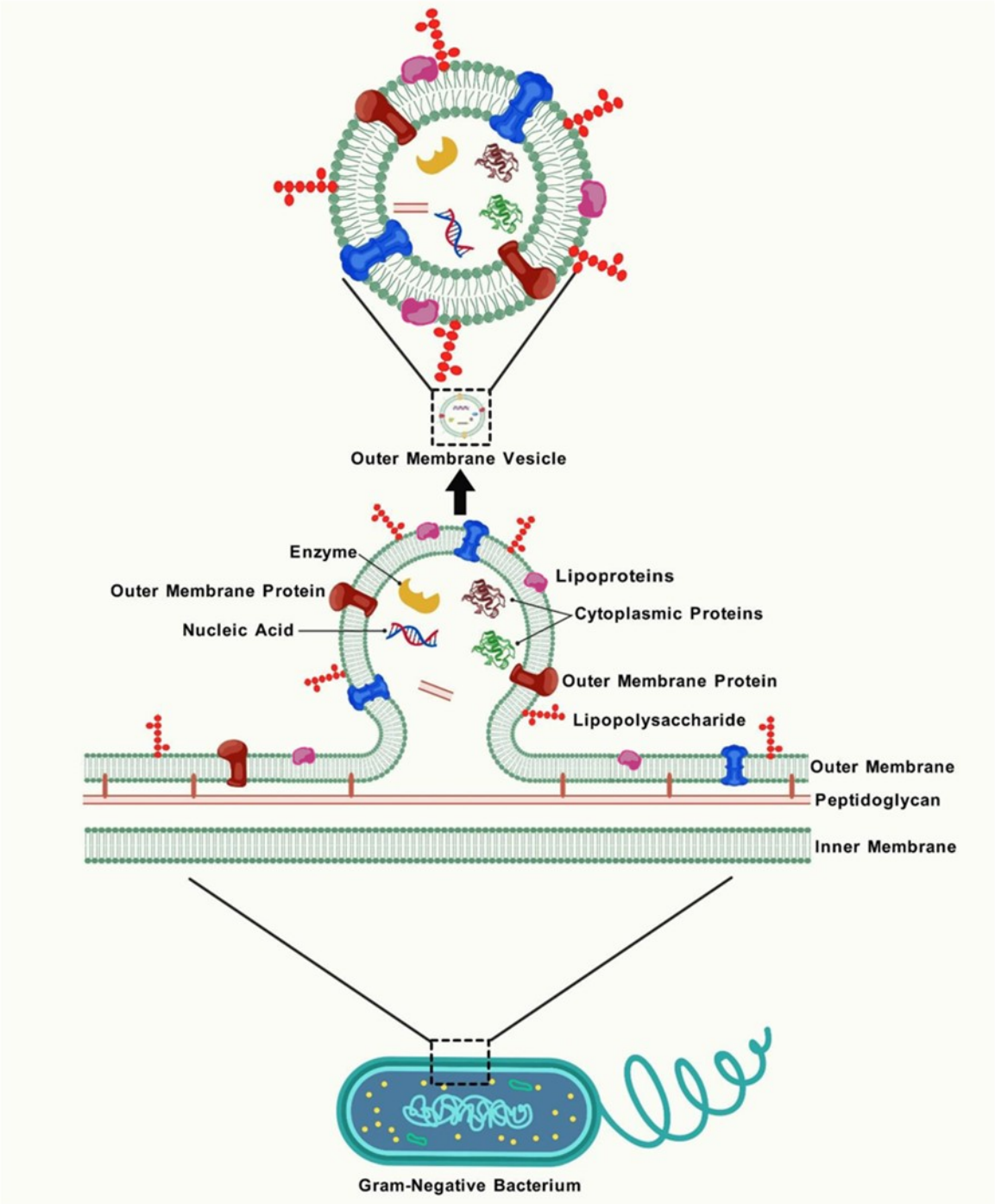

Figure 1. **Structure and molecular composition of Outer Membrane Vesicles (OMV).** OMV are spherical vesicles naturally released from Gram-negative bacteria, consisting of both outer and inner membrane components. The outer membrane is enriched in lipopolysaccharides (LPS), phospholipids, and outer membrane proteins, while the inner membrane contains phospholipids and integral membrane proteins. In addition to membrane-associated molecules, OMV encapsulate internal constituents such as DNA, RNA, and periplasmic

proteins, reflecting their origin from the bacterial envelope and surrounding compartments. Image adapted from Zahid et al_2025 (1)

1.2.2 OMV features for vaccine development

One of the key features of vaccines is their ability to induce a long-lasting immune response that is specifically directed against the target pathogen. This is achieved by simulating the presence of the pathogen in a safe and controlled manner, without causing disease. Through this process, both the innate and adaptive arms of the immune system are activated, leading to the development of immunological memory and sustained protection over time. For a vaccine to be considered effective, it must incorporate three fundamental elements: (1) antigens that are specific to the pathogen, (2) a diverse array of pathogen-associated molecular patterns (PAMPs), and (3) a physical size conducive to optimal immune activation (33). Notably, OMV inherently satisfy all three of the essential criteria for vaccine efficacy. For this reason, OMV represent a promising interface between traditional and next-generation vaccine technologies, offering a versatile platform for the prevention of various infectious diseases (34). They mimic the bacterial outer membrane showing a wide range of bacterial antigens (such as lipoproteins) as well as other constituents (proteins, RNA/DNA, and peptidoglycan) that can be embedded in the OMV lumen from periplasm and cytoplasm compartments (35-37). These components are Pathogen-associated Molecular Patterns (PAMPs) and, interacting with Pattern-Recognition receptors (PRRs), including Toll-like Receptors (TLRs), on host cells, induce a strong innate and adaptive immune responses (38), conferring to OMV a self-adjuvanticity feature (39, 40). Moreover, as OMV are naturally released by Gram-negative

bacteria, they display antigens in their native conformation, preserving both antigenic integrity and conserved epitopes, thereby enhancing immunogenic diversity, addressing antigenic variability, and reducing the risk of immune escape (1, 22-24). Due to their nanometric size (20-300 nm), they can reach lymph nodes either via lymphatic drainage or being phagocytosed and transported by antigen-presenting cells (APCs) (38), promoting systemic distribution and a long-term memory (41). In addition, they are non-replicative particles and thereby they cannot induce disease (1). OMV have shown a marked stability under elevated temperatures and several chemical treatments highlighting their potential as successful vaccine candidates (42). Furthermore, the ease of the manufacturing process, which consists of an initial cultivation and fermentation of the bacteria followed by filtration to collect the OMV released in the culture supernatant, shows their high potential for low-cost vaccine development (43-45). Finally, the availability of bioengineering techniques allows the incorporation of tailored antigens in OMV, thereby amplifying their immune potential and providing broader protection against various strains and species of bacteria (22, 46, 47). These features prove that OMV technology is a suitable platform to design vaccines that can overcome conventional vaccines' limitations, especially for disease caused by bacteria exhibiting complex immune evasion mechanisms or relevant antigenic variation (1).

1.2.3 OMV-based vaccines and generation of Generalized Modules of Membrane Antigens (GMMA)

The OMV platform is employed against various pathogens. Currently, there are two licensed vaccines against N. *meningitidis* (VA-MENGOC-BC™ and

Bexsero™) (25) and others in advanced discovery, against S*higella* spp., *Salmonella* spp., extraintestinal pathogenic *E. coli* (EXPEC), and *V. cholerae* (25, 48). However, spontaneously released of OMV from several bacterial species occurs at low levels from a vaccine manufacturing process perspective. Furthermore, the high presence of LPS with an endotoxic effect can elicit a strong immunogenicity resulting in a strong reactogenicity. Therefore, designing completely safe vaccines based on OMV could present significant challenges (25). To overcome these limitations, several mechanisms and production processes have been developed. Mechanical disruption methods, such as extraction with EDTA sonication, or bacteria vortexing can enhance OMV yields while preserving native membrane characteristics. However, these approaches also introduce non-membrane components, which may increase antigenicity but compromise safety. These vesicles are commonly referred as native OMV (nOMV) (49, 50), while detergent extracted OMV (dOMV) are obtained following the use of detergents. This process improves OMV yield and decreases LPS levels, thereby reducing toxicity, but results in the loss of bacterial antigens and lipoproteins and in the reduction of the relative adjuvant effect (22).

Recently, a genetic modification of OMV-producing bacterial strains has been used as a process to increase the OMV blebbing and reduce the LPS endotoxicity, resulting in the production of mutant-derived OMV (mdOMV), also called Generalized Modules of Membrane Antigens (GMMA). In particular, the over blebbing happens thanks to mutations in genes of the Tol-Pal system which is characteristic of most Gram-negative bacteria, and it is involved in the crosslinking between outer membrane and peptidoglycan layer in the periplasm (51-53). Additionally, due to the

high content of LPS on OMV, further genetic deletion of genes that encode for acyltransferases such as HtrB or MsbB in *Shigella* (54, 55), MsbB and PagP in *Salmonella* (56), or LpxL1 in *N. meningitidis* (57) have been introduced to reduce the lipid A endotoxicity, leading to GMMA detoxification (22, 39, 49, 58, 59). GMMA can be also manipulated to increase the expression of relevant antigens and/or eliminate undesirable ones. Moreover, they can be used as carriers for heterologous polysaccharides and/or protein antigens as the other type of OMV, amplifying the immune response and providing broader protection against various strains and species of bacteria (29, 46, 60, 61) (**Figure 2**).

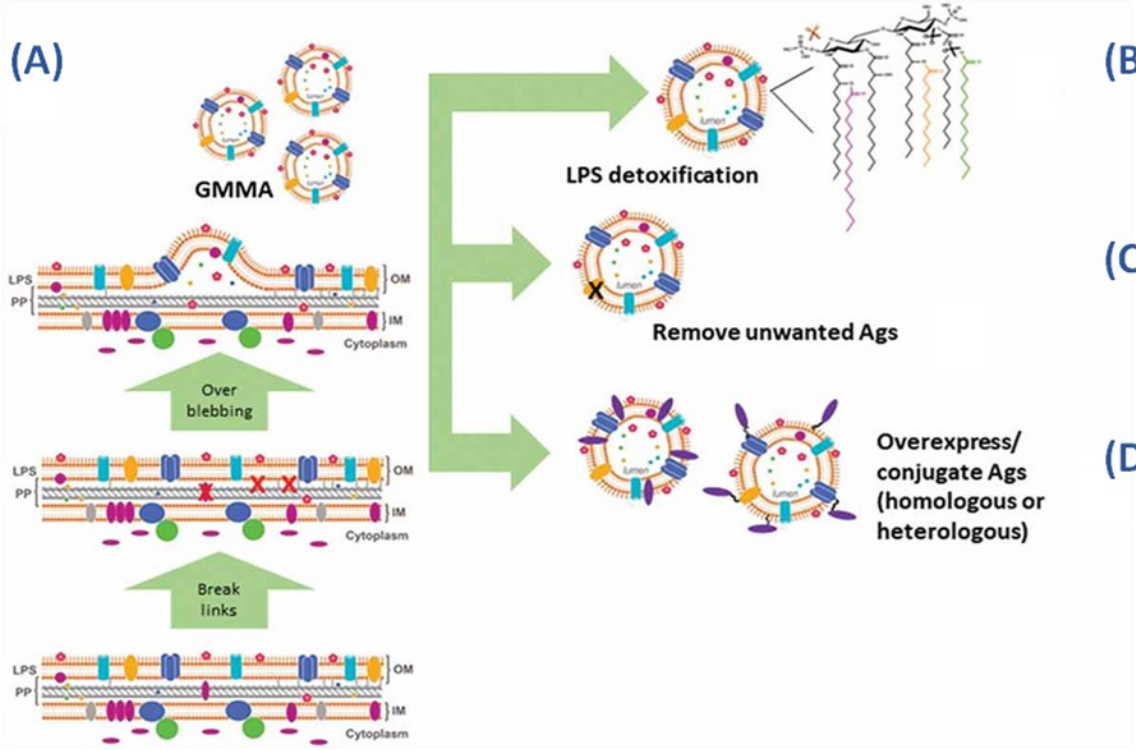

Figure 2. **GMMA' genetic manipulation and bioengineering**. Different genetic manipulations introduced in bacteria used as a source of GMMA production with the goal of: (A) Increase the ability of Gram-negative bacteria to bleb. (B) LPS detoxification to moderate the reactogenic response after GMMA injection. (C) Remove unwanted detrimental antigens for vaccine safety. (D) Overexpression of antigens to make vaccine more immunogenic. (Image adapted from Piccioli et al_2022)(46).

1.3 GMMA immunogenicity

1.3.1 GMMA adjuvanticity and innate response

Adjuvants are fundamental vaccine components that promote adaptive immunity, by directly activating innate immune cells. They are classified into two different groups: immunostimulants and delivery systems (62). The immunostimulants include PAMPs, damage-associated molecular patterns (DAMPs) and their mimicking molecules. They promote antigen presentation on major histocompatibility complexes (MHC) and the upregulation of co-stimulatory molecules such as CD40, CD80, and CD86 on APCs by interacting with PRRs. Moreover, they induce the secretion of inflammatory cytokines (e.g., IL-6, IL-10, IL-12, TNF-α) resulting in further presentation to T cells and their activation. Delivery systems comprise carriers like lipid nanoparticles (LNPs) and poly(lactide-co-glycolide) (PLGA) which promote antigen presentation by enhancing the bioavailability of antigen or creating an immune niche and thus, facilitating the presence of antigens and their potential display on MHC molecules (62). In this context, considering the GMMA composition, the most relevant TLRs that are involved in the recognition of GMMA associated PAMPs are TLR1, TLR2, TLR4, TLR5, TLR6, TLR9 (**Figure 3A**). Among them, LPS has a highly potent immunostimulant property and for this reason it needs particular attention in GMMA-based vaccines development. Indeed, on one hand, LPS has a key role in GMMA-induced effective immune response (39, 54). Notably, the genetic modification of genes encoding enzymes implicated in LPS structures' definition, in GMMA, affects the LPS binding to TLR4 resulting in the reduced immunostimulation.

Another relevant TLR implicated in GMMA immune response is TLR2 that directly binds bacterial lipoproteins. It dimerizes with TLR1 for the recognition of triacylated lipoproteins, or with TLR6 when binding biacylated lipoproteins (63). Other receptors play a minor role in the immunogenicity of GMMA because the PAMPs they recognize, including flagellin via TLR5 (84), unmethylated CpG motifs via TLR9 (85), and bacterial ribosomal RNA via TLR13 (86), are scarcely present in GMMA preparations.

The interaction of GMMA with TLRs expressed by the innate immune system triggers the release of inflammatory cytokines and chemokines, including (TNF)-α, IL-1β, IL-6, IL-8, and macrophage inflammatory protein (MIP)-α and -β as a result of the activation of antigen-presenting cells (monocytes, macrophages and dendritic cells) and human Peripheral Blood Mononuclear Cells (hPBMCs) (64-67). Additionally, flow cytometry and transcriptomics analysis on hPBMCs, reveal monocytes and myeloid DCs as the main cytokine producers (67, 68). GMMA exposure induces the up-regulation of co-stimulatory molecules (e.g. CD80, CD86) and MHC II molecules on APC, increasing their antigen up-take and thus, their ability to prime both CD4+ and CD8+ T cells (25, 66, 68, 69) (**Figure 3B**). For example, *Vibrio cholerae* OMV have been shown to activate human Monocyte-derived DCs (Mo-DCs) as evidenced by the expression of co-stimulatory molecules and to promote the differentiation of CD4+ T cells toward Th2/Th17 phenotype (70). Moreover, mice treated with *Salmonella*-derived GMMA showed that GMMA-primed DCs exhibited *Salmonella* antigens, inducing activation of CD4+ T cells that provided help to B cells for antibody production (71).

The self-adjuvanticity of GMMA is also boosted by their ability to function as carriers and due to their nanometric dimensions which should allow them to reach tissue-drained lymph nodes from the site of injection directly as well as through dendritic cells (DCs) (1, 69). Indeed, this has not been confirmed yet in GMMA context, but it is known that OMV drive DCs maturation (1, 69). For instance, it has been demonstrated that OMV derived from *Salmonella typhimurium* induce maturation of human Mo-DCs, murine bone marrow-derived DCs and CD11c+ splenic DCs (72). Additionally, nOMV derived from *Burkholderia pseudomallei* drive the DCs' maturation and activation both *in vitro* and *in vivo* in mice (73).

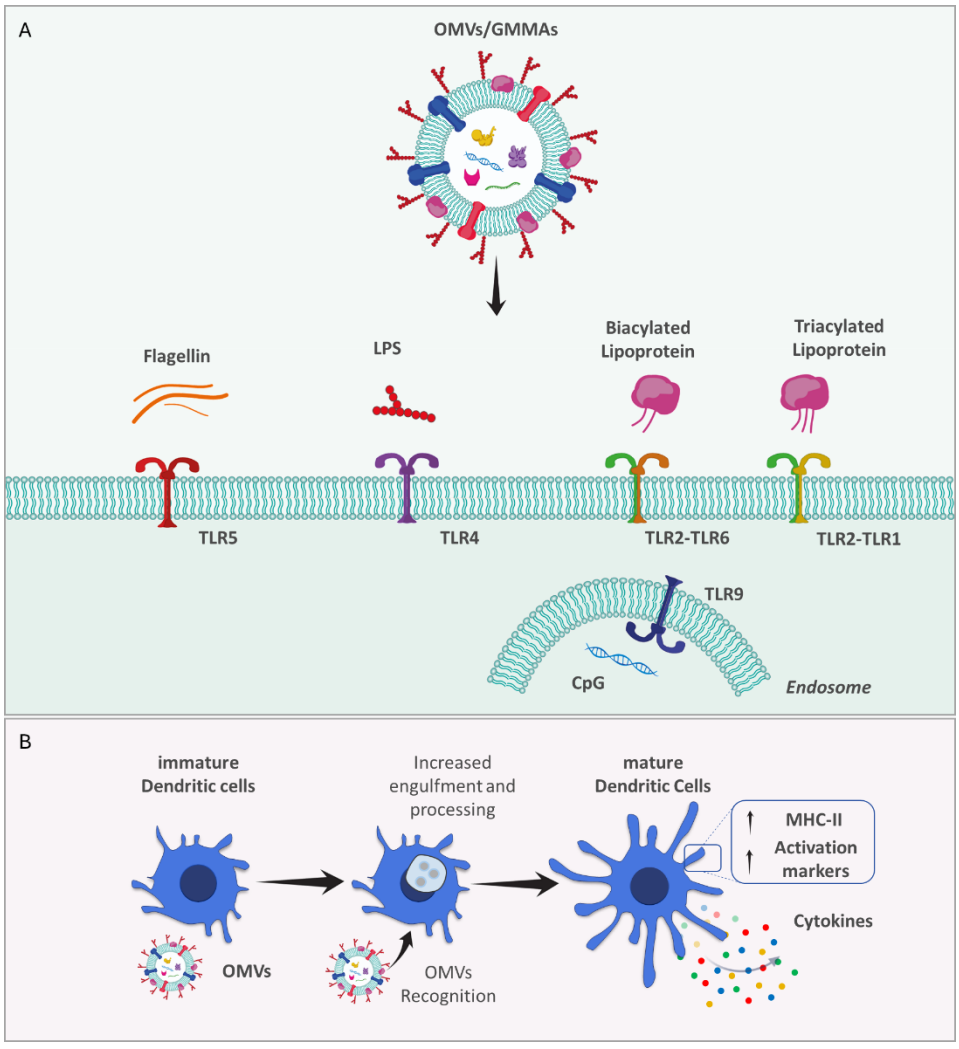

Figure 3. **Employing OMV for vaccination: innate and adaptive immunity connection**. (A) OMV-related pathogen-associated molecular patterns (PAMPs) are recognized by specific Toll-like receptors (TLRs) which are pattern recognition receptors (PRRs). (B) Upon delivery, OMV vaccines are sensed and engulfed by immature dendritic cells following the recognition of OMV' PAMPs by TLRs. The OMV identification and uptake by dendritic cells promote their development, defined by the production of co-stimulatory molecules (activation markers) and cytokine release, as well as antigen presentation.

Although these findings suggest that GMMA is a unique antigen and delivery system, the mechanism of action of GMMA is still not fully elucidated. First, limited evidence is available about the specific immune events occurring at the site of injection. The role of tissue-resident immune cells as well as non-immune cells such as muscle cells and their crosstalk, local cytokine environments, and early APCs recruitment need to be deeply investigated to better characterize factors that shape the GMMA innate immune response.Recently, it has been reported that skeletal muscle cells actively participate in several processes such as tissue repair and immune response. They produce cytokines (e.g. IL-6, IL-8, IL-1β) and chemokines (e.g. CCL2 or MCP-1, CCL3 or MIP-1α, CXCL10 or IP-10), known as myokines, mainly in response to pro-inflammatory stimuli like IFN-γ or TLR ligands (e.g. LPS, CpG), thereby shaping the local immune microenvironment (74). In the context of an intramuscular vaccine injection, this local response contributes to the recruitment and activation of several immune cells like monocyte, neutrophils, and dendritic cells boosting antigen uptake and presentation (75). Overall, these insights indicate that skeletal muscle tissue can influence both the magnitude and quality of GMMA-based vaccine immune response.

However, despite GMMA self-adjuvanticity features, GMMA-based vaccines are formulated in the presence of Alum hydroxide, also known as

Alhydrogel (AH). Aluminium salts are the first licensed adjuvants for human vaccines, generally used for their broad recognized safety and reliability (62, 76). Indeed, the addition of Alum to GMMA-based vaccines (77) has been correlated with reduced pyrogenicity in preclinical models, and it was ascribed to the retention of GMMA at the injection site and the reduced systemic dissemination (78, 79). In contrast, no substantial differences in systemic reactogenicity have been reported between alum-adsorbed and non-adsorbed GMMA formulations in human trials (79). Although alum (Alhydrogel) is used in GMMA-based vaccines to retain the vaccine at the injection site, how Alum influences immune cell recruitment and activation in GMMA formulations remains unexplored.

1.3.2 Adaptive immune response to GMMA

GMMA-induced innate immune response has an important role in the development of a pathogen-specific adaptive immunity via T and B lymphocytes and memory generation. Indeed, the presence of several PAMPs in their native conformation on GMMA' surface, along with their size, facilitates interaction with immune cells, particularly with APCs, that in turn trigger the T-cell response and the development of an effective immunity (39, 46, 49, 80, 81). Indeed, *in vivo* preclinical studies and clinical studies have demonstrated that GMMA-based vaccines elicit a strong adaptive immune response, including both humoral and cellular responses. In mouse models, GMMA vaccination induces both T-cell-dependent and T-cell-independent IgG responses in mouse (66, 82). For instance, in a *Salmonella* GMMA model, mice exhibited strong anti-O-polysaccharide-specific IgG titres with high complement-mediated bactericidal activity conferring protection (83) that also correlated with

long-lived plasma/memory B cells presence (84). Clinical data support these findings. Phase I and II clinical trials for S. *sonnei* GMMA vaccines have demonstrated that vaccines are well tolerated and immunogenic and correlate with a protective profile as resulted by the substantial increase of anti-LPS IgG titers with an high complement-mediated bactericidal activity (69). T-cell responses are less frequently quantified directly. However, murine models showed that there is indirect evidence of T cell involvement for *Shigella* GMMA-based vaccine (66) , while a flow cytometry analysis of the frequency and quality of antigen-specific CD4+ T cells have been evaluated for *Neisseria gonorrhoeae* GMMA-based vaccine demonstrating that the immune response is mainly driven by a Th0 profile (producing IL-2 and TNF-α), with rare frequencies of Th2 and Th17 profiles (85). Moreover, evidence from transcriptomic profiling suggested the involvement of Th1 and Th17 pathways in human PBMC models stimulated with GMMA (68). Additionally, some OMV vaccines such as those based on *Neisseria meningitidis*, showed the activation of both CD4+ and CD8+ T cells, suggesting the OMV vaccine potential in supporting a broad adaptive profile (73, 86). However, The studies on GMMA-based vaccines focus mainly on antibody outcomes and there are few data on their impact in T cell responses including (66) T cell activation and differentiation (69). Overall, despite considerable evidence on GMMA-based vaccines as a promising, self-adjuvanted platform, efficient in inducing strong innate and adaptive immune responses, there are still several open questions about their mechanism of action which needs further and deep investigation.

1.4 GMMA-based Vaccines Against *Shigella* and *Neisseria gonorrhoeae*: Prototypical Therapeutic Strategies for Gram-Negative Pathogens

Shigella and *Neisseria gonorrhoeae* GMMA-based vaccines are selected as models to study the GMMA platform. These pathogens represent urgent vaccine exigencies due to antimicrobial resistance and antigenic variability, while also providing an opportunity to dissect how GMMA structure and origin influence innate immune responses. Insights obtained from these models may support the broader application of GMMA technology.

1.4.1 Shigella spp.

Shigella species (spp.) are facultative anaerobic, non-motile, rod-shaped Gram-negative bacteria belonging to the family *Enterobacteriaceae* (87). These pathogens are responsible for shigellosis, an acute diarrheal disease characterized by a spectrum of clinical manifestations, including watery or bloody diarrhoea, abdominal pain, and fever (88). Shigellosis remains the leading bacterial cause of diarrheal mortality worldwide, accounting for approximately 212,438 deaths annually. Notably, around 30% of these fatalities occur in children under the age of five, predominantly in low- and middle-income countries (LMICs) (88-90).
Shigella comprises four distinct species, *S. dysenteriae*, *S. flexneri*, *S. boydii*, and *S. sonnei*, which are further classified into over 50 serotypes based on the structural variability of the outer polysaccharide antigen (O-antigen, OAg) present on the lipopolysaccharide (LPS) of the bacterial surface (88).*Shigella flexneri* and Shigella *sonnei* are responsible for nearly 90% of shigellosis cases worldwide, with *S. flexneri* predominating in LMICs, and *S. sonnei* being more prevalent in high-income settings (91-

94). Currently, no licensed vaccines against *Shigella* are available. However, several promising candidates are under clinical development, aiming to address the global burden of shigellosis (95).

One of the primary challenges in developing an effective vaccine against *Shigella* is the need to achieve broad coverage across the most epidemiologically relevant serotypes. Several studies have demonstrated that the protection against *Shigella* spp. is primarily serotype-specific, and it correlates with antibodies primarily against *Shigella* OAgs (96-99). As a result, several OAg-based vaccine strategies like live attenuated oral, killed oral, and subunit parenteral vaccines have been evaluated (100). However, no effective vaccine has been licensed, mostly due to limited extent of protection considering the presence of 50 different serotypes of *Shigella* (100). Given these limitations, alternative approaches are being investigated to overcome the challenges of serotype diversity. Among these, GMMA platform has emerged as a promising strategy for the development of broadly protective and cost-effective *Shigella* vaccines.

1.4.2 Shigella GMMA-based vaccine

The development of a tetravalent *Shigella* vaccine, known as altSonflex1-2-3, represents a significant advancement in the fight against shigellosis (101). Since this disease is caused by different serotypes of *Shigella*, researchers wanted to develop a broadly effective vaccine, covering the most epidemiologically relevant serotypes (102). The four-component candidate builds upon bases laid by the first-generation S. *sonnei* GMMA vaccine, called 1790-GMMA (54). The initial S. *sonnei* GMMA vaccine consisted of a single component, 1790-GMMA, derived from the genetically modified S. *sonnei* strain (54). These modifications included

the deletion of *tolR* and *htrB* or *msbB* genes to respectively improve the release of membrane vesicles and reducing reactogenicity (44, 101). The *tolR* gene encodes for a protein that anchors the outer membrane and the peptidoglycan or inner membrane; its disruption weakens this connection, thereby promoting vesicle blebbing. In contrast, *htrB* and *msbB* genes encode two late acyltransferases, specifically HtrB (also known as LpxL) and MsbB (also known as LpxM)- involved in the acylation of lipid A within LPS. Their deletion results in a penta-acylated LPS structure, resulting in a GMMA with reduced endotoxicity (1790-GMMA penta). Consequently, 1790-GMMA (penta-acylated) exhibits lower reactogenicity compared to 1859-GMMA, which retains the wild-type hexa-acylated lipid A structure (59, 91, 92). In agreement with a reduced reactogenicity of 1790-GMMA compared with 1859-GMMA the production of pro-inflammatory cytokines (TNF-α, IL-1β, IL-6, IL-8, IFN-γ, IL-10 and IL-12p70) from hPBMCs after an *in vitro* stimulation with 1790-GMMA penta is lower respect to those elicited by 1859-GMMA (54, 67, 103). A similar behaviour is also observed for additional cytokines like IL-10, IL-13, IL-4, MIP-1a, MIP-1b, IL-2, MCP-1, GM-CSF and IL-12p40. This pro-inflammatory innate response depends on TLR2 and TLR4 activation and, in particular, the immunogenicity given by 1790-GMMA penta is related to TLR2 as demonstrated by blocking of TLRs, alone or in combination, in hPBMCs (55, 56). Indeed, despite the Lipid A modification on LPS, 1790-GMMA penta has still several components of the outer membrane that can act as PAMPs inducing a S. *sonnei* GMMA specific innate response without any possibility to trigger the related disease (104). Moreover, advanced flow cytometry analysis on hPBMCs shows that 1790-GMMA penta activates specific immune cell populations including monocytes, plasmacytoid

dendritic cells (pDCs), B cells, gamma delta (γδ) T cells, NK cell (67). However flow cytometry analysis together with confocal microscopy show monocytes as the primary target population and transcriptomic defines a molecular signature associated with inflammatory response (IFN responses, processes induced by IL1β/TNFα/IL15, and inflammasome activation) but also with antigen-presenting cell differentiation and the T cell regulation (68). The 1790-GMMA penta has been used for the first-generation S. *sonnei* GMMA vaccine candidate known as 1790GAHB which demonstrated to be highly immunogenic with the production of anti-LPS specific IgG and IgM but also antibodies (54, 105). Moreover, Phase I and II clinical trials conducted in healthy European and African adults demonstrated that intramuscular administration of 1790GAHB was well tolerated and elicited a substantial increase in serum IgG levels specific for *Shigella* (106-108). Importantly, the antibodies generated could mediate bacterial killing *in vitro* in the presence of complement. However, a Phase IIb human challenge study using higher doses of O-antigen (OAg) revealed that increased OAg content is likely necessary to achieve clinical protection (109). This finding led to the development of a novel *S. sonnei* GMMA construct, 2929-GMMA, generated through the deletion of the *msbB* and *tolR* genes from the parental *S. sonnei* strain. This new construct contains approximately ten times OAg (relative to protein and lipid A content) than the original 1790-GMMA formulation (102). Despite this difference, both 2929-GMMA and 1790-GMMA, compared at the same protein dose, induced similar level of IL-6 from hPBMCs in a monocyte activation test (MAT) assay. In contrast, *in vivo* study on mice showed that 2929-GMMA induced higher levels of anti-S. *sonnei* LPS IgGs and SBA titres than 1790-GMMA coherently with the

higher amount of OAg on its surface (102). The newly developed construct has been incorporated in a 4-component formulation, called altSonflex1-2-3, which includes GMMA derived from three *S. flexneri* strains 1b, 2a, and 3a adsorbed onto Alhydrogel (102). These *S. flexneri* strains were selected based on their epidemiological relevance and their ability to induce cross-reactive antibodies, with the potential to confer broad protection against the most prevalent *Shigella* serotypes (110). The *S. flexneri* strains underwent the same genetic modifications as the *S. sonnei* strain (Δ*tolR* Δ*msbB*), resulting in GMMA containing penta-acylated LPS. Additionally, *S. flexneri* GMMA exhibited a distinct subpopulation of hexa-acylated, non-wild-type lipid A species, attributed to the activation of the palmitoyl transferase enzyme PagP, which catalyses the palmitoylation of the penta-acylated lipid A (102). Despite these structural differences, the immunogenic profile of S. *flexneri* GMMA closely mirrored that of 1790-GMMA, demonstrating robust safety and immunogenicity (108, 111). A preclinical immunogenicity study assessed on mice and rabbits demonstrated that the combination of the four components didn't impact on the immune response related to each single component resulting in higher anti-OAg IgG response and SBA titres in four-component formulation than single GMMA formulations, also at low doses (66). Of note, sera from vaccinated mice and rabbit elicited a robust, dose-dependent production of functional antibodies against OAg of all serotypes inside the vaccine as well as additional S. *flexneri* serotypes with an epidemiological relevance (namely *S. flexneri* serotypes 4a, 5b, 6, X, Y) suggesting broad protective potential (66). Remarkably, toxicology studies where rabbits are treated with the full human dose demonstrated a mild inflammatory response supporting the vaccine's safety (66). These

findings were also reinforced by *in vitro* assays including the monocyte activation tests (MAT) assay which showed that the IL-6 amount from hPBMCs was comparable to that observed for 1790GAHB (66).

These promising preclinical results allowed to proceed to clinical trials (clinicaltrial.gov NCT05073003). The altSonflex1-2-3 was administrated intramuscularly in three different doses firstly in European adults (stage 1) and subsequently in a shigellosis-endemic population in Kenya (stage 2) following an age-descalation strategy (first in adults 18 to 50 years of age, secondly in children 24 to 59 months of age and finally in infants 9 months of age) with the aim to define immunogenicity and safety of the vaccine candidate but also to define the optimal dose for vaccine administration in 9 month of age target population. Data from stage 1 showed excellent tolerability with mild reactogenicity (e.g. pain and headache) (112) similar to prior formulation 1790GHAB (113). Immunogenicity data reported a strong immune response with the production of functional antibodies titres against all vaccine serotypes, particularly S. *flexneri* 2a and S. *sonnei*, with a bactericidal activity. A recapitulation of immune responses was observed with additional doses highlighting the vaccine's potent initial effects and sustained antibody levels post-vaccination (112). Accordingly with preclinical results, data reported a higher response to S. *sonnei* for altSonflex1-2-3 than 1790GHAB (102, 107, 109). These findings permitted the progression toward the currently ongoing stage 2 of the clinical stage that consist in the vaccination of shigellosis endemic population in Africa with a age de-escalation to finally test the vaccine in a younger population which is the target one (102).

Altogether, these findings support the continued clinical development of altSonflex1-2-3 as a promising vaccine candidate with the potential to

provide broad, safe, and effective protection against the most epidemiologically relevant *Shigella* serotypes. However, despite the encouraging preclinical and clinical results, the underlying mechanisms by which GMMA-based vaccines elicit immune responses remain incompletely understood and warrant further investigation.

1.4.3 Neisseria gonorrhoeae

The gram-negative bacterium *Neisseria gonorrhoeae* (Ng) poses a significant global health threat, contributing to invasive gonorrhoea, a sexually transmitted infection (STI) that likely affected 86.9 million people among 15–49 years of age, globally in 2016 (114). Gonorrhoea triggers mostly urethritis in men and cervicitis in women but usually remains asymptomatic, mainly in women, provoking an underdiagnosis and consequently the progression of the disease, which can be characterized by pelvic inflammatory disease (endometritis and/or salpingitis), infertility (115, 116) and increased risk of HIV acquisition (117). Alarmingly, in recent years, gonorrhoea case rates have notably risen even in industrialized countries (7). Gonorrhoea cases increased by 67% from 2013 to 2017 in the USA (7, 118) and by >200% from 2008 to 2017 in the European Union/European Economic Area (EU/EEA) (8). Following a historic low in 2009, gonorrhoea incidence increased by 82.6%, rising from 98.1 cases per 100,000 population in 2009 to 179.1 cases per 100,000 in 2018, corresponding to a total of 583,405 reported cases (119). Effective antimicrobial therapy remains critical for the prevention and control of gonorrhoea. The Centers for Disease Control and Prevention (CDC) currently recommend a dual therapy regimen consisting of 250 mg intramuscular ceftriaxone and 1 g oral azithromycin for the treatment of uncomplicated gonorrhoea. However, the emergence of strains with

reduced susceptibility to ceftriaxone and azithromycin has raised concerns regarding the potential for untreatable infections. Consequently, novel strategies are urgently needed to prevent gonorrhoea and address the growing threat of antibiotic-resistant *N. gonorrhoeae* (119).

One promising approach is the development of a gonococcal vaccine. Although no licensed vaccine currently exists and past efforts have been unsuccessful, recent evidence suggests that serogroup B meningococcal vaccines containing *Neisseria meningitidis*-derived outer membrane vesicles (MenB OMV) may confer modest protection against gonorrhoea (120). These findings have revitalized research efforts and provided a foundation for the rational design of gonococcal vaccine candidates.

However, *N. gonorrhoeae* has a remarkable ability to evade the immune system through antigenic and phase variation, molecular mimicry, and immune suppression (115, 121-125). These mechanisms enable repeated infections in previously exposed individuals. Especially, virulence surface factors such as Type IV pili, opacity-associated (Opa) proteins, and lipo-oligosaccharides (LOS), which, together with the abundant outer-membrane protein PorB, correspond to the main vaccine targets for *N. gonorrhoeae*, undergo frequent genetic mutations, resulting in immune avoidance and limiting the development of a stable protective immunity (115, 125). The bacterium also binds complement-regulatory proteins (FHbp and C4bp), suppressing complement activation and enhancing serum resistance. Additionally, Neisserial porins contribute to immune evasion by inducing programmed cell death in human antigen-presenting cells, thereby impairing antigen presentation. They also inhibit dendritic cell–mediated T-cell proliferation and suppress both Th1- and Th2-driven adaptive immune responses, ultimately dampening host immunity and

complicating vaccine development efforts (126). These sophisticated evasion tactics present major obstacles to gonococcal vaccine development. Furthermore, the absence of a protective immune response after a natural infection as well as lack of an efficient animal model that can be predictive of *N. gonorrhoeae* pathogenesis are considerable challenges in vaccine development (127). Several vaccine candidates and/or different formulations, such as DNA-based platforms (128), viral replicon particles (129), and outer membrane-derived formulations (130), have been developed but only three vaccine candidates reached clinical trial phases, all of which ultimately failed. These included a heat-killed whole-cell vaccine (131), a pilin-based formulation effective only against homologous strains(132), and an outer membrane vaccine enriched in antigens like PorB and LOS, which also failed to protect (133). A key development in the *N. gonorrhoeae* vaccine development came with retrospective studies of MeNZB, an OMV vaccine developed for *N. meningitidis* serogroup B. These studies reported a cross-protection of 31% against *N. gonorrhoeae* infection in the vaccinated individuals (120), a finding subsequently corroborated by several ecological data from several countries (120, 134, 135). Further investigations with 4CMenB (Bexsero), a more forward OMV-containing vaccine, demonstrated 33–46% efficacy against gonorrhoea (136-138). This cross-protection is likely due to the identity between *N. gonorrhoeae* and *N. meningitidis* protein antigens, most of which are present on OMV incorporated in the MeNZB and 4CMenB vaccines (139, 140). Despite the evidence about the significant 4CMenB's impact on gonorrhoea infection, there is no evidence of effective and durable protection against N. *gonorrhoea*.

1.4.4 Neisseria gonorrhoeae (Ng) GMMA-based vaccine

N. gonorrhoeae-specific OMV vaccines are under preclinical and clinical investigation (141). These include NGoXIM (142) and dmGC_0817560 (143) vaccines based on nOMV, in late preclinical phases, and a *N. gonorrhoeae* (Ng) GMMA-based vaccine currently in phase 1/2 trials in healthy adults aged from 18 to 50 years old (NCT05630859). The Ng GMMA vaccine candidate is based on GMMA derived from *N. gonorrhoeae* FA1090 strain in which genes for Rmp and LpxL1 have been deleted. The reduction modifiable protein (Rmp) is a protein involved in immunosuppression processes (144). Indeed, subsequent studies about the first Ng OMV vaccine demonstrated that anti-Rmp antibodies generated after vaccination induced a decrease in SBA activity by anti-LOS and anti-Por with a reduction of protection (116, 144). Therefore, its deletion improves the immunogenicity of Ng GMMA. The *lpxL* gene encodes for the late acetyltransferase LpxL implicated in the acetylation of the Lipid A in LPS, and its deletion leads to a detoxification (145) of LOS as happened in *Shigella* spp. GMMA. Indeed, *in vitro* studies on hPBMCs have demonstrated that the production of pro-inflammatory cytokine IL-6 is highly reduced following stimulation with GMMA prepared from FA1090 Δ*lpxL1*Δ*rmp* (Ng GMMA) compared to the response elicited by FA1090 WT nOMV. Moreover, *in vivo* studies on mice have shown that Ng GMMA immunization triggered a CD4+ T cells response against various types of gonococcal GMMA and bacteria. Specifically, the CD4+ T cells population is cross-reactive against MenB OMV and GMMA from FA1090 and SK92-679 as well as heat-killed (HK) FA1090 and SK92-679 bacteria, while a slight response has been observed against *Salmonella* GMMA. The quality of the cellular-mediated immune response is dominated by a Th0 profile

characterized by the production of IL-2 and TNF-α, while low frequencies are observed for Th2 and Th17 profiles defined by the low levels of IL-17 and IL-4/13 respectively. Moreover, Ng GMMA immunization induced also higher levels of IgG and IgA in both sera and vaginal washes compared to those elicited by the 4CMenB showing stronger immunogenicity and antibody activity. Using a human serum bactericidal assay (hSBA) and a bacterial adhesion inhibition (BAI) assay, it has been demonstrated that sera from mice immunized with Ng GMMA showed a higher bactericidal activity against a panel of 11 gonococcal strains compared to those immunized with 4CMenB or alum and inhibited the bacterial adhesion to human urogenital epithelial cell lines (SV-HUC1 ureteral cells as male representative epithelial cell line and Ect1 ectocervical cells as female's one), rising up to 67-92% inhibition for both homologous FA1090 and heterologous SK92-679 strains. No relevant inhibition activity was observed for 4CMenB-immunized mice sera, suggesting the superior effectiveness of Ng GMMA. The antibodies generated after the Ng GMMA vaccine immunization are against both proteins and LOS which correspond to the major target antigens since it has been demonstrated that anti-LOS antibodies can activate the complement system to kill Ng (146) and had the potential to prevent re-infection by homologous strains as shown in male urethral experimental gonococcal infection model (147). Anti-LOS antibodies showed a predominant bactericidal activity against several gonococcal strains while anti-protein antibodies inhibited FA1090 homologous strain adhesion suggesting an extensive functional protection exceeding that observed with 4CMenB-immunization (85). Overall, the promising results supported the investigational NgG vaccine as a potential vaccine candidate against *N. gonorrhoeae* and it has

entered the clinical development phase. Specifically, it is in Phase 1/2 clinical trial with the aim of assessing the safety, reactogenicity, immunogenicity, and efficacy of the NgG vaccine candidate in eight countries: the USA, the United Kingdom, France, Germany, Spain, Brazil, the Philippines and South Africa (NCT05630859). So, these results demonstrated that GMMA represent a relevant platform in the development of a suitable and effective vaccine against N. *gonorrhoeae*.

1.5 Aim of the project

GMMA technology is considered as a qualified vaccine platform since GMMA vaccines can be defined as a low-cost multivalent vaccine (61). Moreover, GMMA, resembling the bacterial outer membrane, show several antigens in their native conformation conferring a strong self-adjuvanticity propriety and can also be used as a carrier for antigens from different bacteria (46). Preclinical and clinical studies have demonstrated the GMMA vaccines ability to induce strong innate and adaptive immune responses (69). However, multiple variables including antigenic composition, both in terms of serotype diversity and bacterial origin, presence of adjuvants like alum and route/site of administration can influence the quality, magnitude, and nature of the immune response (69). This project aims to elucidate the mechanism of action of GMMA-based vaccines, focusing on how GMMA, through their inherent self-adjuvanticity, interact not only with immune cells but also with non-immune cells such as muscle cells at the injection site. Such interactions are likely to shape the innate immune response, a critical step for the downstream adaptive immunity and thus, an effective vaccination. Notably, being a GMMA-based vaccine formulated with alum hydroxide, I

also investigate how the GMMA-induced activation of innate immune cells is influenced by alum to clarify the relative contribution of GMMA's self-adjuvanticity as well as the alum's immunoregulatory role. Another important variable that can influence GMMA-induced innate response is the bacterial origin of GMMA. Indeed, the species of origin defines GMMA's specific antigenic composition which may shape their immunological profile, influencing the type and quality of innate immune response and thereby the further adaptive response they promote. For this reason, I study the mechanism of action of *Shigella* and *N. gonorrhoeae* GMMA-based vaccine, as models, evaluating whether their ability to activate innate immune cells or muscle cells is linked primarily to their self-adjuvanticity and structural platform features, or to their bacterial origin. Moreover, since the adaptive immune response, including firstly the activation and differentiation of T cells and further of B cells, is dictated by signals provided during the innate phase I want also to investigate how innate immune cells treated with these model vaccines guide T cell polarization, providing insights on the influence of GMMA-based vaccines on the type of T cell response triggered. Additionally, by developing a primary muscle cell model (PMCM), which combines immune cells with myotubes to recapitulate the cellular crosstalk between immune and non-immune cells, including muscle cells at the injection site, this project aims to deepen the current knowledge about GMMA's local immunological impacts, bringing new insights of the Mode of action (MoA) of GMMA-based vaccines in a more physiological context. Altogether, this project will provide a comprehensive overview of GMMA-based vaccines' MoA, enhancing the rational design of future GMMA-based multivalent vaccines.

2. MATERIALS AND METHODS

2.1 hPBMCs *in vitro* stimulation

2.1.1 hPBMCs thawing

Frozen hPBMCs from healthy donors were obtained from Tivoli Hospital (Belgium). The study was approved by local Ethics Committees and conducted according to good clinical practice in accordance with the declaration of Helsinki (1975). Cryopreserved hPBMCs were thawed at 37°C and washed twice (1200 rpm, 10 min RT) with a pre-warmed "thawing solution" (PBS w/o Ca++ Mg++, Gibco Life Sciences, 2.5 mM EDTA, Euroclone, and 20 µg/ml DNAse, Sigma Aldrich). hPBMCs were then resuspended in "complete medium" (RPMI-1640 supplemented with 1% non-essential amino acids and 1% sodium pyruvate (Gibco Life Sciences), 1% Penicillin/Streptomycin/Glutamine (Euroclone), and 10% heat-inactivated FBS (Hyclone), and counted to assess cell viability based on Trypan blue dye exclusion (Vi-Cell-blue, Beckman Coulter). The viability of thawed hPBMCs was between 90 and 98% of total cells.

2.1.2 hPBMCs stimulation

After thawing, $1x10^6$ live cells/well were seeded in round-bottom 96 wells plates (Corning) and then stimulated for the immune characterization's experiments with the following stimuli: 1) Shig 4vForm+alum (*Shigella* GMMA-based vaccine or altSonflex1-2-3), 2) Shig 4vForm (the *Shigella* GMMA 4 valent formulation), 3) single GMMA : S. *sonnei* 2929 GMMA penta, S. *flexneri* 1b, S. *flexneri* 2a, S. *flexneri* 3a GMMA (GSK Vaccines Institute for Global Health, GVGH), 4) N. *gonorrhoeae* (Ng) GMMA, 5) Ng GMMA + Alum (Ng GMMA-based vaccine),6) S. *sonnei* GMMA esa as positive control, 7) Alum alone, 8) Medium alone (MED) as negative

control. All stimuli are used at 1 µg/ml for both flow cytometry experiments and cytokine detection in cell culture supernatants (SN); hPBMCs were incubated for 4 hours at 37°C, 5% CO_2.

2.1.3 Flow cytometry analysis: Immunophenotyping and Activation Markers Expression by stimulated hPBMCs

Following 4 hours of stimulation, hPBMCs were centrifuged at 1700 rpm for 5 min at RT to pellet them. Cell-free SN was collected from each well and stored at -20°C for cytokine quantification assay. Cells were stained with Fixable Viability Stain 440UV (cat. 566332, Invitrogen) for 20 min in the dark at room temperature (RT). After washing twice with 150µl/well of 1X PBS (1700 rpm, 5 min, RT), cells were incubated with 2% rabbit serum (Gibco) for 20 minutes at 4°C to saturate Fc receptors present on hPBMCs thus avoiding unspecific binding of antibodies through their Fc portion. Cells were then washed twice with 1X PBS and stained on the surface for 20 minutes on ice for phenotypic characterization of cells subsets. The following mix of mouse monoclonal anti-human mAbs (BD Biosciences) were used: anti-CD3 (APC-H7), anti-CD11c (PE Cy- 5.5), anti-HLA-DR (BV570), anti-CD4 (BUV395), anti-CD8 (BUV737), anti-CD14 (BUV496), anti-CD16 (BV786), anti-CD19 (BB790), anti-CD56 (APCR700), anti-CD69 (BB750), anti-CD86 (PE Cy-7), anti-CD123 (BUV615), anti-CD32 (BUV563), anti-CD1c (BV421), anti-CD40 (BV650), anti-TCRγδ (BUV661), anti-CD64 (BV480), anti-CD83 (PE -Cy5) (BD Biosciences). Following incubation, cells were washed twice with PBS and fixed with Cytofix (BD Bioscience) for 20 minutes at +4°C. Finally, cells were washed twice with PBS and resuspend to 150 µg PBS-EDTA 2,5 mM. Samples were acquired on BD FACSymphony A3 Analyzer. Data were analyzed using FlowJo 10 software (Becton, Dickinson and Company).

2.1.4 Gating strategy identification of immune hPBMC populations

The flow cytometry gating strategy applied is shown in **Figure 4**. The analysis of hPBMCs form a healthy donor stimulated for 4 hours with Alum is shown as an example. (Panel A) Discrimination between live (gated region) and dead cells was assessed by Live/Dead staining. Then the leukocytes cells were selected using forward scatter (FSC) and side scatter (SSC); (3) the cellular aggregates were excluded gating for singlets based on their width (side scatter area, SSC-A, versus side scatter width SSC-W). (Panel B) Among live singlet cells, the T cells were identified gating on CD3+: CD4 cells were identified as CD4+CD8- cells, CD8 cells were CD8+CD4-, whereas TCRγδ were discriminated as TCRγδ on CD4-CD8-. (Panel C) (4) Among CD3- cells, the B cells population was identified as CD19+, (5) NK cells were identified as CD19-CD56+. NKs dim were distinct from NK bright as CD16+CD56- since NKs bright were CD16-CD56+. Among CD3- also monocytes and dendritic cells were discriminated (6). Non classical monocytes were identified as HLA-DR+ gating first and then CD16+CD14-, whereas classical as CD14+CD16-Intermadiate monocytes were selected as CD14+CD16+. (7) Dendritic cells were identified as HLA-DR+ cells gating first on CD14- cells, then as CD123+CD11c- for pDCs and CD123lowCD11c+ for mDCs.

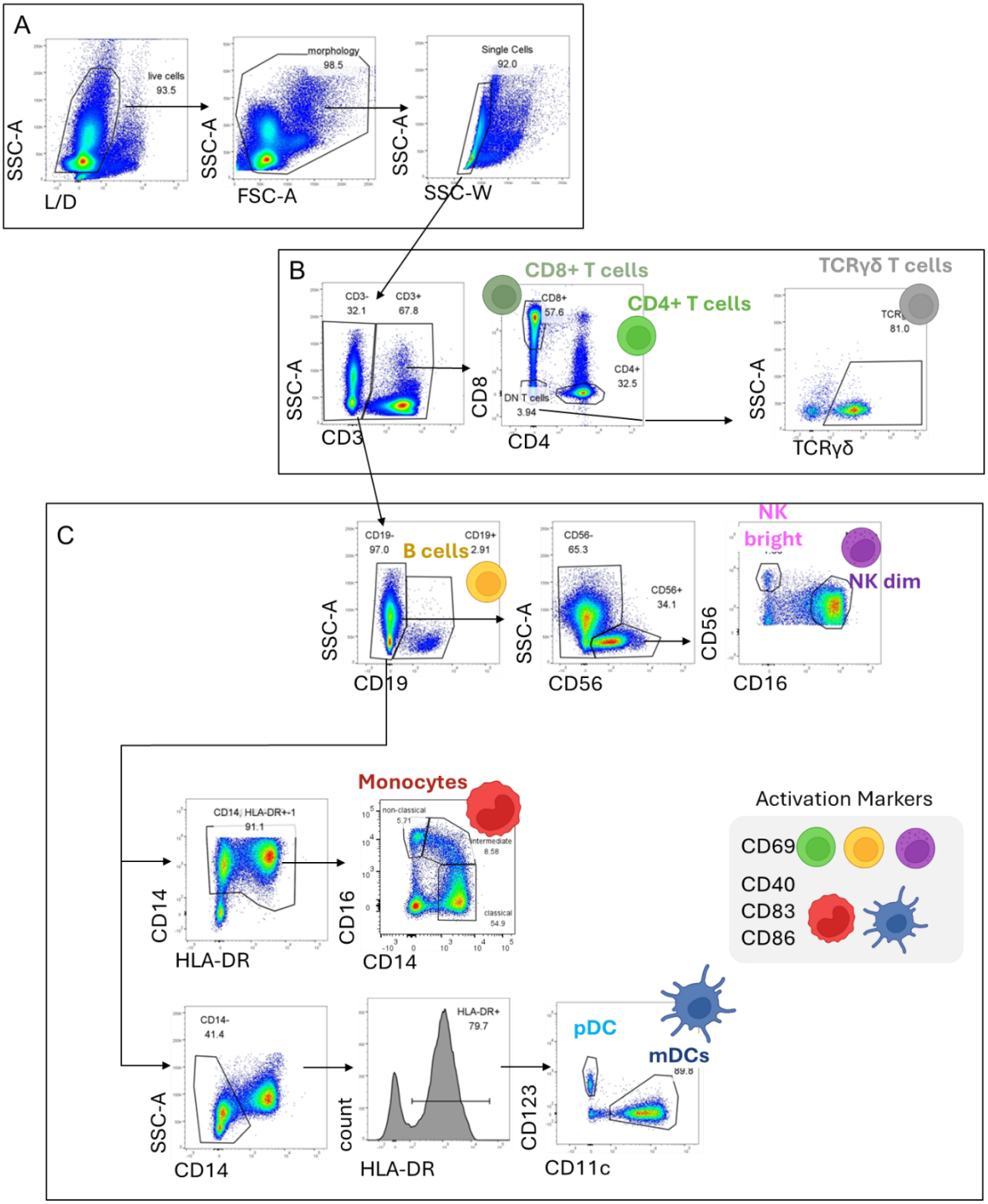

Figure 4. **Representative gating strategy used to define PBMCs' cell subsets**

2.2 Monocyte-derived dendritic cells (Mo-DCs) generation and *in vitro* stimulation

2.2.1 Monocyte Isolation from healthy donors' hPBMCs

Following hPBMCs thawing (refer to paragraph 3.1.1), monocytes were isolated using the EasySep™ Human Monocyte Isolation Kit (cat. 19359, Stemcell Technologies). This kit enables immunomagnetic negative isolation of untouched human CD14+CD16- monocytes. The isolation process was carried out in accordance with the manufacturer's protocol. The yield of monocyte isolation was evaluated by flow cytometry (refer to paragraph 3.1.3). In particular, the percentage of monocytes detected in pre-isolation samples were compared to that detected in post-isolation samples as shown in **Figure 5**.

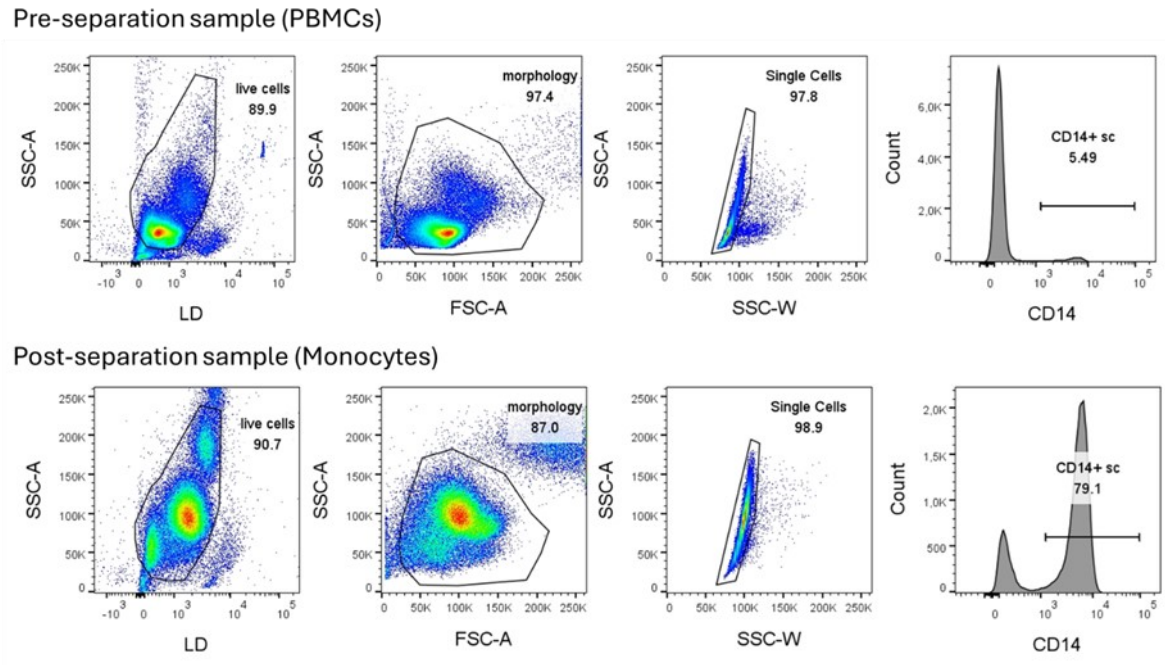

Figure 5. **Representative gating strategy of monocytes isolation check.**

2.2.2 Monocyte-derived Dendritic Cell (Mo-DC) generation and stimulation

Monocytes isolated from hPBMCs were differentiated *in vitro* into immature monocyte-derived dendritic cells (iMo-DCs). Following isolation, monocytes were seeded in 6 well plate (Corning) at a density of 2×10^6 cells per well in 4 ml of a commercially available monocyte-derived dendritic cell differentiation medium (Miltenyi Biotec, cat. 130-094-812). After six days of incubation (37 °C, 5% CO_2), the differentiated cells were harvested, pooled, and assessed for viability and concentration using the Vi-CELL automated cell counter. On day 6, 0,25 x 10^6 cells live iMo-DCs were plated into round-bottomed 96 well plates (Corning) and stimulated for 48h at 37°C, 5% CO_2 with 1 µg/ml of: 1) Shig 4vForm+alum, 2) Shig 4vForm, 3) single GMMA : S. *sonnei* 2929 GMMA penta, S. *flexneri* 1b, S. *flexneri* 2a, S. *flexneri* 3a GMMA 4) Ng GMMA, 5) Ng GMMA + Alum, 6) Alum, 7) S. *sonnei* GMMA esa (0,001 µg/ml) as positive control, 8) complete medium (MED) as negative control.

2.2.3 Flow cytometry: Immunophenotyping and Activation Markers Expression by stimulated hPBMCs, Monocytes, iMo-DCs and mMo-DCs

To evaluate monocyte isolation yield (see paragraph 3.2.1), iMo-DC differentiation, mMo-DCs maturation and quantification of activation markers following Mo-DCs stimulation, the following surface staining protocol was applied. Briefly (detailed surface staining protocol is reported in paragraph 3.1.3), samples were centrifuged at 1700 rpm for 5 minutes RT. Cell-free SN was collected from each well and stored at -20°C for cytokine quantification assay. Cells were stained using Fixable Viability

Stain 440UV and then incubated with 2% rabbit serum for 20 minutes at 4°C, preventing unspecific antibody binding. Then cells underwent surface staining for 20 minutes on ice for phenotypic characterization. The following mix of mouse monoclonal anti-human monoclonal antibodies (mAbs) from BD Biosciences was used: anti-CD3 (APC-H7), anti-CD11c (PE Cy 5.5), anti-HLA-DR (BV570), anti-CD4 (BUV395), anti-CD8 (BUV737), anti-CD14 (BUV496), anti-CD16 (BV786), anti-CD19 (BB790), anti-CD56 (APCR700), anti-CD69 (BB750), anti-CD86 (PE Cy-7), anti-CD123 (BUV615), anti-CD32 (BUV563), anti-CD1c (BV421), anti-CD40 (BV650), anti-TCRγδ (BUV661), anti-CD64 (BV480), anti-CD83 (PE -Cy5) (BD Biosciences). Cells were then washed and fixed with Cytofix for 20 minutes at +4°C. Finally, cells were washed twice with PBS and resuspend to 150 µl PBS-EDTA 2,5 mM for the acquisition by BD FACSymphony A3. Analysis was done using FlowJo Software version 10 (Becton, Dickinson and Company).

2.2.4 Gating strategy for Mo-DCs definition

The flow cytometry gating strategy applied is shown in **Figure 6**. The analysis of Mo-DCs from a healthy donor without any stimulation is shown as an example. (**Panel A**) Live cells, Mo-DCs morphology and single cells were defined as reported in paragraph 3.1.3. for monocytes, immature and mature Mo-DCs. (**Panel B**) Among live singlet cells, the up-regulation of Mo-DCs population markers CD1c, CD11c and HLA-DR alongside the downregulation of monocytes' marker CD14, were evaluated to check the effective differentiation of monocyte to immature Mo-DCs. (**Panel C**) The maturation of Mo-DCs upon 48 hours stimulation was evaluated measuring the up regulation of activation markers CD40, CD83, CD86.

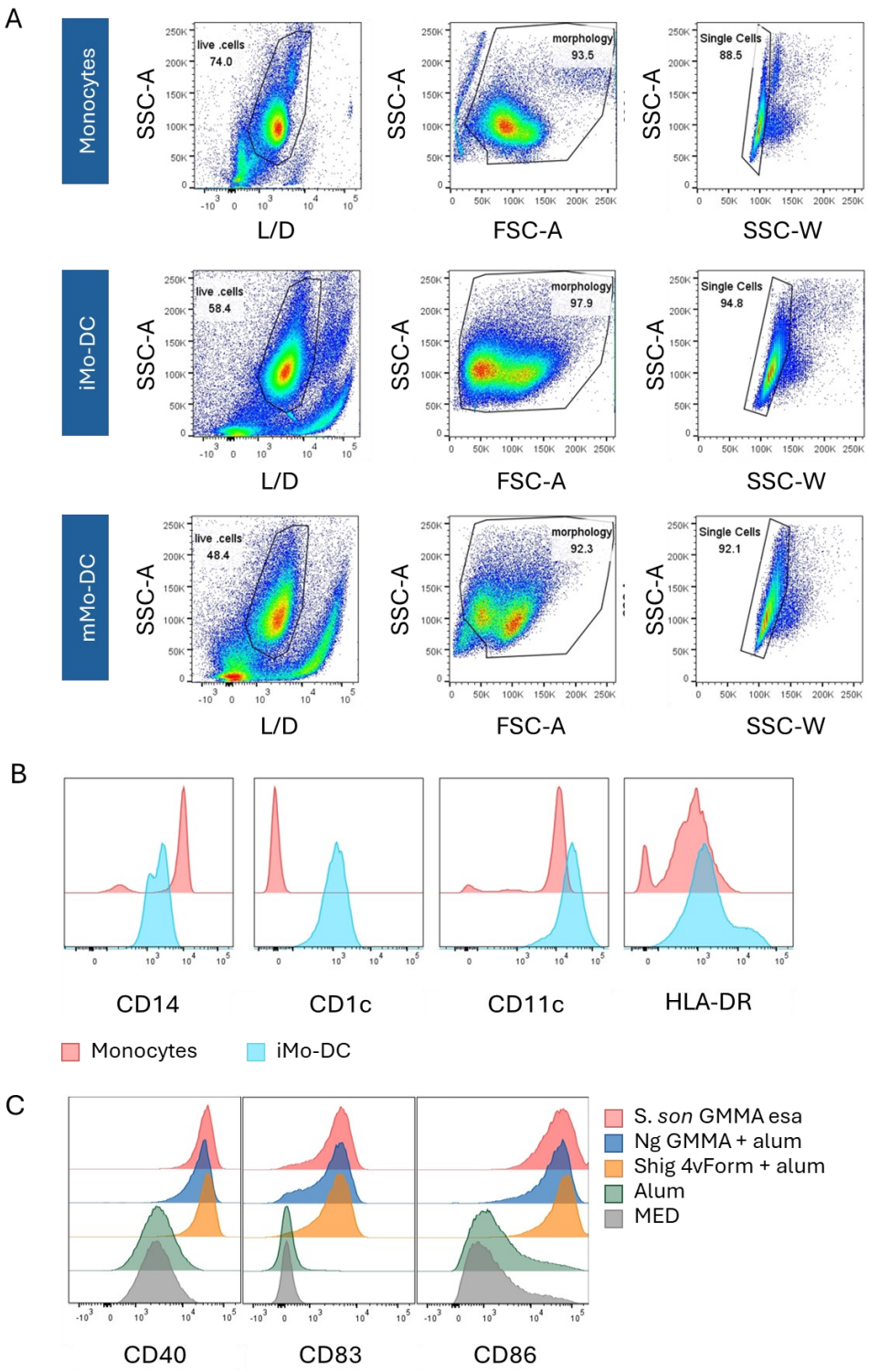

Figure 6. **Representative gating strategy and flow cytometry analysis for differentiation and maturation of Mo-DCs.**

2.3 Human Skeletal Muscle Cells: *in vitro* culture, differentiation from myoblast to myotube, stimulation and generation of the muscle cell *in vitro* model

2.3.1 Culturing of Skeletal muscle myoblasts

Commercial human primary skeletal muscle myoblasts (HSMM, CC-2580, Lonza, Basel, CH) were propagated using Skeletal Muscle growth medium (SkGM Medium, CC-3246, Lonza) supplemented with SkGM-2 Single Quots kit (CC-3244, Lonza) which included human Epidermal Growth Factor (hEGF), Dexamethasone, L-glutamine, Fetal Bovine Serum (FBS), and Gentamicin/Amphotericin-B (GA). Cells were maintained at 37°C with 5% CO_2 in T175 flasks and upon reaching and 50–70% confluence, cells were detached using the ReagentPack subculture reagents (CC-5034, Lonza) which includes HEPES buffered saline for cell wash, Trypsin/EDTA and trypsin neutralizing solution for cell detachment. Cells viability was assessed by Trypan blue dye exclusion assay on TC20 automated cell counter (BIO-RAD). The viability was between 70 and 80% of total cells.

2.3.2 Differentiation of myoblast into myotubes and generation of the muscle cells in vitro model

To obtain myotubes, myoblasts were first detached as described in Paragraph 3.3.1. Subsequently, 0.1 x 10^6 cells per well were seeded into 24-well plates (Corning) pre-coated with Cultrex 3-D Culture Matrix. The coating process involved diluting Cultrex 3-D Culture Matrix (cat. 3533-010-02, R&D System) at a 1:100 ratio in SkGM medium, incubating 1 hour at RT. Cells were initially incubated for 24 hours at 37°C with 5% CO2. Following this initial incubation, they were cultured for an additional 5 days under the same conditions using differentiation medium, composed of

DMEM F12 Glutamax (cat. 31331-028) supplemented with 2% horse serum (HS, cat. 26050070, Gibco Life Sciences). The medium was refreshed every two days. (cat. 3533-010-02, R&D System). After 5 days, differentiated myotubes, refreshed in 150 ul of RPMI per well, were stimulated with 50 µl per well of complete RPMI supplemented with 50 µl of: Shig 4vForm + Alum, Shig 4vForm, Ng GMMA + alum, Ng GMMA, alum, S. *sonnei* GMMA concentrated 5X (final concentration 0,1 µg/ml). Subsequently, 1x 10^6 thawed hPBMCs were added in 50 µl per well to a final volume of 250 µl per well. The Myotube and PBMCs cultures were also stimulated with the same stimuli. For all 3 conditions, complete medium RPMI was used as negative control (MED). Myotubes, PBMCs and the Myotubes/PBMCs co-culture were incubated overnight (O/N) at 37°C, 5% CO2 and at the end of incubation, SN were collected and stored at -80°C for further Luminex and O-link analysis, while cells were analysed by flow cytometry to evaluate cellular activation.

2.4 Optimization of an *in vitro* model for polarizing naïve CD4+ T Helper (Th) cells

2.4.1 Isolation of Naïve CD4 T helper (Th) cell

Naïve CD4 T helper (Th) cell subsets were isolated from frozen hPBMCs from healthy donors using EasySep Human Naïve CD4+ T Cell Isolation Kit II (cat.17555, STEMCELL). This kit facilitates immunomagnetic negative isolation, ensuring the collection of untouched naïve CD4+ Th cells. The isolation process was conducted in accordance with the manufacturer's protocol. The isolation yield was assessed via flow cytometry by

comparing the percentage of naïve CD4+ Th cells present in samples before and after isolation as shown in **Figure 7**.

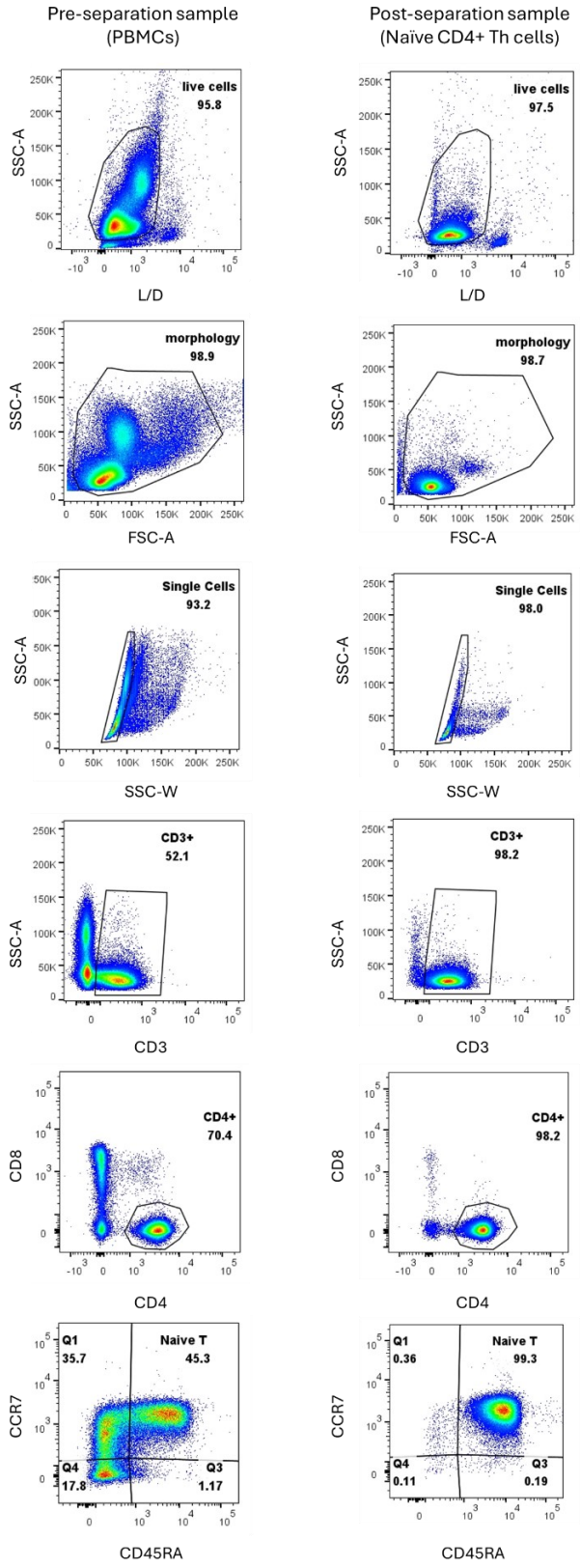

Figure 7. **Representative gating strategy for Naïve T helper cell isolation check.**

2.4.2 In vitro polarization of naïve CD4+ T cells

Following isolation, 0.1 × 10^6 naïve $CD4^+$ Th cells per well were seeded into a flat-bottomed 96-well plate (Corning) in complete medium (100 µl). To induce Th cell activation, polarization, and expansion, Dynabeads Human T-Activator CD3/CD28 (bead-to-cell ratio of 1:1, cat. 11132D, Invitrogen) were added to the culture. A schematic workflow outlining the *in vitro* polarization process of naïve $CD4^+$ Th cells is shown in **Figure 8**.

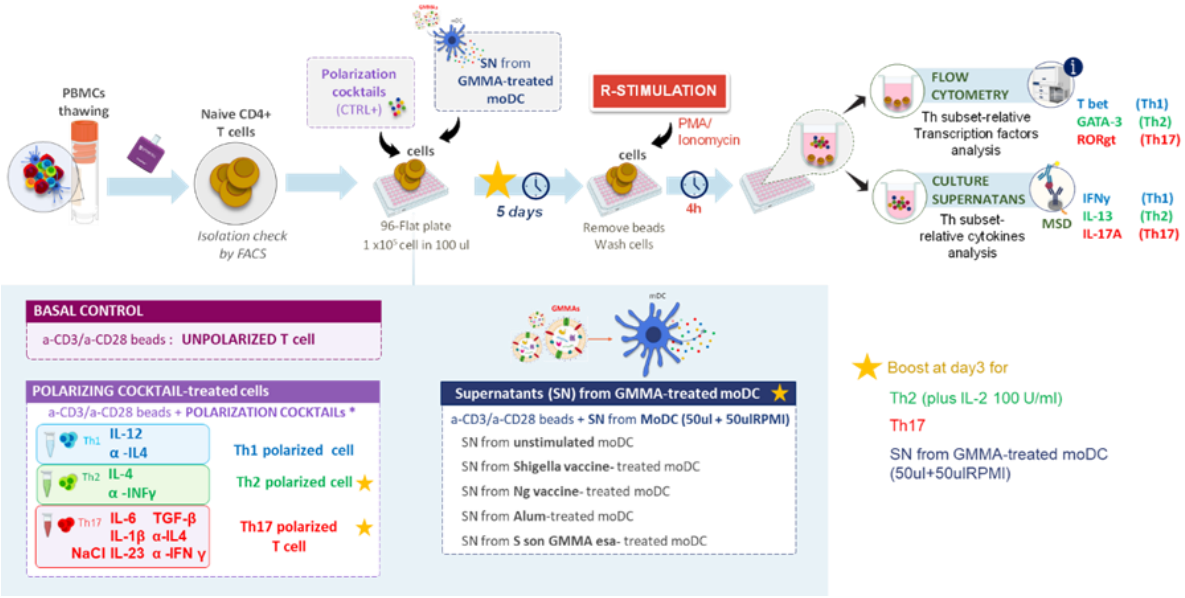

Figure 8. **Schematic workflow for the Naïve CD4+ Th polarization *in vitro* model.**

Th1, Th17 and Th2 polarization cocktails were used as positive control of the naïve CD4+ Th cells *in vitro* polarization system. The final concentrations of polarizing cytokines and neutralizing antibodies for each Th subsets are detailed in the **Table 1:**

Table 1. Polarization cocktails for naïve T cell polarization towards Th1, Th2 and Th17 cell subsets.

Th subset	**Polarization cocktail**
Th1	• rIL-12 → 2 ng/ml (Peprotech) • mAb anti-IL-4 → 5 µg/ml (R&D System)
Th2	• rIL-4 →2,5 ng/ml (Peprotech) • mAb anti-IFNγ → 5 µg/ml (R&D System)
Th17	• rIL-6 →10 ng/ml (Peprotech) • rIL-23 → 20 ng/ml (Peprotech) • rIL-1β → 10 ng/ml (Peprotech) • rTGF-β → 5 ng/ml (Myltenyi) • anti-IL-4→ 5 ng/ml (Myltenyi) • anti-IFNγ → 5 ng/ml (Myltenyi) • NaCl → 40 mM (cat. S9888-25G, Sigma-Aldrich). The addition of NaCl has been shown to markedly induce the naïve CD4+ Th cell polarization into Th17 cell subsets (148).

In parallel to the positive control, to evaluate the polarization potential of GMMA-based vaccines, naïve CD4+ Th cells were stimulated with 100 µl of undiluted supernatants (SN) derived from Mo-DC stimulated with Shig 4vForm + Alum, Ng GMMA + Alum, Alum, S. *sonnei* GMMA esa (positive control), complete medium RPMI (MED) as negative control. After three

days of incubation at 37°C with 5% CO_2, Th2, Th17, and SN-stimulated cells were boosted as outlined in **Table 2**:

Table 2. Boosting cocktails for Th cell subsets.

Stimulation condition	**Boost**
Th1	• Complete medium
Th2	• rIL-4 →12,5 ng/ml (Peprotech) • mAb anti-IFNγ → 25 µg/ml (R&D System • rIL-2 →100 U/ml (R&D System)
Th17	• rIL-6 →50 ng/ml (Peprotech) • rIL-23 → 100 ng/ml (Peprotech) • rIL-1β → 50 ng/ml (Peprotech) • rTGF-β → 25 ng/ml (Myltenyi) • anti-IL-4→ 25 ng/ml (R&D System) • anti-IFNγ → 25 ng/ml (R&D System)
SN-treated T cells	• Culture supernatants for each stimulus → 50 µl • Complet medium → 50 µl

Cells were then incubated for additional two days at 37°C, 5% CO_2. Following incubation, cells were restimulated with 200 µl per well of RPMI supplemented with PMA (10 ng/ml) and Ionomycin (1mM) (Sigma Aldrich) for 4 hours. At the end of the incubation, SN were transferred in round-bottomed 96 well plates and stored at -80°C for a further cytokine analysis;

cells were stained to for transcription factors upregulation by flow cytometry.

2.4.3 CD4+ T helper (Th) subsets characterization

Phenotypic characterization of naïve $CD4^+$ T cell samples (pre- and post-isolation) as well as stimulated polarized naïve $CD4^+$ T cells was performed using surface and intracellular staining of transcription factor. In particular, cells were washed twice with PBS and then stained with Fixable Viability Stain 440UV for 20 minutes in the dark and washed twice with PBS. Next, cells were incubated with 2% rabbit serum in PBS for 20 minutes at RT to block nonspecific binding of the antibodies. Cells were stained for surface markers with anti-CD45RA (BUV563), anti-CCR7 (BV711) for 20 min at RT. Next, cells were washed twice with PBS and permeabilized with Fixation/Permeabilization Concentrate (cat. 00-5123-43) diluted 1:4 in Fixation/Perm diluent (cat. 00-5223-56) (eBiosciences) at RT for 30 minutes. After two washes with Permeabilization Buffer (PermBuffer) (cat. 00-8333-56, eBiosciences), cells were stained with 2% rabbit serum in PermBuffer for 20 minutes at RT to avoid the intracellular a-specific binding of antibodies and then, stained with anti-CD3 (APC-H7), anti-CD4 (BUV395), anti-CD8 (BV605), anti-Tbet (R718), anti-GATA3 (BV421), anti-RORgt (PE-CSF594). For each stimulated sample, a control population was stained with related isotype antibodies for transcription factors (BV421-conjugated and R718-conjugated mouse IgG 1K monoclonal isotype standards, PE-CSF594-conjugated mouse IgG2b monoclonal isotype standard (BD Biosciences). After an incubation of 20 min at RT, cells were washed firstly in PermBuffer and secondly in PBS. Finally, cells were resuspended to 150 ul of PBS and were acquired at BD

FACSymphony A3. Raw data were processed by FlowJo10 Software (Becton, Dickinson and Company).

2.4.4 Gating strategy for CD4+ T helper (Th) subsets characterization

The flow cytometry gating strategy applied is shown in **Figure 9**. The analysis of Th cell from a healthy donor stimulated for 5 days with the Th1 polarizing cocktail is shown as an example. (**Panel A**) Live cells (gated region) are discriminated from dead cells by Live/Dead staining. Then the leukocytes cells were selected using forward scatter (FSC) and side scatter (SSC) and single cells (gated region) are distinguished from aggregates based on their width (side scatter area, SSC-A, versus side scatter width SSC-W). (**Panel B**) On single cell population, the up-regulation of the transcription factors (TFs) T-bet, GATA-3 and RORgt was evaluated to assess the polarizing process compared to the TFs expression of unpolarized Th cell (control). The TFs positive population gate is defined on the base of Isotype control for each TFs.

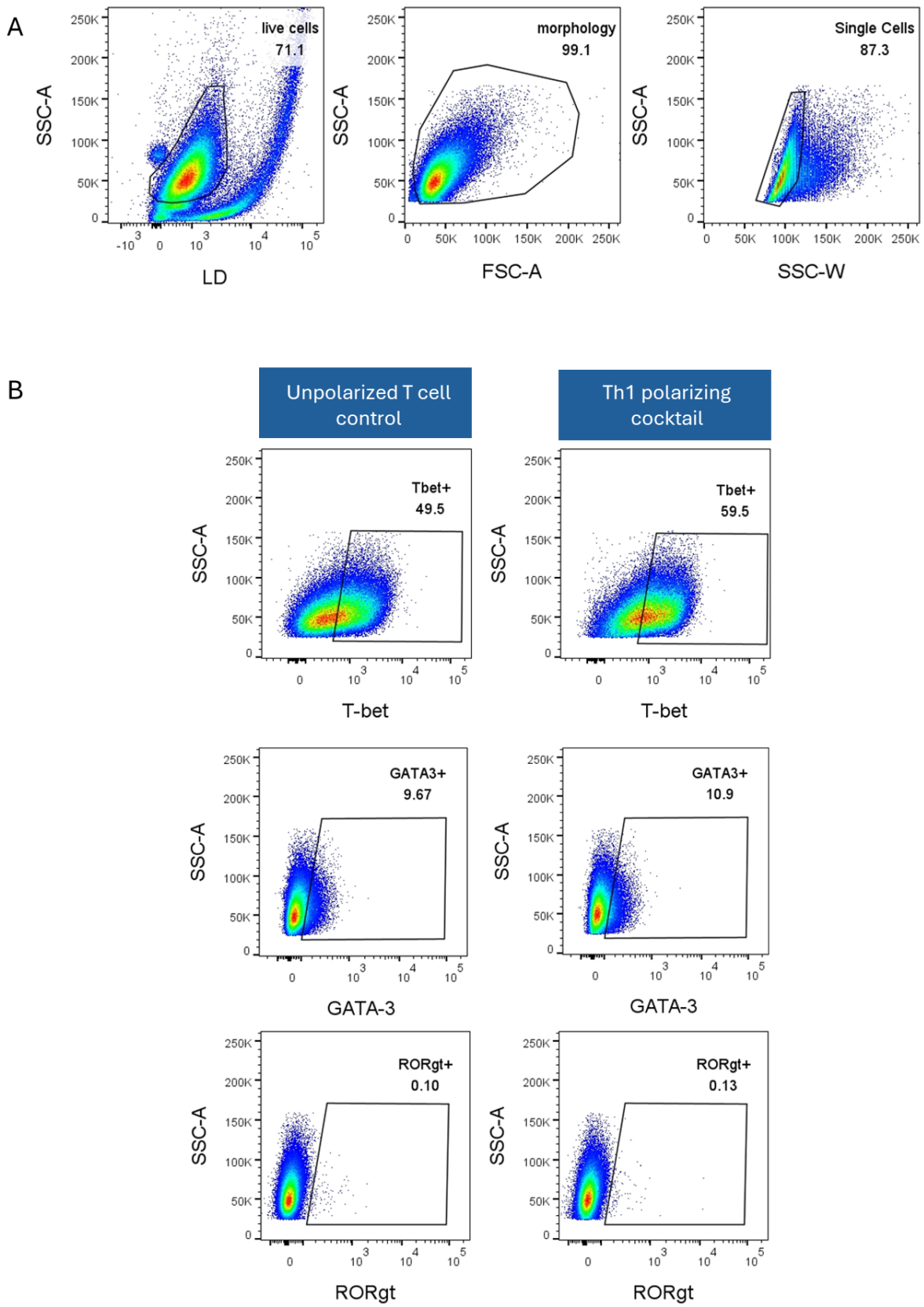

Figure 9**. Representative gating strategy used to define CD4$^+$ T helper cell polarization based on transcription factor expression**. Gates for each transcription factor were set according to isotype controls.

2.5 Cytokine and chemokine quantification

Cytokines profiles were defined analyzing culture supernatants (SN) by different technologies: Mesoscale, Luminex and O-link.

2.5.1 Mesoscale Technology for cytokine detection

Cytokine and chemokine levels in 4h-treated PBMCs, 48h-treated MoDC and 6days-stimulated naïve CD4+ T cells culture supernatants (SN) were assessed using different kits (Mesoscale technology):

- U-PLEX Custom Biomarker (hu) Assay containing 10 analytes: IFN-γ, IL-10, IL-12p40, IL-1α, IL-1β, IP-10, MCP-1, MIP-1α, MIP-1β, TNF-α
- V-PLEX Human 30-Plex Kit containing 29 analytes : IFN-γ, IL-10, IL-12p70, IL-13, IL-1β, IL-2, IL-4, IL-8, TNF-α, Eotaxin, Eotaxin-3, IP-10, MCP-1, MCP-4, MDC, MIP-1α, MIP-1β, TARC, GM-CSF, IL-12p40, IL-15, IL-16, IL-17A, IL-1α, IL-5, IL-7, TNF-β, VEGF
- U-PLEX Custom Biomarker (hu) Assay containing 20 analytes : GM-CSF, IL-13, IL-18, IL-2, IL-21, IL-22, IL-29, MIP-1α, MIP-1β, TNF-α, IFN-α2a, IFN-β, IFN-γ, IL-10, IL-12p70, IL-17A, IL-1β, IL-6, IL-8, IP-10

Cytokine and chemokine quantification assays were performed in accordance with the manufacturer's instructions. Mesoscale Technology combines electrochemiluminescence and multi-array technology. The multi-array MSD plates' wells have ten independent spots coated with capture antibodies which bind specific analytes. The detection is done using the electro-chemiluminescent label SULFO TAG conjugated to detect antibodies which bind analytes, giving a sandwich immunoassay. The MSD instrument applies electricity to the plate electrodes with a subsequent SULFO TAG labels light emission which is measured to quantify analytes in the sample. MSD plates were read using MESO

QuickPlex SQ 120 and analyzed with the DISCOVERY WORKBENCH software. Cytokine and chemokine concentrations were expressed as pg/mL and were calculated based on the standard curve provided by the kits. All values within the detection range were accepted and considered as such. Values above the detection range were replaced with twice the upper limit of detection (2X ULOD); values below the detection range were replaced with half of the lower limit of detection (1/2 LLOD). GraphPad Prism v10 (GraphPad Software, San Diego, California USA, www.graphpad.com) was used to generate boxplots and linear graph to define an immune profiling.

2.5.2 Luminex technology

Cytokine and chemokine levels in the culture SN collected after the stimulation of myoblasts, myotubes, PBMCs, and the myotube/PBMC co-culture system were quantified using a Luminex assay.

The Luminex assay is a sandwich immunoassay designed for the precise quantification of multiple analytes within a single sample. Utilizing bead-based technology, the assay enables multiplex detection of up to 500 analytes simultaneously. The system employs color-coded microspheres, internally dyed with varying proportions of red and infrared fluorophores, each corresponding to a unique spectral signature or bead region. Antibodies specific to the target analytes are conjugated to distinct bead regions and incubated with the sample. Following the removal of unbound materials through washing, the beads are incubated with biotinylated detection antibodies and a streptavidin-phycoerythrin (PE) reporter molecule. The Luminex instrument uses one laser to excite the beads, identifying the bead region and its associated analyte, while a second

laser measures the PE-derived fluorescence signal, which is proportional to the concentration of the bound analyte. Multiple readings are taken for each bead region, ensuring reliable and robust detection.

The analysis was performed with the Custom Human ProcartaPlex Mix&Match 21-plex kit (Thermo Fisher Scientific), which enabled the simultaneous detection of multiple analytes, including IFN-α, IFN-γ, IL-10, IL-12p70, IL-17A, IL-2, IP-10, GM-CSF, IL-1α, IL-13, IL-18, IL-21, IL-22, IL-4, MCP-1, MIP-1α, VEGF-A, IL-6, IL-8, IL-1β, and TNF-α. Specifically, the quantification of IL-6 and IL-8 in SN collected from 4-hour stimulated hPBMCs was performed after diluting the SN 1:10 in complete medium. In contrast, for all other cytokines, the supernatants were analysed without dilution. Assay was performed in accordance with the manufacturer's instructions. Luminex plates were read using Luminex TM 200TM and analysed with the Bio-Plex Manager 6.1 software. Cytokine and chemokine concentrations were expressed as pg/mL and were calculated based on the standard curve. All values within the detection range were accepted and considered as such. Values above the detection range were replaced with twice the upper limit of detection (2X ULOD); values below the detection range were replaced with half of the lower limit of detection (1/2 LLOD). GraphPad Prism v10 (GraphPad Software, San Diego, California USA, www.graphpad.com) was used to generate boxplots and linear graph to define an immune profiling.

2.5.3 O-link technology

The levels of cytokines and chemokines in the culture supernatants, collected following *in vitro* stimulation with GMMA-based vaccines, were quantified using O-link technology, Inflammation kit (92 analytes).

Specifically, as detailed in paragraph 3.3.2, supernatants were harvested following an O/N stimulation in cultures consisting of muscle cells alone, human peripheral blood mononuclear cells (hPBMCs) alone, and co-cultures of muscle cells and hPBMCs. O-link technology is based on the Proximity Extension Assay (PEA) technology that combines antibody-based immunoassay with the powerful properties of polymerase chain reaction (PCR). Indeed, 92 capture antibody pairs which are labelled with 92 unique oligonucleotides, can bind the target protein (immunoassay step). The specific target protein binding allows the DNA oligos hybridization and subsequently their extension by proximity-dependent DNA polymerization event resulting in a DNA barcode for each target protein (Extension step). Then, DNA barcodes are amplified and detected using real-time PCR by O-link Signature Q100. O-link provides internal and external controls for data normalization and quality control of both each step of the assay and individual samples. Internal controls are included in each sample and consist of two Immunoassay controls, an Extension control and a Detection control. The immunoassay controls are two non-human antigens (phycoerythrin (PE) and green fluorescent protein (GFP) with matching antibodies/assays and monitor all steps of Olink assay. Extension control is an antibody linked to two matched oligonucleotides; it is important for monitoring the extension and readout steps independently of antigen binding and it is used for data normalization across samples. Lastly, the Detection control is a synthetic double-stranded template and checks the readout step. Sample for which any of these controls are not in a pre-determined range will be flagged and are not considered in statistical analysis. The external controls comprise the Inter-plate control (IPC) that is use for a second normalization step

between different acquisition plates; the negative control consisting in the running buffer to monitor the background noise and it is used to calculate the limit of detection; the positive control that consists of a pool of plasma samples, useful to assess the variation within plate. Data analysis is performed starting from a pre-processing normalization. For each sample and data point the related Cq-value (cycle threshold) for the Extension control is subtracted, normalizing samples for technical variation within a run. Next, these values are adjusted based on an Olink-defined correction factor. The normalization process gives values in the Normalized Protein Expression (NPX) unit that is expressed on a log2 scale where higher numbers indicate huge level of proteins, with the background around zero.

2.6 Analysis of GMMA localization in Mo-DCs and Myotubes by microscopy

To visualize the localization and the interaction of GMMA with different cell subsets, specifically iMo-DCs and Myotubes, we employed live imaging using OPERA Phenix system. For iMo-DCs, live imaging was conducted O/N, while myotubes underwent staining following an O/N incubation.

iMo-DC at a concentration of 0.1 x 10^6 cells/well, differentiated as described in paragraph 3.2-1, were seeded into flat-bottomed 96-well polylysine-coated plates (cat. 655090, Greiner bio-one). The cells were then stimulated with 5 µg/ml of pHrodo-conjugated Shigella *flexneri* 2a GMMA (pHrodo-S. flex 2a GMMA). Plates were immediately loaded onto the OPERA Phenix instrument (PerkinElmer) for O/N acquisition using live imaging. pHrodo Red is pH-sensitive dye that allows to evaluate the phagocytosis ability of cells. Indeed, it becomes fluorescent only inside the cells, specifically in phagosomes where the pH is lower than that observed outside the cell.

In the case of muscle cells, myoblast differentiation into myotubes was carried out as described in paragraph 3.3.2 but using Cell Imaging 24-well plates (cat. 0030741021, Eppendorf), which are suitable for acquisition with the OPERA Phenix instrument.

On day 5, myotubes were stimulated with 5 µg/ml Alex488 dye-conjugated S. flex 2a GMMA (A488- S. flex 2a GMMA). Following an O/N incubation at 37°C 5% CO_2, cells were fixed with 4% Formaldehyde for 30 minutes at RT. Then, cells were washed once with PBS and incubated with rabbit anti-GMMA S. flex 2a polyclonal antibody diluted 1:1000 in 1% BSA for 1 hour at RT. Thereafter, cells were washed twice with PBS and incubated 30 minutes at RT in the dark with a mix of: secondary antibody Alexa Fluor 568 goat anti-rabbit IgG (Invitrogen, cat n° A11011), DAPI (Thermo Scientific, cat. 62248) and Cell Mask Deep Red Plasma Membrane (Invitrogen, cat. C10046) diluted 1:1000 in 1% BSA. Then, cells were washed twice with PBS and resuspended in a final volume of 200 µl of PBS. Cells were then acquired on Opera Phenix instrument.

2.7 Statistical analysis

RM One-way ANOVA parametric test was used to compare results obtained from stimulated and unstimulated (control) samples as well as those derived from different stimuli in the experiments on hPBMCs and Mo-DC immune characterization and on *in vitro* T cell polarization. Specifically, Holm-Šídák's and Tukey's multiple comparisons tests were used to compare cytokine production among different experimental conditions.

3. RESULTS

3.1 Unveiling the immune signature induced by GMMA-based vaccines in human PBMCs and Mo-DCs

3.1.1 Individual Shigella vaccine components and their combination induced a similar response in both hPBMCs and Mo-DCs

The next generation *Shigella* GMMA-based vaccine comprises four different *Shigella* GMMA: S. *sonnei* 2929-GMMA penta derived from a mutated *Shigella sonnei* strain, and S. *flexneri* 1b GMMA, S. *flexneri* 2a GMMA and S. *flexneri* 3a GMMA derived from S. *flexneri* 1b, 2a, 3a respectively, all having the same mutations, which confer higher blebbing (ΔtolR) and reduced endotoxicity (ΔmsbB). In this vaccine formulation, called Shig 4vForm + Alum, the four different *Shigella* GMMA are adsorbed on Alum hydroxide or Alhydrogel (AH) to retain GMMA at the site of injection decreasing systemic dissemination (78, 79). As described by Tondi et al. (67) the response of immune cells following the treatment with S. *sonnei* 1790-GMMA penta was previously characterized by integrating data obtained from cytokine production and expression of cellular activation markers in hPBMCs (67). In this study, I therefore investigated whether the immune cell response elicited by the four-component combination of GMMA variants (Shig 4vForm) differs from that induced by the individual vaccine components, namely S. son 2929-GMMA penta, S. flex 1b GMMA, S. flex 2a GMMA, and S. flex 3a GMMA. To this end, hPBMCs and monocyte-derived dendritic cells (Mo-DCs) were stimulated *in vitro* for 4 hours with 1 µg/ml of both individual GMMA components and their combination; following stimulation, the quantification of cytokines secreted in supernatants was evaluated, alongside the cellular activation by flow cytometry. In hPBMCs samples, results showed that each *Shigella*

species (spp.) GMMA and their combination, Shig 4vForm, induced comparable levels of pro-inflammatory cytokines, including IL-1α, IL-1β, TNF-α, IL-6, IL-8, alongside chemokines such as MCP-1 and MIP-1α, and the anti-inflammatory cytokine IL-10. Additionally, IFN-γ, MIP-1β and IL-12 are also similarly produced but in lower concentrations, while IP-10 is not produced either by individual GMMA components or their combination. Moreover, applying a flow cytometry gating strategy on the heterogeneous hPBMCs population, several cellular subsets were identified and for each cell subset population, the up-regulation of population-specific markers was evaluated. Cellular activation results showed that both individual components and the four-component formulation led to the upregulation of CD83, an activation marker of monocytes and myeloid dendritic cells (mDCs) as well as of CD83 and CD86, which are usually upregulated on activated plasmacytoid dendritic cells (pDCs). Furthermore, both single GMMA components and their four-valent formulation similarly induced a modest activation of natural killer (NK) cell subsets (NK dim and NK bright) and CD4+ T cells, assessed by measuring up-regulation of CD69 (**Figure 10**). Notably, the activation of NK and T cells could be the result of a bystander effect due to the nearby activated cells rather than a direct activation by GMMA. Thus, both the individual components and their combination activated different cell subpopulations of hPBMCs, triggering the production of pro-inflammatory cytokines and chemokines, without notable differences in the response magnitude.

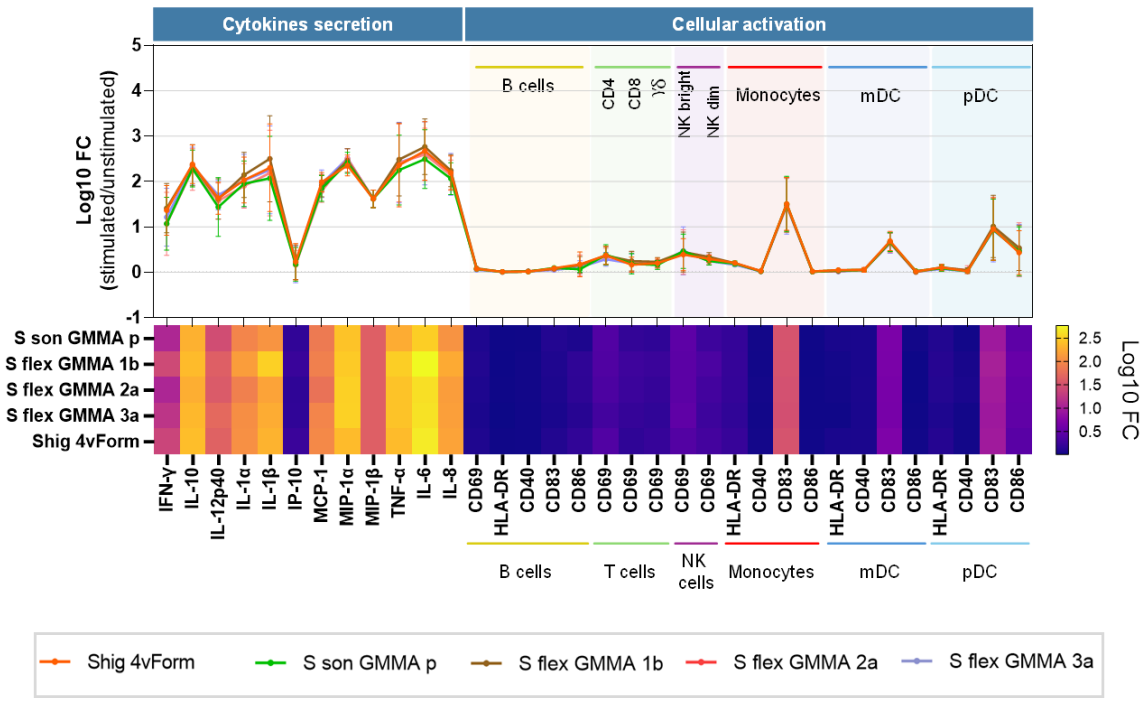

Figure 10. **Cytokine secretion and cellular activation profiles in hPBMCs stimulated with four-component GMMA formulation (Shig 4vForm) and its individual components (S. son 2929-GMMA penta, S. flex 1b GMMA, S. flex 2a GMMA and S. flex 3a GMMA).** hPBMCs of eight healthy donors were stimulated *in vitro* for 4 hours with 1 µg/ml of the following GMMA formulations: S. sonnei GMMA penta, S. flexneri GMMA 1b, 2a, 3a, and the combined four-component formulation (Shig 4vForm). Results are expressed as the Log10 of the average fold change (Log10 FC) across the eight donors, relative to unstimulated controls incubated for 4h with medium. The upper panel displays line graphs representing the average Log10 FC ± standard deviation for each formulation: S. sonnei GMMA penta (green line), S. flexneri GMMA 1b (brown line), 2a (pink line), 3a (light cyan line), and the Shig 4vForm (orange line). The lower panel presents a heatmap of the average Fold change values (Log10 FC) (relative to unstimulated controls incubated for 4 hours with medium) for the same cytokines and formulations, with colour intensity ranging from dark purple to bright yellow, indicating the magnitude of the immune response.

I then investigated whether the results observed in the total hPBMCs population were also confirmed in the individual antigen presenting cell (APCs) subpopulation. To this end, the Mo-DCs model was used as a simplified *in vitro* system to evaluate the direct effect of Shig 4vForm on

this cell population which I previously identified as one of the two main Antigen Presenting Cells (APCs) subpopulations, along with monocytes, directly targeted by 1790-GMMA (67). Quantification of an extensive panel of pro-inflammatory cytokines and chemokines compared with that used to assess hPBMCs response to GMMA, along with the upregulation of Mo-DCs-specific activation markers, revealed a comparable immune profile in Mo-DCs treated with the individual components and their four-valent combination (**Figure 11**). Indeed, all single GMMA components as well as their combination induced comparable levels of IFN-γ, IL-1α, IL-1β, IL-12p40, IL-8, IL-6, TNF-α, IL-10 and chemokines like MIP-1α and MIP-1β and IP-10. Moreover, for both individual components and their combination, a comparable slight secretion of MCP-1, IL-13, IL-15, IL-17A, IL-12p70, IL-5, IL-7, IL-2, Eotaxin and TGF-β was also observed; VEGF appeared to be higher induced upon stimulation with the four-valent combination compared to single components, but is not statistically relevant, owing to high variability between donors for that cytokine. MDC, MCP-4, TARC, Eotaxin-3, GM-CSF, IL-16, IL-4 were not produced either upon stimulation with single components or their combination. These cytokines and chemokines are involved in pro-inflammatory processes which can be triggered after vaccine injection and thus, providing an insight of the activation of APCs. Furthermore, flow cytometry analysis revealed that both single components and their combination induced a comparable up regulation of HLA-DR, and co-stimulatory molecules CD40 and CD86 on Mo-DCs, demonstrating that both stimulations induced the maturation and activation of Mo-DCs.

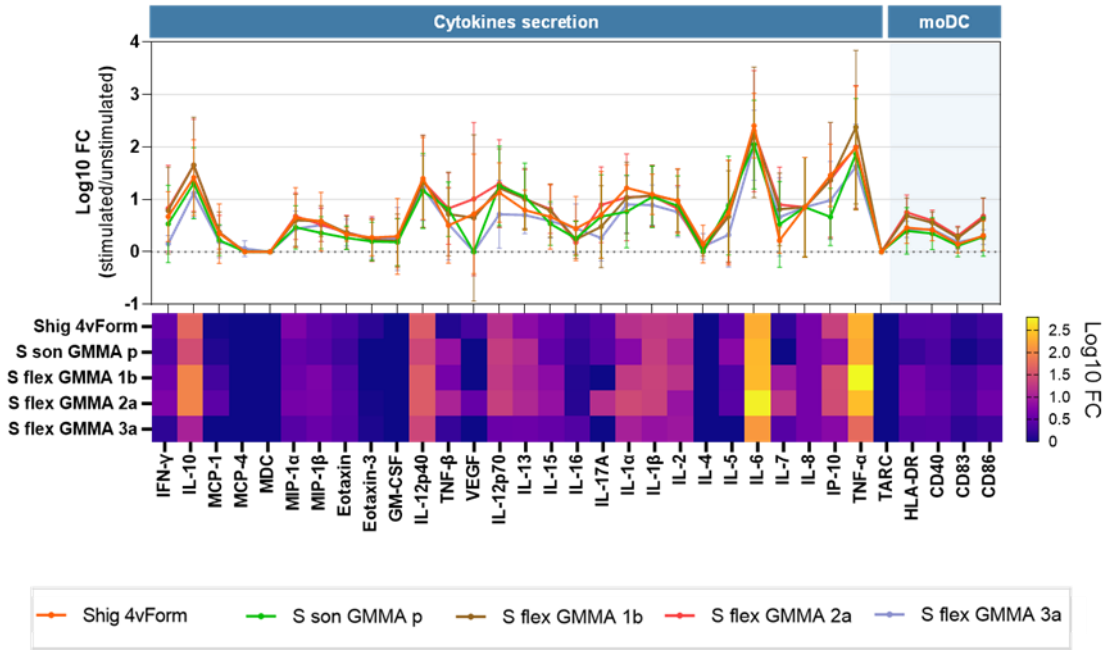

Figure 11. **Cytokine secretion and cellular activation profiles in monocyte-derived dendritic cells (Mo-DCs) stimulated with four-component GMMA formulation (Shig 4vForm) and its individual components (S. son 2929-GMMA penta, S. flex 1b GMMA, S. flex 2a GMMA and S. flex 3a GMMA).** Mo-DCs were first differentiated *in vitro* from monocytes isolated from hPBMCs of six healthy donors and subsequently stimulated for 48 hours with 1 ug/ml of the following GMMA formulations: S. sonnei GMMA penta, S. flexneri GMMA 1b, 2a, 3a, and the combined four-component formulation (Shig 4vForm). Results are expressed as the Log10 of the average fold change (Log10 FC) across the five donors, relative to unstimulated controls incubated for 4h with medium. The upper panel displays line graphs representing the average Log10 FC ± standard deviation for each formulation: S. *sonnei* GMMA penta (green line), S. *flexneri* GMMA 1b (brown line), 2a (pink line), 3a (light cyan line), and the Shig 4vForm (orange line). The lower panel presents a heatmap of the average Fold change values (Log10 FC) (relative to unstimulated controls incubated for 4 hours with medium) for the same cytokines and formulations, with colour intensity ranging from dark purple to bright yellow, indicating the magnitude of the immune response.

Collectively, these findings demonstrated that both the individual components and their four-valent combination in the vaccine Shig 4vForm, elicited a similar innate immune cell activation defined by both the production of mainly pro-inflammatory cytokine and chemokines, in

both hPBMCs and Mo-DCs, alongside hPBMCs activation and Mo-DCs maturation/activation.

3.1.2 Alum has an impact on the cytokine and cellular immune activation induced by Shigella GMMA-based vaccine in both hPBMCs and Mo-DCs

To understand whether the impact of Alum on the in vitro immune response induced by the Shigella GMMA-based vaccine, I compared Alum-adjuvanted *Shigella* GMMA vaccine formulation with the non-adjuvanted formulation. Using the experimental setting described in paragraph 4.1.1. I found that both the Alum-adjuvanted *Shigella* four-valent formulation (Shig 4vForm + Alum) and the non-adjuvanted *Shigella* four-valent formulation (Shig 4vForm) elicited comparable responses in hPBMCs and Mo-DCs, characterized by the secretion of the same set of pro-inflammatory cytokines and chemokines, like IFN-γ, IL-1α, IL-1β, TNF-α, IL-6, IL-8, MIP-1α, MIP-1β, MCP-1, as well as the anti-inflammatory cytokine IL-10 (**Figure 12 A-B**). Notably, the chemokine IP-10 was exclusively secreted from Mo-DCs upon both stimulations. The analysis on Mo-DCs revealed additional cytokines such as IL-13, IL-15, IL-17A, IL-12p70, IL-12p40, IL-5, IL-7, IL-2, Eotaxin, TGF-β and VEGF (**Figure 12B**). Accordingly, both Alum-adjuvanted and non-adjuvanted *Shigella* four-valent formulations induced comparable activation of monocytes and mDCs, assessed by the CD83 up-regulation, and pDCs activation through CD83 and CD86 up-regulation. Moreover, no differences in the activation of NK dim and CD4+ T cells were observed under these conditions (**Figure 12A**). Remarkedly, in addition to inducing cytokine secretion, the two formulations promote the maturation of Mo-DCs as shown by the up-regulation of HLA-DR, CD40, CD83 and CD86 (**Figure 12B**).

Notwithstanding Shig 4vForm, in presence or in absence of alum, induced a qualitatively similar response in both hPBMCs and Mo-DCs *in vitro*, comparison of the magnitude revealed that alum enhanced both the upregulation of activation markers and cytokines secretion in these cell types. This effect was higher in the Mo-DCs *in vitro* model compared to hPBMCs *in vitro* system.

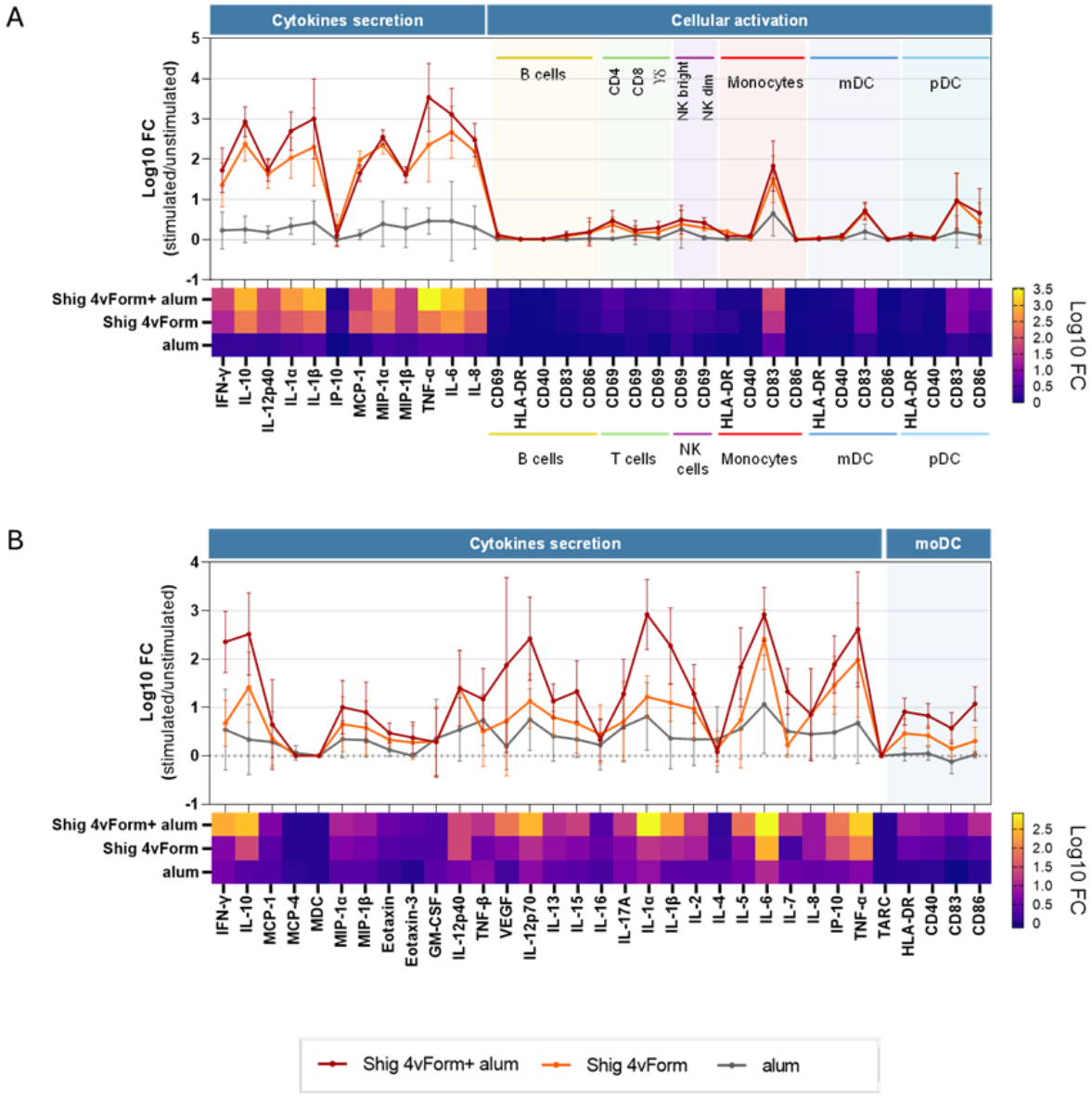

Figure 12. **Cytokine secretion and cellular activation profiles in hPBMCs and Mo-DCs stimulated with four-component GMMA formulation (Shig 4vForm) with or without Alum.** hPBMCs from eight healthy donors (Panel A) and Mo-DCs differentiated *in vitro* from the

corresponding monocytes from six of the same donors (Panel B) were stimulated *in vitro* for 4 hours and 48 hours, respectively, with 1 µg/ml of a four-component GMMA formulation, either adjuvanted (Shig 4vForm + Alum), non-adjuvanted (Shig 4vForm), or with Alum alone. Cytokine quantification in supernatants (Mesoscale) and cell activation (FACS) results are expressed as the Log10 of the average fold change (Log10 FC) across the eight and six donors respectively, relative to unstimulated controls. Linear graphs show the average Log10 FC ± standard deviation for each formulation: Shig 4vForm + Alum (red line), Shig 4vForm (orange line), and Alum (grey line). Heatmaps display the average Log10 FC values for the same cytokines and formulations, with colour's intensity ranging from dark purple to bright yellow, indicating the magnitude of the immune response.

Specifically, following stimulation with alum-adjuvanted *Shigella* formulation, statistically significant increases were observed in IFN-γ, IL-10, IL-1α, IL-1β and TNF-α levels in both cell types, opposite to IL-6 which was significantly higher in hPBMCs. Additionally, IL-12p70, IL-13 and IL-15 levels increased in Mo-DCs (**Figure 13A-B**). Notably, IL-12p70 is a crucial cytokine for the polarization of naïve CD4+ T helper (Th) cell into Th1 cells, required to fight mainly intracellular pathogens (149). Therefore, its high secretion by Mo-DCs upon *Shigella* GMMA vaccine stimulation, suggests the *Shigella* GMMA vaccine potential in priming Mo-DCs to skew a Th1 cell response.

hPBMCs

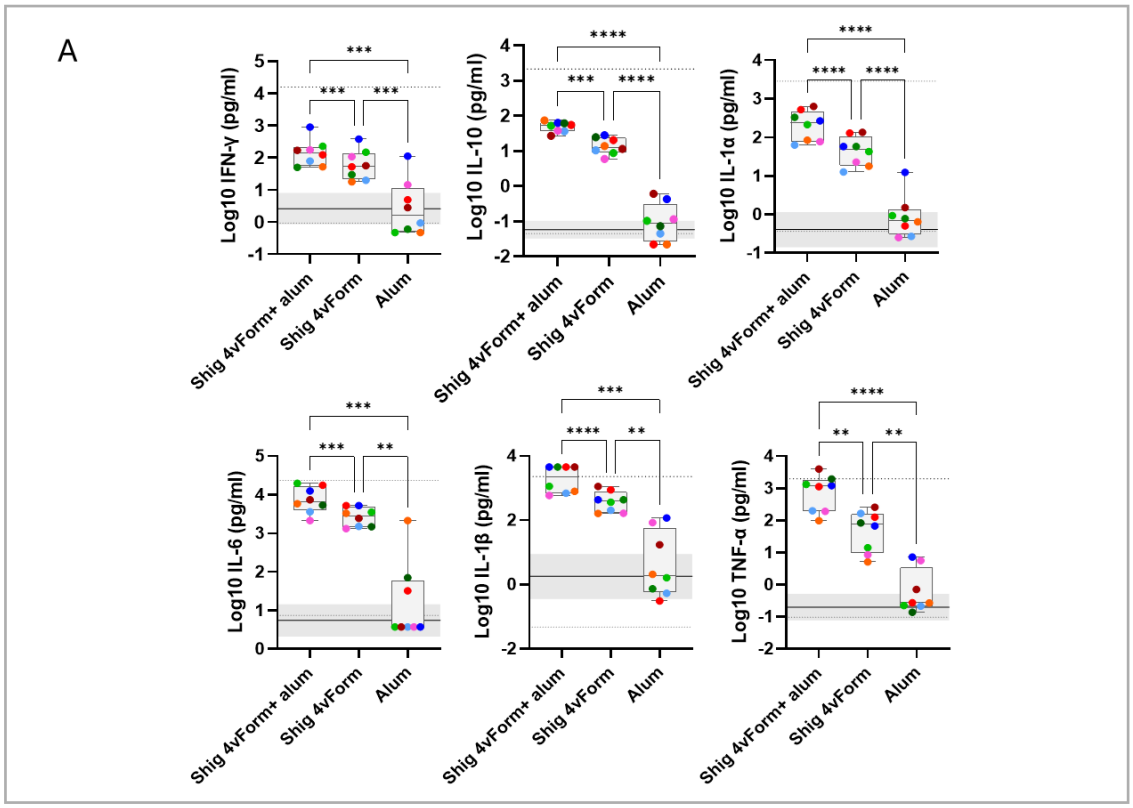
A
Log10 IFN-γ (pg/ml)
Log10 IL-10 (pg/ml)
Log10 IL-1α (pg/ml)
Log10 IL-6 (pg/ml)
Log10 IL-1β (pg/ml)
Log10 TNF-α (pg/ml)
Shig 4vForm+ alum
Shig 4vForm
Alum

Mo-DC

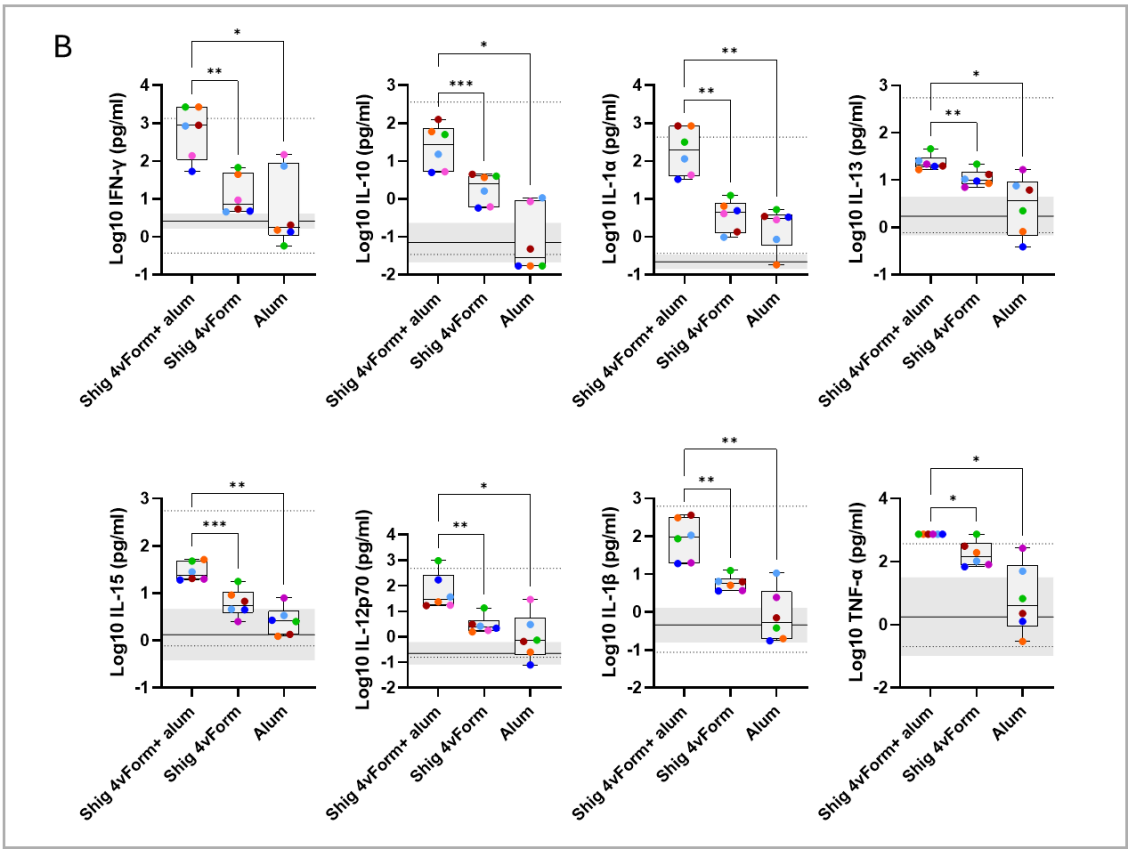
B
Log10 IFN-γ (pg/ml)
Log10 IL-10 (pg/ml)
Log10 IL-1α (pg/ml)
Log10 IL-13 (pg/ml)
Log10 IL-15 (pg/ml)
Log10 IL-12p70 (pg/ml)
Log10 IL-1β (pg/ml)
Log10 TNF-α (pg/ml)
Shig 4vForm+ alum
Shig 4vForm
Alum

Figure 13. **Cytokine quantification in culture supernatants collected *following in vitro* stimulation of hPBMCs and Mo-DCs with *Shigella* GMMA-based vaccine.** hPBMCs from eight healthy donors (Panel A) and Mo-DCs differentiated *in vitro* from the corresponding monocytes from six of the same donors (Panel B) were stimulated in vitro for 4 hours and 48 hours, respectively, with 1 µg/ml of a four-component GMMA formulation, either adjuvanted (Shig 4vForm + Alum), non-adjuvanted (Shig 4vForm), or with Alum alone. Cytokine concentrations in supernatants were measured using a 10-analyte U-PLEX assay (Panel A) and V-plex assay (Panel B). Box plots display log10-transformed cytokine values, representing the minimum, first quartile (25th percentile), median (50th percentile), third quartile (75th percentile), and maximum. Each coloured dot corresponds to an individual donor. Dotted black lines denote the Upper limit of detection (ULOD) and lower limit of detection (LLOD). Values above the detection range were replaced with twice the upper limit of detection (2X ULOD); values below the detection range were replaced with half of the lower limit of detection (1/2 LLOD). The unstimulated sample (MED) is reported as mean value (continued black line) with its confidence interval (CI) (grey area). Significances observed between groups were determined using the RM one-way ANOVA with Geisser-Greenhouse correction (*p-value < 0.05, **p-value<0.005, ***p-value<0.0005, ****p-value<0.00005; ns stands for nonsignificant and are not reported, p-value > 0.05).

Overall, the Alum-adjuvanted *Shigella* four-valent formulation induced a stronger immune response in terms of cytokine secretion as well as cellular activation compared to the non-adjuvanted formulation in the analysed *in vitro* systems. Interestingly, this effect was not attributable to Alum itself, as Alum alone did not elicit any significant cellular activation nor cytokine secretion suggesting that the response elicited could be related to a synergic effect with GMMA and/or the different size of the alum-adsorbed formulation.

3.1.3 Alum's impact on the cytokine and cellular immune activation induced by Neisseria gonorrhoeae (Ng) GMMA vaccine in both hPBMCs and Mo-DCs is similar to that observed upon Shigella GMMA vaccine stimulation

To determine whether the observed impact of Alum is specific to *Shigella* GMMA-based vaccine or applicable to the GMMA-platform, I compared in the same *in vitro* model the response elicited by a GMMA-based vaccine against *Neisseria gonorrhoeae* (Ng). The *N. gonorrhoeae* GMMA-based vaccine consists of Ng GMMA derived by the mutated *N. gonorrhoeae* strain FA1090 adsorbed on Alum hydroxide (Alhydrogel). As for *Shigella* GMMA-based vaccine, I compared Alum-adjuvanted Ng formulation (Ng GMMA + alum) and non-adjuvanted formulation (Ng GMMA). Using the same experimental setting (paragraph 4.1.1), data showed that, both formulations, with and without alum, induced a pro-inflammatory cytokine profile in both hPBMCs and Mo-DCs alongside the activation of monocytes, mDCs and pDCs cell subpopulations in hPBMCs samples and the maturation/activation of Mo-DCs. However, as with *Shigella* GMMA-based vaccines, the presence of alum induced a greater response in Ng GMMA-based vaccine compared to non-adjuvanted Ng GMMA, both in terms of cytokine secretion and cellular activation (**Figure 14A-B**) and, also in this case, the Alum's impact on the Ng GMMA vaccine-induced response is more evident in Mo-DCs *in vitro* model (**Figure 14B**).

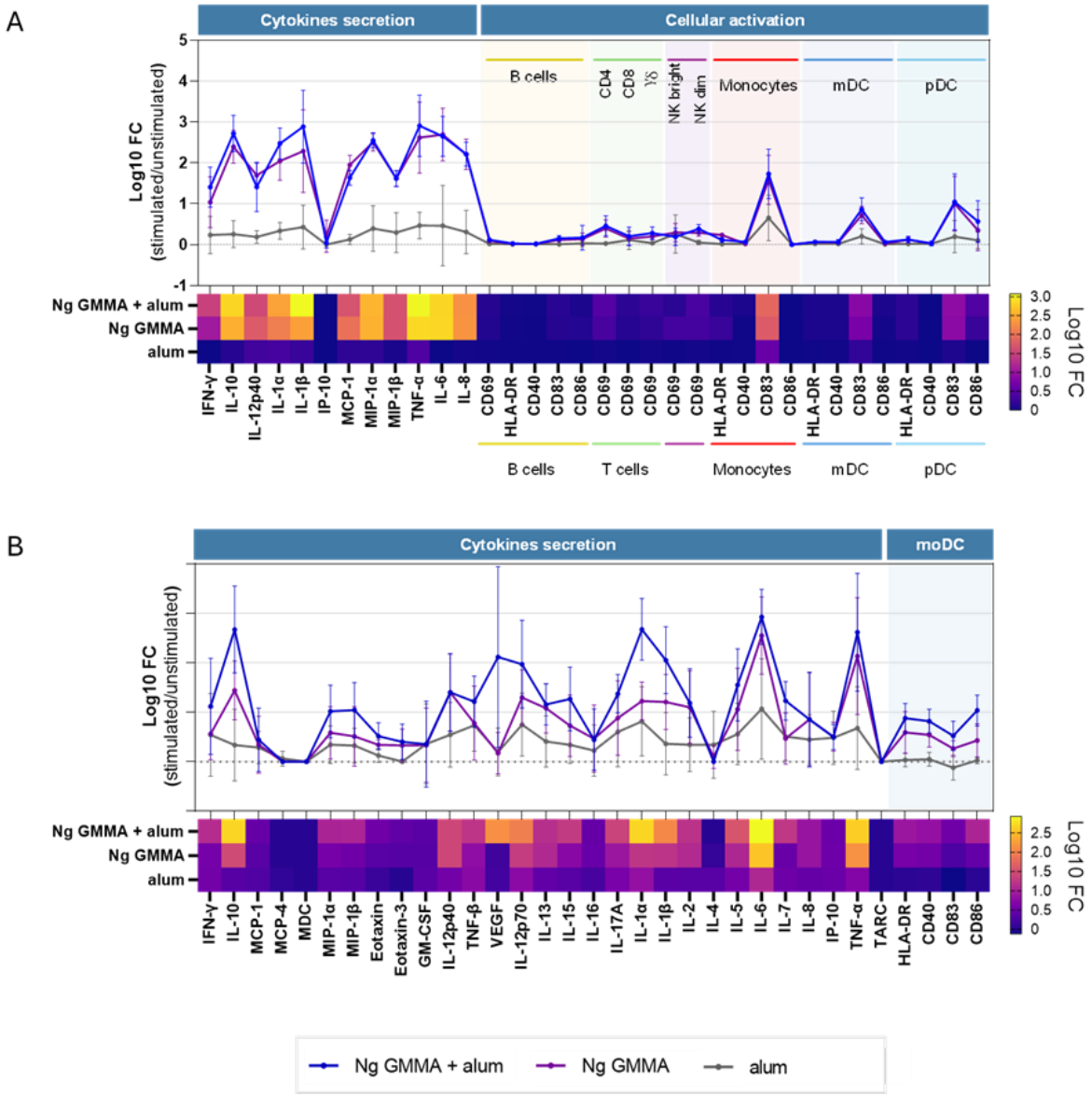

Figure 14. **Cytokine secretion and cellular activation profiles in hPBMCs and Mo-DCs stimulated with *N. gonorrhoeae* GMMA (Ng GMMA), with or without Alum.** hPBMCs from eight healthy donors (Panel A) and Mo-DCs differentiated *in vitro* from the corresponding monocytes from six of the same donors (Panel B) were stimulated *in vitro* for 4 hours and 48 hours, respectively, with 1 µg/ml of Ng GMMA formulation, either adjuvanted (Ng GMMA + Alum), non-adjuvanted (Ng GMMA), or with Alum alone. Cytokine quantification in supernatants (Mesoscale) and cell activation (FACS) results are expressed as the Log10 of the average fold change (Log10 FC) across the eight and six donors respectively, relative to unstimulated controls. Linear graphs show the average Log10 FC ± standard deviation for each formulation: Ng GMMA + Alum (blue line), Ng GMMA (purple line), and Alum (grey line). Heatmaps display the average Log10 FC values for the same cytokines and formulations, with

colour's intensity ranging from dark purple to bright yellow, indicating the magnitude of the immune response.

In this case too, although for a smaller number of cytokines such as IL-10, IL-1α and IL-1β levels, in both cell types, as well as IFNγ and TNF-α in hPBMCs and IL-15 and IL-12p70 in Mo-DCs, statistical differences were observed between the Alum-adjuvanted Ng GMMA (Ng GMMA + Alum) and non-adjuvanted Ng GMMA formulation (**Figure 15**).

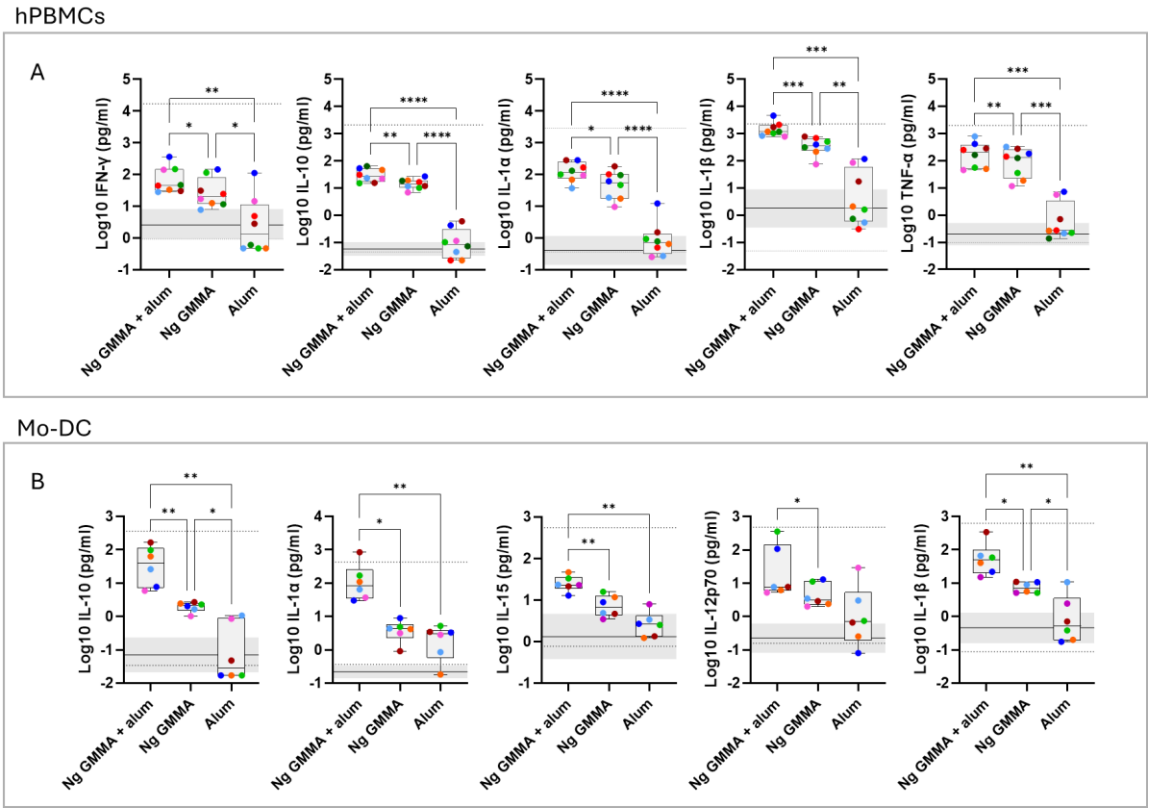

Figure 15. **Cytokine quantification in culture supernatants collected following *in vitro* stimulation of hPBMCs and Mo-DCs with Ng GMMA-based vaccine.** hPBMCs from eight healthy donors (Panel A) and Mo-DCs differentiated *in vitro* from the corresponding monocytes from six of the same donors (Panel B) were stimulated *in vitro* for 4 hours and 48 hours, respectively, with 1 µg/ml of a Ng GMMA formulation, either adjuvanted (Ng GMMA + Alum), non-adjuvanted (Ng GMMA), or with Alum alone. Cytokine concentrations in supernatants

were measured using a 10-analyte U-PLEX assay (Panel A) and V-plex assay (Panel B) Box plots display log10-transformed cytokine values, representing the minimum, first quartile (25th percentile), median (50th percentile), third quartile (75th percentile), and maximum. Each coloured dot corresponds to an individual donor. Dotted black lines denote the Upper limit of detection (ULOD) and lower limit of detection (LLOD). Values above the detection range, were replaced with twice the upper limit of detection (2X ULOD); values below the detection range, were replaced with half of the lower limit of detection (1/2 LLOD). The unstimulated sample (MED) is reported as mean value (continued black line) with its confidence interval (CI) (grey area). Significances observed between groups were determined using the RM one-way ANOVA with Geisser-Greenhouse correction (*p-value < 0.05, **p-value<0.005, ***p-value<0.0005, ****p-value<0.00005; ns stands for nonsignificant and are not reported, p-value > 0.05).

3.1.4 Shigella and Ng GMMA-based vaccines induced a similar immune profile, albeit differences in magnitude for certain cytokines

After evaluating the impact of Alum in the two vaccine formulations in the established immune cells *in vitro* models, I asked whether their different bacterial origins could influence the immune cells response. To this end, hPBMCs and Mo-DCs were stimulated with both *Shigella* and Ng GMMA vaccines for 4 hours at the same concentration; at the end of treatment the cytokine release in supernatants alongside the cellular activation were evaluated by flow cytometry. Results showed that the two vaccines induced similar pattern of cytokine secretion and cellular activation across the cell types studied (**Figure 16 A-B**).

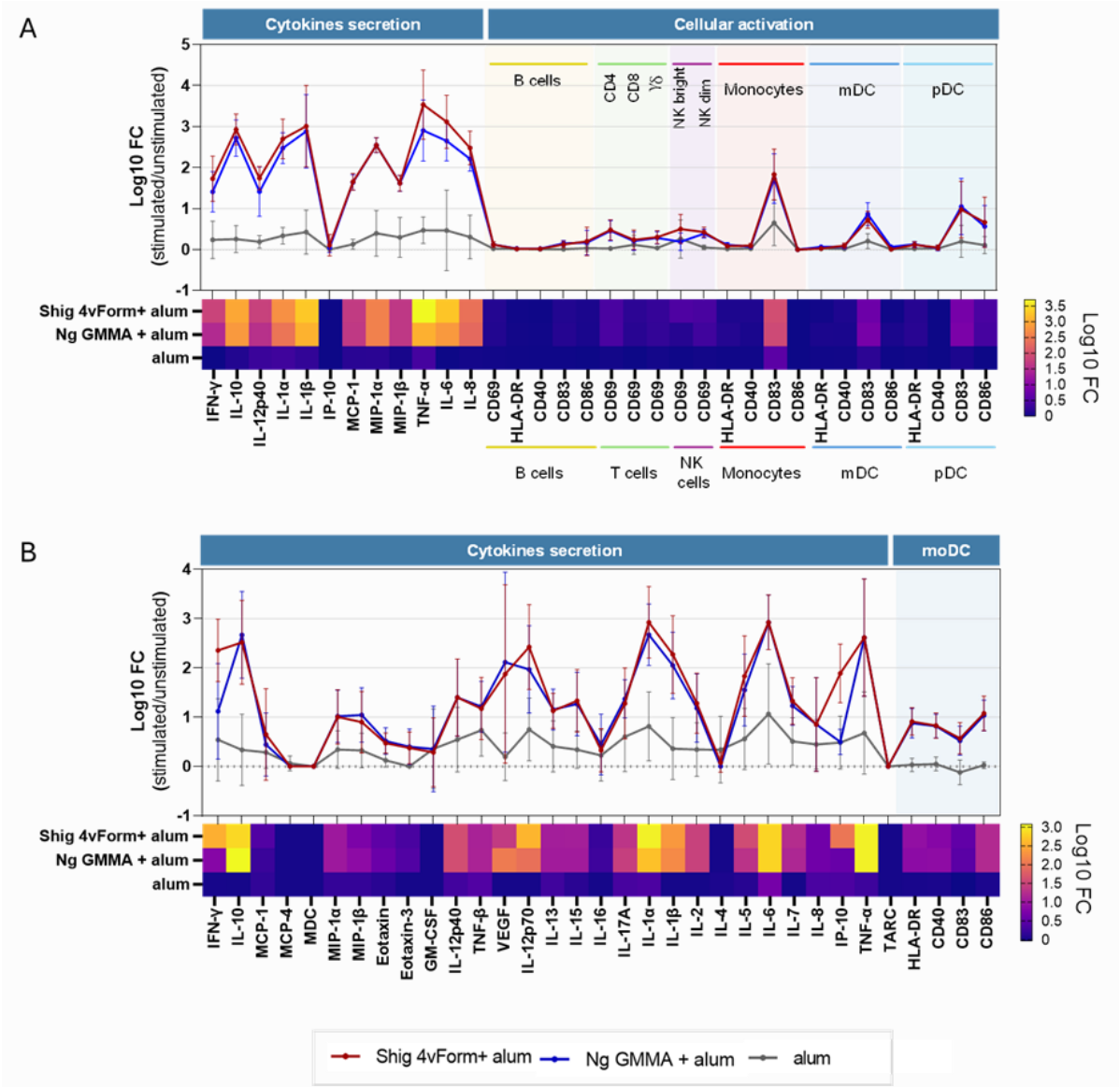

Figure 16. **Cytokine secretion and cellular activation profiles in hPBMCs and Mo-DCs stimulated with *Shigella* and Ng GMMA-based vaccines.** hPBMCs from eight healthy donors (Panel A) and Mo-DCs differentiated *in vitro* from the corresponding monocytes from six of the same donors (Panel B) were stimulated *in vitro* for 4 hours and 48 hours, respectively, with 1 µg/ml of *Shigella* GMMA vaccine (Shig 4vForm + alum), Ng GMMA vaccine (Ng GMMA + alum) and Alum alone. Cytokine quantification in supernatants (Mesoscale) and cell activation (FACS) results are expressed as the Log10 of the average fold change (Log10 FC) across the eight and six donors respectively, relative to unstimulated controls. Linear graphs show the average Log10 FC ± standard deviation for each formulation: Shig 4vForm + alum (red line), Ng GMMA + Alum (blue line), and Alum (grey line). Heatmaps display the average Log10 FC values for the same cytokines and formulations, with colour intensity ranging from dark purple to bright yellow, indicating the magnitude of the immune response.

Interestingly, *Shigella* GMMA-based vaccine induced a higher secretion of IFNγ in hPBMCs and Mo-DCs, IL-1α, IL-6, and TNF-α in hPBMCs, IL-12p70 and IP-10 in Mo-DCs, compared to Ng GMMA-based vaccine. Conversely Ng GMMA-based vaccine induces a slight increase of IL-10 compared to Shigella GMMA-based vaccine (**Figure 17 A-B).** It suggested that *Shigella* and Ng GMMA-based vaccines, despite their different bacterial origin, induced a similar response in our models but with different magnitudes for certain cytokines.

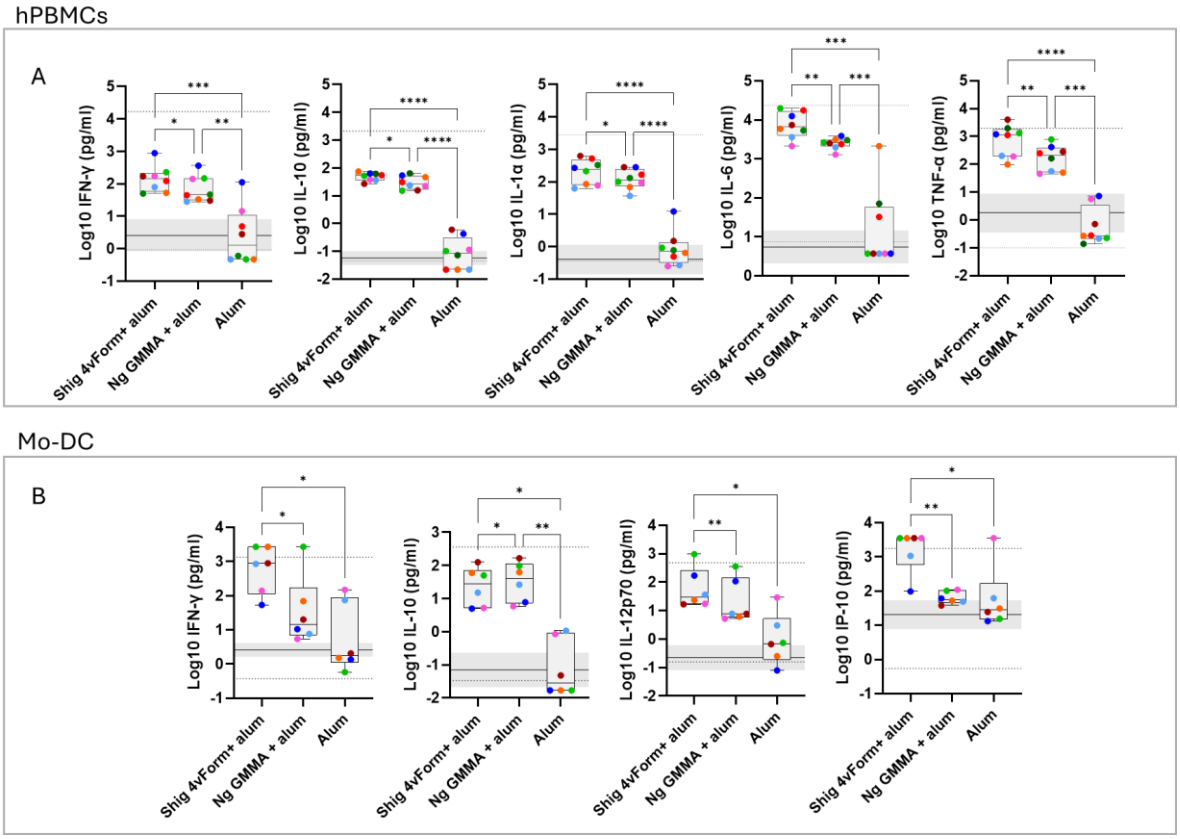

Figure 17. **Cytokine quantification in culture supernatants collected following *in vitro* stimulation of hPBMCs and Mo-DCs with *Shigella* and Ng GMMA-based vaccines.** hPBMCs from eight healthy donors (Panel A) and Mo-DCs differentiated *in vitro* from the corresponding monocytes from six of the same donors (Panel B) were stimulated *in vitro* for 4 hours and 48 hours, respectively, with 1 µg/ml of a Shig 4vForm + Alum, Ng GMMA + Alum, or with Alum alone. Cytokine concentrations in supernatants were measured using a 10-analyte U-PLEX

assay (Panel A) and V-plex assay (Panel B) Box plots display log10-transformed cytokine values, representing the minimum, first quartile (25th percentile), median (50th percentile), third quartile (75th percentile), and maximum. Each coloured dot corresponds to an individual donor. Dotted black lines denote the Upper limit of detection (ULOD) and lower limit of detection (LLOD). Values above the detection range were replaced with twice the upper limit of detection (2X ULOD); values below the detection range were replaced with half of the lower limit of detection (1/2 LLOD). The unstimulated sample (MED) is reported as mean value (continued black line) with its confidence interval (CI) (grey area). Significances observed between groups were determined using the RM one-way ANOVA with Geisser-Greenhouse correction (*p-value < 0.05, **p-value<0.005, ***p-value<0.0005, ****p-value<0.00005; ns stands for nonsignificant and are not reported, p-value > 0.05).

3.2 GMMA internalization by monocyte-derived Dendritic cells (Mo-DCs)

The data reported in section 4.1 demonstrated that both *Shigella* and *N. gonorrhoeae* (Ng) GMMA-based vaccines are capable of inducing activation and maturation of APCs, such as Mo-DCs. As described in paragraph 2.3.1, this activation is typically associated with engagement of pattern recognition receptors (PRRs), particularly Toll-like receptors (TLRs), which recognize pathogen-associated molecular patterns (PAMPs) present on GMMA surfaces (39, 69). However, GMMA are complex vesicular structures that can also be internalized by APCs, potentially influencing intracellular signalling pathways, antigen processing, and presentation mechanisms (69, 81).

Understanding whether GMMA-induced APCs activation is solely mediated by surface receptor engagement (e.g., TLRs) or also involves active internalization and intracellular trafficking is crucial for elucidating the full immunological mechanism of action of GMMA-based vaccines. Internalization could contribute to enhanced antigen presentation via

MHC class I and II pathways, influence cytokine secretion profiles, and modulate the overall adaptive immune response (150).

To investigate the capacity of APCs to internalize GMMA, immature Mo-DCs (iMo-DCs) were exposed to *Shigella* GMMA labelled with pHrodo, a pH-sensitive fluorescent dye that becomes brightly fluorescent in acidic environments such as phagolysosomes but remains non-fluorescent at neutral pH found on the cell surface or in the cytosol (**Figure 18**). This property makes pHrodo an ideal tool for tracking GMMA uptake and intracellular trafficking in real time. Live-cell imaging was performed overnight to monitor the internalization process and assess the dynamics of GMMA entry into APCs.

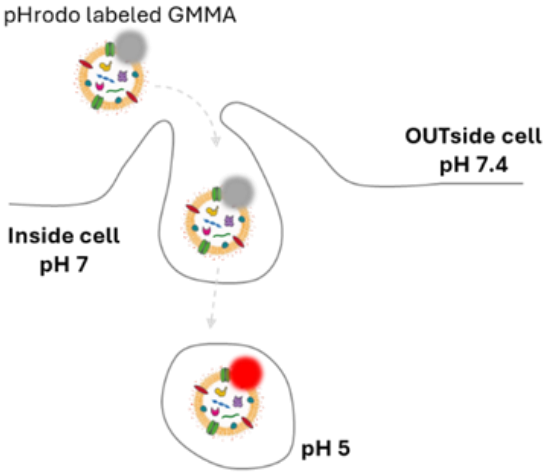

Figure 18. **Tracking GMMA internalization in APCs using pHrodo.**
Fluorescence. Schematic representation of the pHrodo-based method used to monitor GMMA internalization by antigen-presenting cells (APCs). GMMA vesicles are labelled with pHrodo, a pH-sensitive fluorescent dye that remains non-fluorescent at neutral pH (e.g., on the cell surface or in the cytosol). Upon internalization, GMMA are trafficked into acidic compartments such as endosomes and phagolysosomes, where the pHrodo dye becomes fluorescent, emitting a bright red signal. This fluorescence serves as a real-time indicator of successful uptake and intracellular localization of GMMA. The approach enables dynamic visualization of

the internalization process using live-cell imaging, providing insights into the kinetics and extent of GMMA uptake by APCs.

As shown in **Figure 19**, at t0 (starting point), no fluorescence signal was detected, as expected. However, as time progressed, cells began to phagocytize and internalize the pHrodo-labelled GMMA which are likely to be processed as suggested by the loss of fluorescence. Interestingly, cellular morphology changes from a round shape to a more elongated, dendritic structure by the end of the time lapse (Yellow circles, **Figure 19A**). A detailed analysis of the pHrodo-positive regions within each well revealed a notable increase in internalization compared to untreated cells, demonstrated by the increase of regions exhibiting pHrodo fluorescence (**Figure 19B**). These data demonstrated that GMMA are effectively internalized by Mo-DCs.

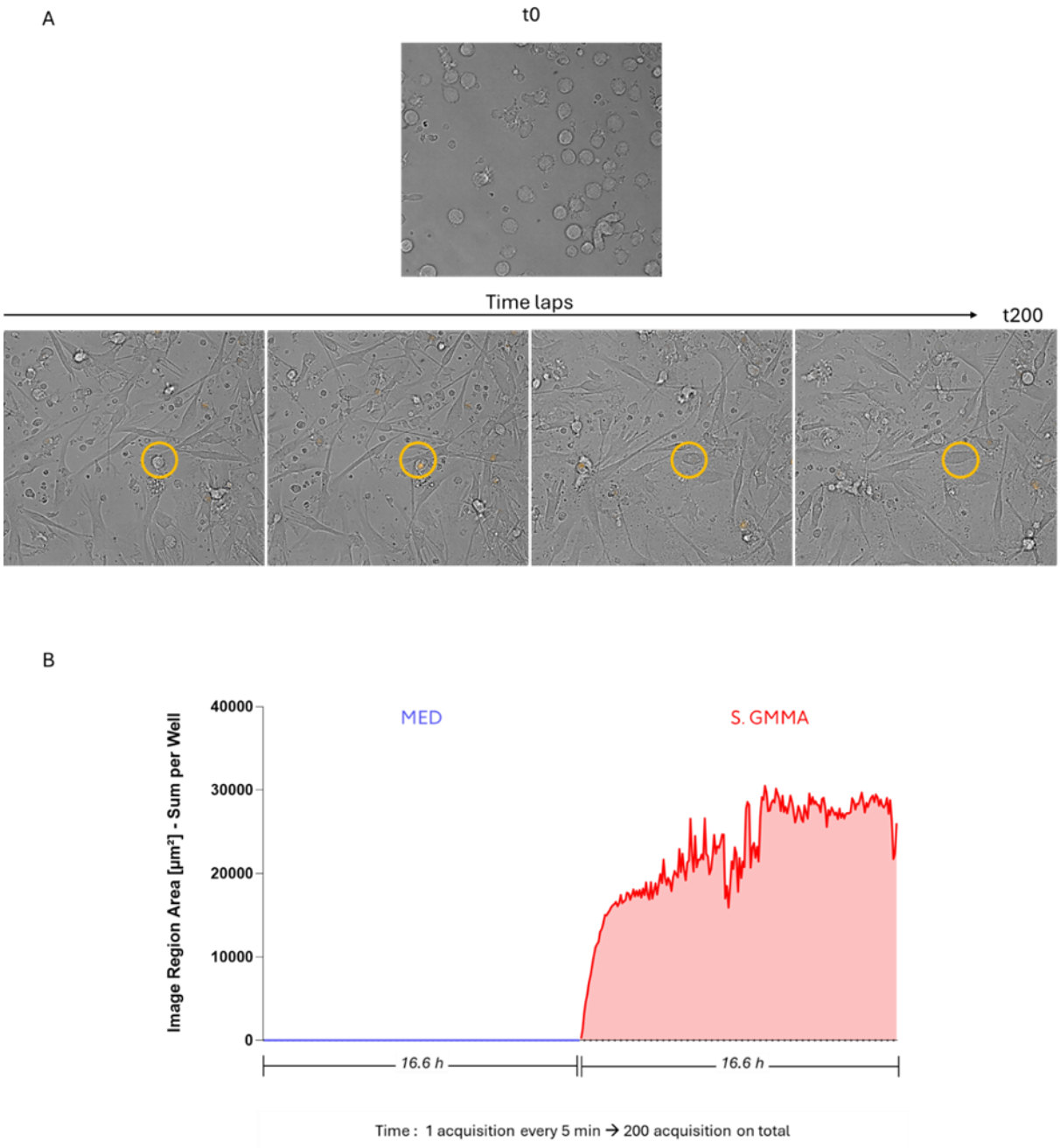

Figure 19. **Live imaging of S. GMMA internalization by Mo-DCs using pHrodo-labelled vescicles. A)** Representative time-lapse microscopy images of Mo-DCs exposed to pHrodo-labelled *Shigella* GMMA, captured over 16.6 hours (200 acquisitions, one every 5 minutes). Yellow circles highlight regions of increasing fluorescence, indicating GMMA internalization and trafficking into acidic compartments. B) Quantification of fluorescence signal over time, expressed as the sum of image region area per well (μm^2). The blue curve corresponds to the unstimulated control (MED) while the red curve represents cells stimulated with S. GMMA. The increase in fluorescence in the S. GMMA condition reflects progressive internalization and acidification of GMMA-containing vesicles.

3.3 GMMA-based vaccines and adaptive immunity

Due to the observation of a significant enhancement in the production of cytokines such as IL-12p70, IL-1β, and IL-6, which are known to drive Th cells response (150), in Mo-DCs upon stimulation with GMMA-based vaccines compared to unstimulated sample, I investigated whether GMMA vaccines-stimulated Mo-DCs have the ability to induce naïve CD4+ T helper cells to differentiate into effector cells and potentially which kind of the Th cell response they can dictate.

3.3.1 Optimization of Naïve CD4+ T helper cell polarization in vitro model

To investigate whether GMMA-based vaccines can modulate the adaptive immune response, an *in vitro* polarization model was developed. In particular, I focused my attention on the 3 main Th subsets: Th1, Th2 and Th17 whose differentiation is induced by IL-12, IL-4/IL-13, and a combination of IL-6, IL-23, IL-1β and TGF-β respectively.

Th1 cells are characterized by upregulation of the transcription factors (TF) T-box expressed in T cells (T-bet) and produce IFNγ, thereby providing protection against intracellular pathogens. Th2 cells upregulate GATA-binding protein-3 (GATA-3) and produce IL-13 and IL-4, which offer protection against helminths and are also implicated in allergic responses. Th17 cells are characterized by the upregulation of retinoic acid receptor-related orphan receptor gamma t (RORγt) and produce IL-17F, IL-17A, IL-21, and IL-22, providing an effective defense against extracellular bacteria and fungi, and playing a pivotal role in mucosal immunity (**Figure 20A**).

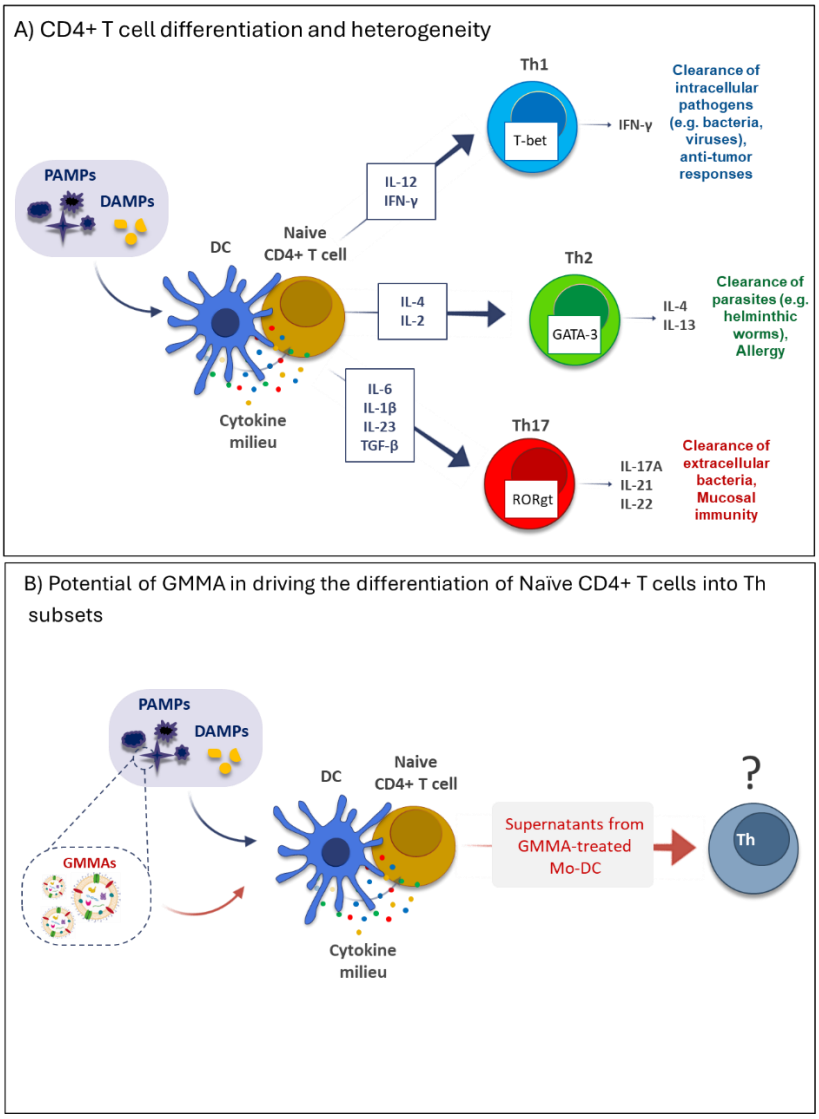

Figure 20. **CD4⁺ Th cells differentiation and heterogeneity of mechanisms of Th cells differentiation induced by GMMA-Treated Dendritic Cells.** The diagram illustrates the immunological pathways leading to T-helper (Th) cell differentiation mediated by dendritic cells (DCs). A) Based on different Pathogen-associated molecular patterns (PAMPs) and damage-associated molecular patterns (DAMPs), Dendritic cells (DCs) can shape the adaptive response by directing the differentiation naïve CD4+ Th cell into specific Th effector cells.B) GMMA-based vaccines were employed to stimulate monocyte-derived dendritic cells (Mo-DCs), after which the resulting supernatants were collected to assess the cytokine milieu produced. These supernatants were subsequently tested on naïve CD4+ T helper (Th) cells to evaluate the polarization potential of GMMA. This approach aimed to determine the specific Th effector subsets induced in a simplified *in vitro* environment.

I first optimized the *in vitro* CD4+ Th cell polarization protocol by modifying existing published methods by Annunziato et al. (151), which did not work well in our hands. In particular, I introduced NaCl in addition to the already published Th17 polarization cocktail and added a boost step, at day 3, for Th2 and Th17 phenotypes. The boosting consisted in adding the same polarization cocktail supplemented with IL-2 for Th2 phenotype and adding the same polarization cocktail lacking NaCl for Th17 phenotyping. Moreover, I reduced the time of stimulation, from seven to five days, and used a different Th cell polarization readout compared to that used by Annunziato et al. (151), evaluating the up-regulation of the Th cell- specific transcription factors through flow cytometry and secretion, in culture supernatants, of Th cells-specific cytokine by Mesoscale. Therefore, to induce the differentiation of naïve CD4+ T cell towards Th1, Th2 and Th17 cell subsets, specific polarization cocktails tailored to each Th cell subset (rIL-12 + mAb ant-IL-4 for Th1, IL-4+ mAb ant-IFNγ for Th2, and rIL-6,rIL-23,rIL-1β,rTGF-β, mAb ant-IL-4, mAb ant-IFNγ and NaCl for Th17) were used in combination with α-CD3/α-CD28 beads for T cell activation over a period of five days. To assess polarization, flow cytometry was employed to determine the proportion of cells positive for the master transcription factors T-bet, GATA-3 and RORγt which are associated with Th1, Th2 and Th17 respectively. Additionally, Th- specific cytokines like IFN-γ, IL-13 and IL-17A were quantified in the supernatants of Th1, Th2 and Th17 cultures, respectively. As illustrated in **Figure 21**, after five days of stimulation, naïve CD4+ T cells treated with Th1 polarizing cocktail showed elevated expression of T-bet (**Figure 21A**) and higher IFN-γ production compared to unpolarized cells and those treated with Th2 and Th17 cocktails (**Figure 21B**). Naïve CD4+ T cells exposed to Th2 polarization cocktail exhibited

upregulation of GATA-3 (**Figure 21C**) and increased levels of IL-13 (**Figure 21D**) compared to unpolarized cells and those treated with Th1 and Th17 cocktails. Treatment with the Th17 polarization cocktail led to a modest increase in RORγt expression (**Figure 21E**) compared to other conditions, along with substantial IL-17A production (**Figure 21F**) relative to unpolarized and Th1 cultures. Notably, significant levels of IL-17 were also detected in Th2 cultures.

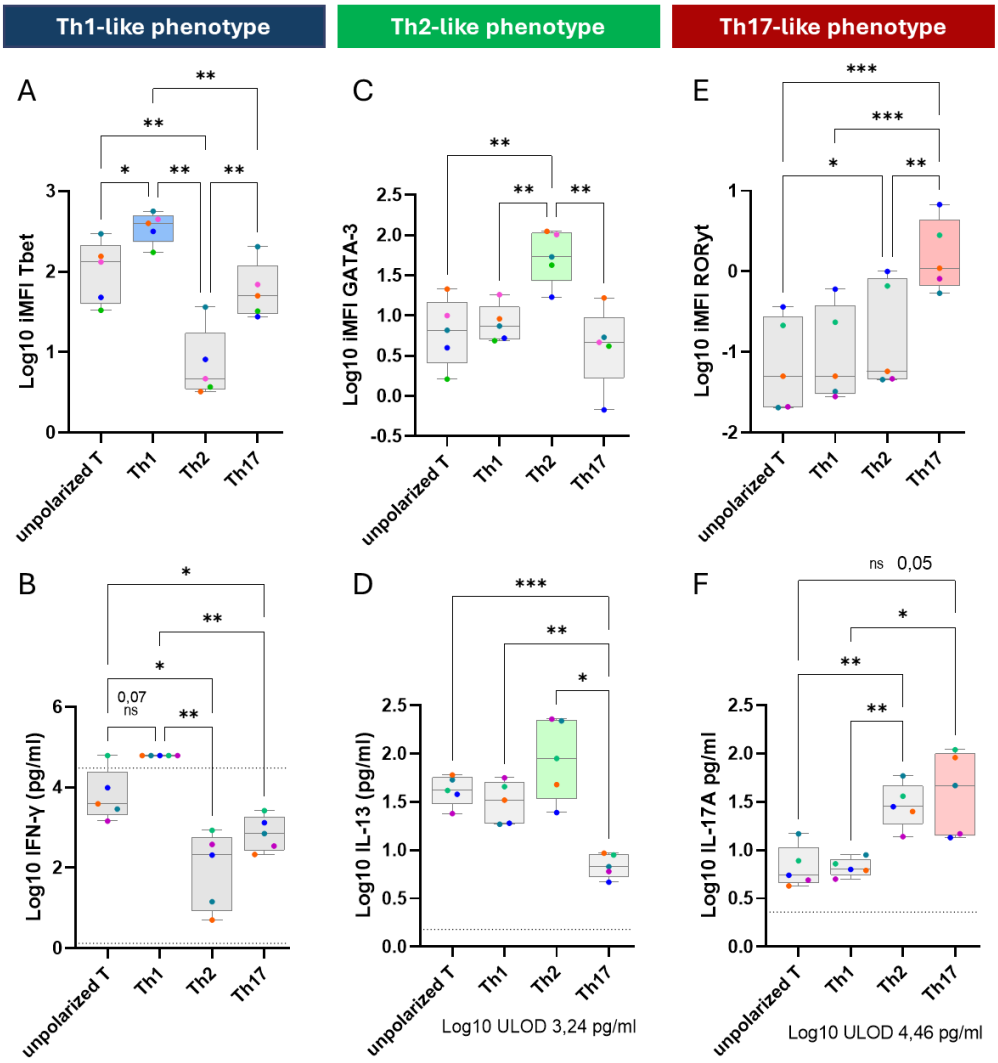

Figure 21. ***In vitro* model of Naïve CD4+ T helper (Th) cell polarization**. Box plots show the expression levels of transcription factors (Panel A: T-bet, Panel C: GATA-3, Panel E: RORγt) and cytokines (Panel B: IFNγ, Panel D: IL-4, Panel F: IL-17A) associated with Th1-, Th2-, and Th17-like phenotypes. Data are reported as log10 values in box plots, illustrating the minimum, first quartile (25th percentile), median (50th percentile), third quartile (75th percentile), and

maximum. Each dot represents an individual donor, five donors in total. Groups include unpolarized controls and phenotype-specific polarizing conditions Th1, Th2 and Th17. **Panel A-C-E:** Quantification of transcription factor (TFs) expression at the single cell levels by flow cytometry. TFs expression is reported as integrated mean fluorescence intensity (iMFI), calculated by multiplying the percentage of cells positive for each TFs by the geometric mean fluorescence intensity (geoMFI) and then dividing the product by 100. **Panel B-D-F:** Cytokine quantification in culture supernatants by Mesoscale (U-PLEX Biomarker Assay 20 analytes). Dotted black lines represent the ULOD and LLOD. Values above the detection range were replaced with twice the upper limit of detection (2X ULOD); values below the detection range were replaced with half of the lower limit of detection (1/2 LLOD). Significances observed between groups were determined using the RM one-way ANOVA with Geisser-Greenhouse correction (*p-value < 0.05, **p-value<0.005, ***p-value<0.0005, ****p-value<0.00005; ns stands for nonsignificant and are not reported, p-value > 0.05).

3.3.2 Shigella and Ng GMMA-based vaccines shaped the adaptive immunity towards Th1 phenotype with the up-regulation of T-bet and the secretion of IFNγ

Upon optimization, the CD4+ Th polarization *in vitro* model was employed to assess the polarization potential of the cytokine environment generated by Mo-DC following *in vitro* stimulation with GMMA-based vaccines as reported schematically in **Figure 20B**. In **Figure 22** are reported the box plots illustrating the expression levels of transcription factors (**Panel A**: T-bet, **Panel C**: GATA-3, **Panel E**: RORγt) and cytokines (**Panel B**: IFN-γ, **Panel D**: IL-4, **Panel F**: IL-17A) associated with Th1-, Th2-, and Th17-like phenotypes in response to *Shigella* and Neisseria *gonorrhoeae* (Ng) GMMA vaccines. The expression of T-bet and secretion of IFN-γ were significantly elevated, compared to MED and Alum, in cells exposed to *Shigella* GMMA formulations (Shig 4vForm + alum), indicating a robust Th1-like response. Ng GMMA vaccine (Ng GMMA + alum) also induced T-bet and IFN-γ, albeit to a lesser extent (**Figure 22, panel A-B**). In contrast, Th2- (GATA-3 and IL-

4) and Th17-(RORγt and IL-17) associated markers were not induced across all GMMA conditions, suggesting limited Th2 and/or Th17 polarization. These findings suggest that GMMA-based vaccines primarily promote Th1-biased immunity.

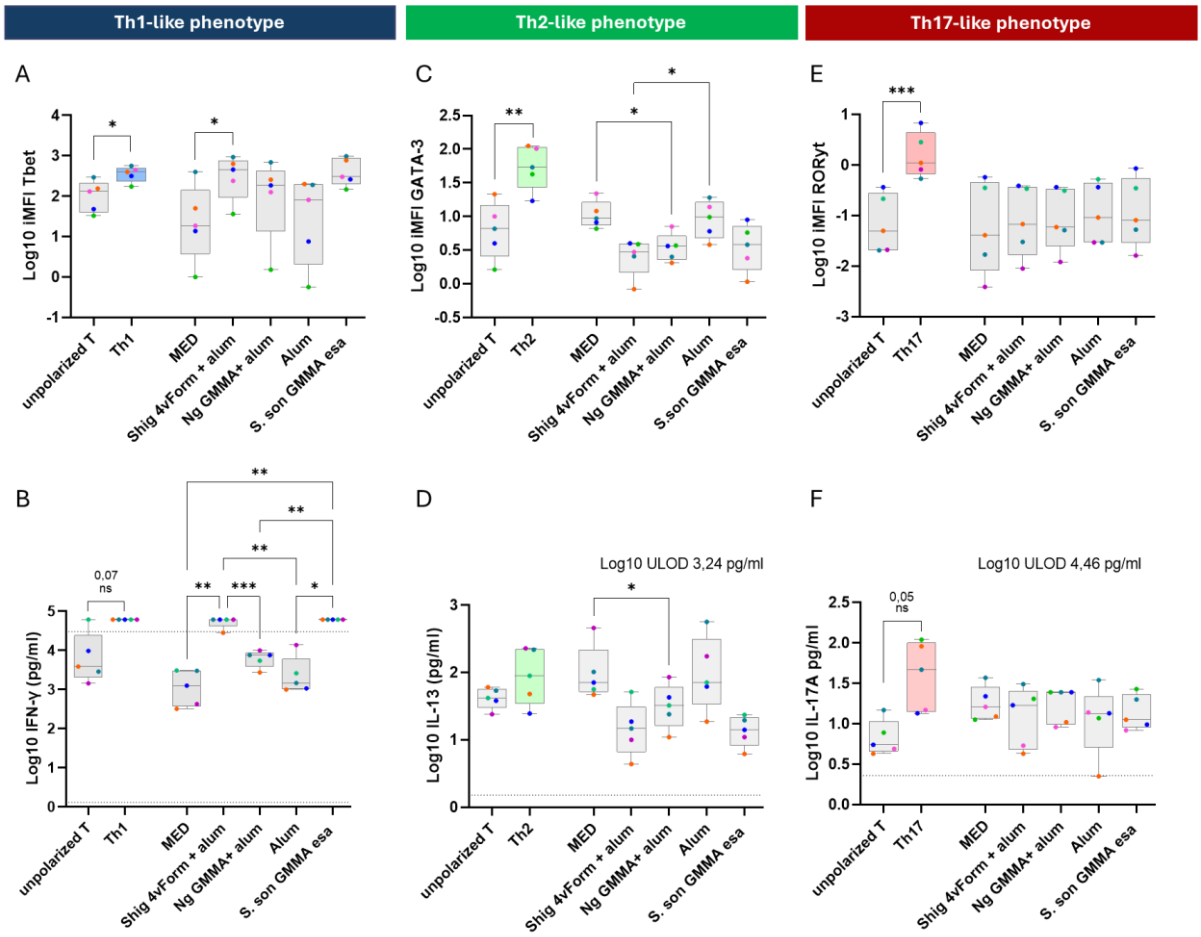

Figure 22. **Expression of transcription factors (TFs) and cytokines associated with Th1-, Th2-, and Th17-like phenotypes in response to GMMA-based vaccines.** Box plots show the expression levels of transcription factors (Panel A: T-bet, Panel C: GATA-3, Panel E: RORγt) and cytokines (Panel B: IFNγ, Panel D: IL-4, Panel F: IL-17A) associated with Th1-, Th2-, and Th17-like phenotypes in response to Shigella sonnei and Neisseria gonorrhoeae (Ng) GMMA vaccines. Data are reported as log10 values in box plots, illustrating the minimum, first quartile (25th percentile), median (50th percentile), third quartile (75th percentile), and maximum. Each dot represents an individual donor, five donors in total. Groups include unpolarized controls, phenotype-specific polarizing conditions (Th1, Th2, Th17), and stimulation with supernatants derived from the *in vitro* stimulation of Mo-DCs with: GMMA-based vaccines (*Shigella*: Shig 4vForm+alum; *N. gonorrhoeae*: Ng GMMA + alum), Alum, *S. sonnei* GMMA esa

(S. son GMMA esa, positive control) and unstimulated cells (MED, negative control). **Panel A-C-E:** Quantification of transcription factor (TFs) expression at the single cells levels by flow cytometry. TFs expression is reported as integrated mean fluorescence intensity (iMFI), calculated by multiplying the percentage of cells positive for each TFs by the geometric mean fluorescence intensity (geoMFI) and then dividing the product by 100. **Panel B-D-F:** Cytokine quantification in culture supernatants by Mesoscale (U-PLEX Biomarker Assay 20 analytes). Dotted black lines represent the ULOD and LLOD. Values above the detection range were replaced with twice the upper limit of detection (2X ULOD); values below the detection range were replaced with half of the lower limit of detection (1/2 LLOD). Significances observed between groups were determined using the RM one-way ANOVA with Geisser-Greenhouse correction (*p-value < 0.05, **p-value<0.005, ***p-value<0.0005, ****p-value<0.00005; ns stands for nonsignificant and are not reported, p-value > 0.05).

3.4 Myotubes: Muscle cell *in vitro* model

The innate immune response following vaccination depends not only on the direct interactions and activation of immune cells but is also greatly shaped by the local immunological environment at the injection site. Since GMMA-based vaccines are administered intramuscularly, and given the well demonstrated role of skeletal muscle cells in shaping the immunological microenvironment (74, 75, 152), I used a muscle cells *in vitro* model to mimic the injection site and thus, to investigate the interaction of GMMA-based vaccines with cells in that environment .

3.4.1 Myotubes are responsive to Shigella and Ng GMMA vaccines

As a first step, I demonstrate that human skeletal muscle myoblasts are responsive to GMMA (data not shown). However, despite skeletal muscle myoblasts represent a well-established and widely used *in vitro* model to investigate muscle cell responses, it does not fully recapitulate the physiological characteristics of muscle tissue at the site of vaccine injection. Therefore, I differentiated human skeletal muscle myoblasts into myotubes, which represent the closest physiological state to muscle fibres (153). Using this model, I evaluated the secretion of cytokines and chemokines in the culture supernatants following a 22-hours stimulation with different GMMA-based vaccine formulations. Specifically, I tested both Alum-adjuvanted and non-adjuvanted *Shigella* and *N. gonorrhoeae* GMMA vaccines and Alum alone. *S. sonnei* GMMA-esa (wild-type LPS) and complete medium (MED) were used as positive and negative controls, respectively. All conditions were tested at a concentration of 0,1 µg/ml. I employed O-link technology which is based on the Proximity Extension Assay (PEA) technology that combines antibody-based

immunoassay with the powerful properties of polymerase chain reaction (PCR) (see paragraph 3.5.3). This system provide a highly specific and sensitive detection of proteins even at very low concentrations. Moreover, it detects a wide range of cytokines. These features can help in obtaining accurate cytokines profiling in a complex *in vitro* system. For this study, I used the "Inflammation kit", which detects 92 proteins broadly implicated in the inflammation process. Cytokine concentrations were expressed in Normalized Protein Expression (NPX) units, a relative quantification metric on a log2 scale, where higher NPX values indicate greater protein abundance. As shown in **Figure 23**, upon stimulation with both alum-adjuvanted and non-adjuvanted GMMA formulations, myotubes significantly secreted higher levels of CCL20, CXCL1, CXCL5, CXCL6, CXCL8 and IL-6 as well as following treatment with S. son GMMA esa (positive control) compared to the control (MED). Furthermore, the trend

of myokine levels showed a stronger impact following *Shigella* GMMA-based vaccine stimulation than Ng GMMA-based vaccine.

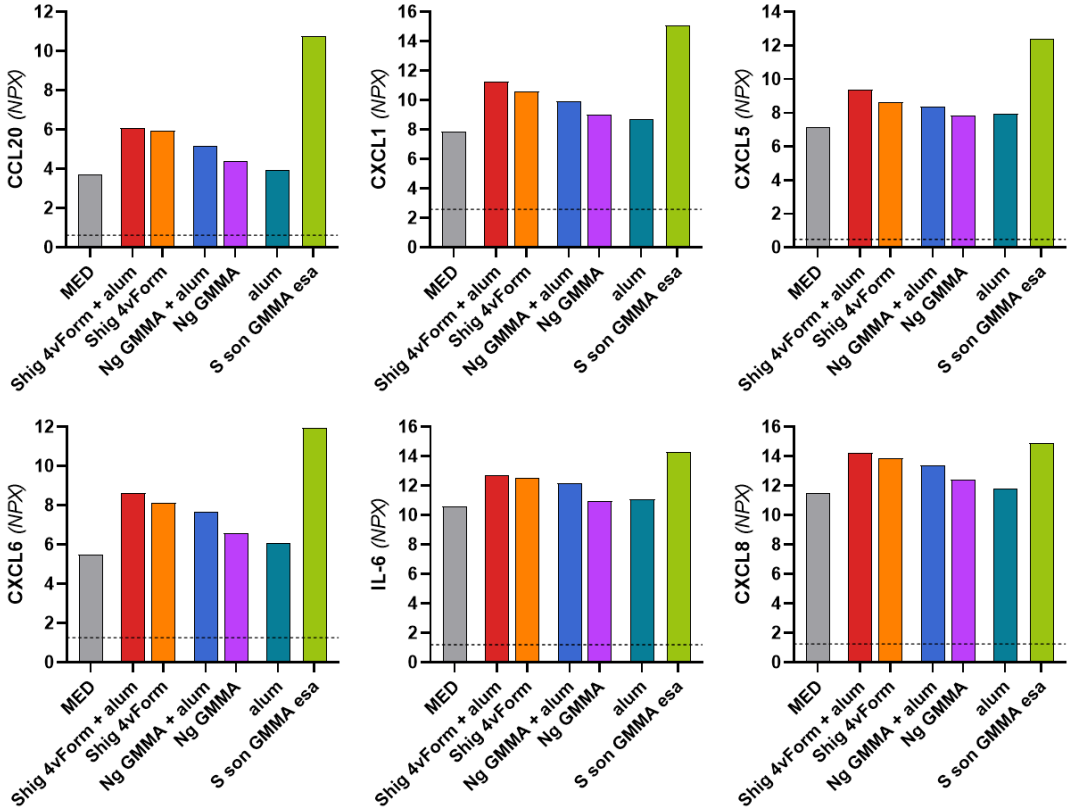

Figure 23. **Cytokine secretion by myotubes following stimulation with GMMA-based vaccine formulations.** Myotube were stimulated for 22 hours with *Shigella* four-component GMMA vaccine adjuvanted with Alum (Shig 4vForm + Alum), non-adjuvanted *Shigella* GMMA formulation (Shig 4vForm), *Neisseria gonorrhoeae* GMMA vaccine with Alum (Ng GMMA + Alum), non-adjuvanted Ng GMMA, Alum alone, and *S. sonnei* GMMA ESA (positive control), all at a final concentration of 1 µg/ml. Complete medium (MED) was used as negative control. Cytokine levels in culture supernatants were quantified using Olink technology and expressed as Normalized Protein Expression (NPX) units on a log2 scale. The dotted black line indicates the lower limit of detection (LOD). Data are related to a single experiment.

3.4.2 Myotubes can internalize GMMA

The GMMA-dependent secretion of cytokines and chemokines from myotubes suggest that they are likely to shape the microenvironment at

the injection site. However, whether this activation is only mediated by TLRs engagement, which are expressed by muscle cells (154) or involves other mechanisms, needs to be investigated. In particular, the question of whether skeletal muscle myotubes can act as non-professional APCs remains unresolved particularly in the context of intramuscular vaccination, where muscle tissue is the primary site of antigen deposition (155). Although, cytokines stimulated myotubes have been reported to express MHC-I and II, as well as co-stimulatory molecules such as CD40, BB-1, and ICOS-L (156, 157) there is still a lack of data demonstrating their ability to participate in the antigen presentation cascade including antigen uptake, processing, peptide-MHC complex formation, and subsequent T-cell activation. Given that the first step in antigen presentation by professional APCs is the recognition and uptake of foreign substances/pathogens, I investigated the ability of myotubes to internalize GMMA by confocal microscopy analysis on skeletal muscle myotubes differentiated *in vitro* from human skeletal muscle myoblasts (see paragraph 3.3.2). Myotubes were incubated for 22 hours with 5 µg/ml of S. *flex* 2a GMMA fluorescently labelled with Alexa Fluor 488 (A488-S. GMMA) or left untreated. Following stimulation, cells were incubated with an anti-GMMA antibody followed by a secondary antibody conjugated to Alexa Fluor 568 to specifically identify extracellular GMMA.

A dual-staining approach was employed instead of a pHrodo-based strategy due to differences in biological context and technical objectives between Mo-DCs and muscle cells. For Mo-DCs, which are professional APCs, the aim was to monitor the dynamics of GMMA uptake and processing in real time. pHrodo, a pH-sensitive dye that exhibits strong fluorescence in acidic environments such as endosomes and lysosomes,

is well suited for live-cell imaging and tracking internalization into degradative compartments.Conversely, muscle cells are not professional phagocytes; their uptake is typically slower and less efficient, making live imaging less practical. Therefore, an endpoint dual-staining strategy was applied to distinguish internalized GMMA (A488+ signal only) from GMMA bound to the cell surface (A568+ signal). This approach provided a semi-quantitative assessment of uptake and surface binding, as well as spatial distribution. As shown in **Figure 24**, S. GMMA were detected both on the surface and inside skeletal muscle myotubes under these conditions, indicating that S. GMMA are likely to bind myotubes prior to internalization. However, the pathway through which the internalization happens and whether this internalization evolves in a complete antigen presentation (processing, peptide-MHC complex formation, and T-cell activation) remains undetermined and warrants further investigation. Our data showed that GMMA are internalized and actively processed by Mo-DCs, a representative model for professional APCs (paragraph 4.2; Figure 19).

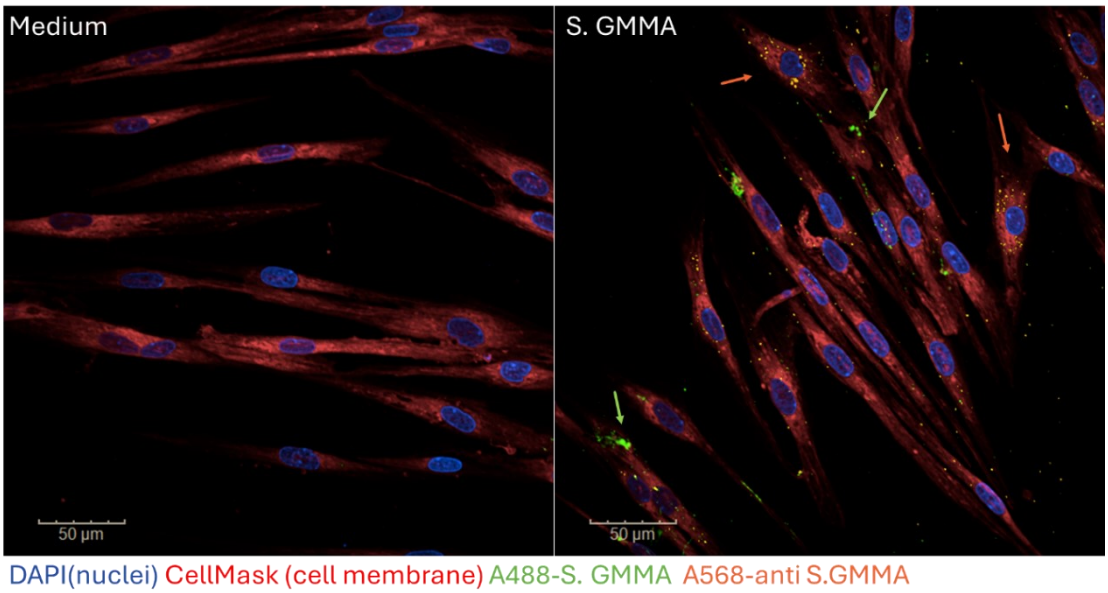

Figure 24. **Confocal microscopy analysis of S. *flexneri 2a* GMMA internalization in skeletal muscle myotubes.** Fluorescent images acquired using Opera Phenix confocal microscopy

compare untreated myotubes (Medium) with myotubes treated for 22 hours with S. *flex* 2a GMMA conjugated to Alexa Fluor 488 (A488-S. GMMA). Cell nuclei are stained with DAPI (blue), and cell membranes with Cell Mask Deep Red (red). A polyclonal secondary antibody conjugated to Alexa Fluor 568 (orange) was used to label extracellular GMMA, allowing discrimination between surface-bound (orange) and internalized (green) GMMA. Internalized GMMA retains the green A488 signal, as they are inaccessible to the secondary antibody.

3.4.3 Establishment of an in vitro model of the injection site with myotubes and immune cells

To better mimic the local site of injection, I established an *in vitro* cell model comprising both myotubes and hPBMCs thereafter referred to as the primary muscle cell model (PMCM). *Shigella* or *Neisseria gonorrhoeae* GMMA-based vaccines (final concentration of 0,1 µg/mL) were added to the PMCM in the presence or absence of alum and incubated for 22 hours. Culture supernatants were then collected and analyzed for cytokine secretion using O-link technology, employing the "Inflammation panel kit" which quantifies 92 proteins typically involved in the inflammatory processes. Control samples, including PMCM maintained in complete medium, treated with Alum or with *S. sonnei* GMMA esa (positive control), were set up in parallel with treated samples. In addition, to dissect the contribution of each cellular component of the PMCM model, parallel stimulations with GMMA-based vaccines were performed on PBMCs and myotubes cultured separately.

I first analysed whether the combination of the two cell types in the PMCM (P_M) model in the absence of GMMA had an impact on the quantity and quality of cytokines secreted compared with single cultures of PBMCs (P) and Myotubes (M). To this end a principal component analysis (PCA) based on cytokine secretion profiles from the three unstimulated conditions was

carried out. In the PCA plot (**Figure 25**), each point represents a donor, and colours indicate the experimental model: blue for P_M, pink for P, and green for M. Samples were projected onto the first two principal components (PC1 and PC2), which accounted for 55.36% and 17.4% of the total variance, respectively. To facilitate interpretation, a biplot was generated, overlaying loading vectors that represent the contribution of individual cytokines to the principal components. The direction of each arrow indicates the gradient of cytokine expression across the sample space, while its length reflects the magnitude of its influence on the components. The PCA revealed a clear separation among the three models, suggesting specific cytokine profiles for each model. Notably, cytokines such as IL-6, CSF-1, and CCL20 were hallmarks of the P_M model, while cytokines like IFN-γ, TRANCE, and TNFSF14 of the PBMCs model. The M model instead, was not marked by a pronounced contribution from any single cytokine. These findings suggest that the microenvironment generated by the inclusion of muscle cells and immune cells in the PMCM model is not merely the sum of molecules secreted by the individual components but is likely the result of cellular crosstalk.

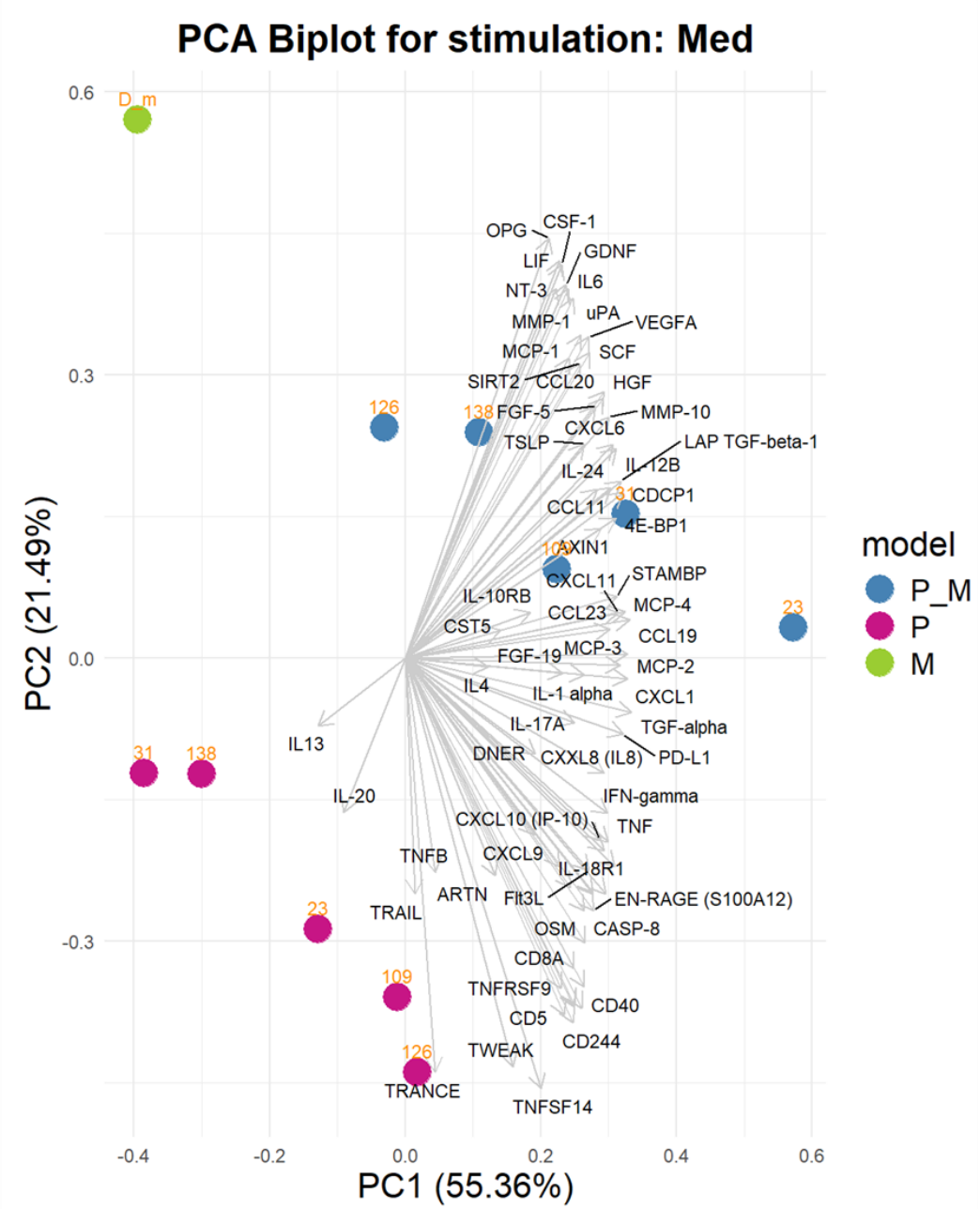

Figure 25. **Principal Component Analysis (PCA) of cytokine profiles in unstimulated *in vitro* models.** Principal component analysis of the 92 cytokines detected in the culture supernatants from unstimulated Myotubes (M), PBMCs (P) single models and PMCM co-culture model (P_M). In the P_M and P models, each dot represents a donor , with blue and pink colors indicating the respective model conditions. The M model is represented by a single green dot corresponding to the myotube monoculture. Arrows indicated the contribution of each cytokine to the principal components: the direction reflects the gradient of cytokine expression across the sample space, while the length indicates the strength of the contribution to the components.

To further identify cytokines and chemokines with both high statistical significance (low p-value) and substantial expression differences (high fold change) between the PMCM co-culture (P_M) and the PBMCs single culture (P) under basal condition I performed a differential cytokine expression analysis visualized in the volcano plot (**Figure 26**), which displays statistical significance (P-value) against the magnitude of change (fold change).

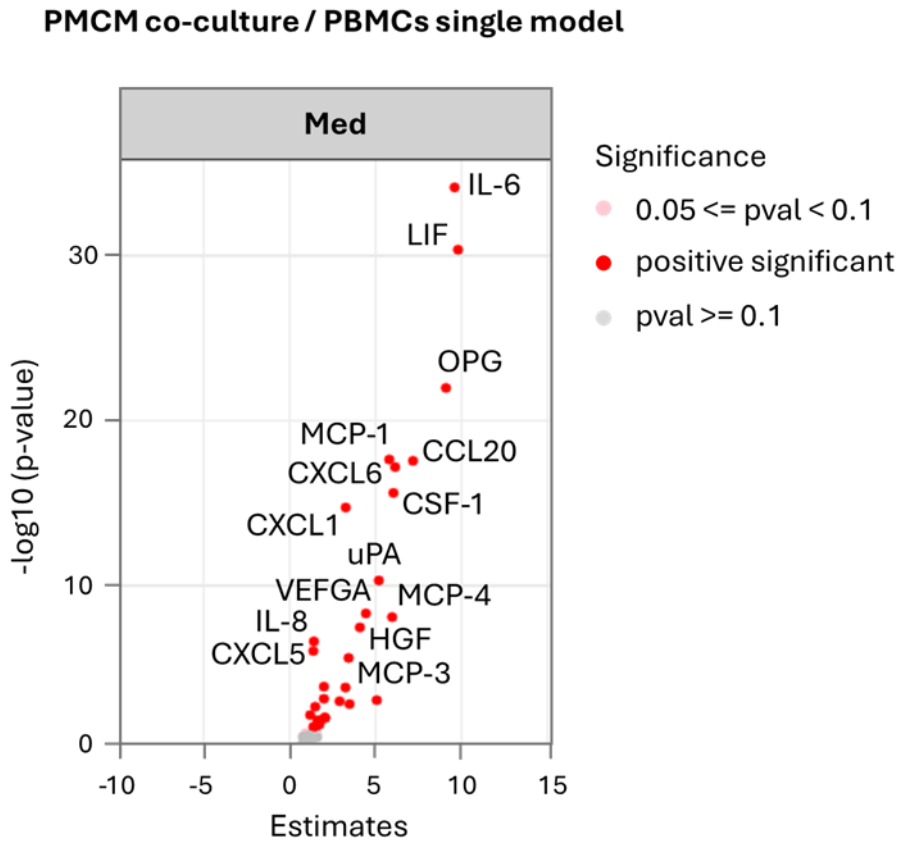

Figure 26. **Volcano plot of differential cytokine expression between unstimulated PBMCs and PMCM co-culture models.** Volcano plot represents the differential cytokine secretion between unstimulated PMCM co-culture and PBMCs single models. Cytokine levels were quantified in culture supernatants collected after 22 hours of incubation for both models. X axes reports the estimated that represent the log2 scaled differential Normalized protein expression (NPX) compared to the PBMCs single model, while Y axes represent the statistical

significance of the modulation [-log10 scaled p-value]. Cytokines that are highly secreted in the PMCM co-cultured model respect to PBMCs single model are represented as red dots.

As shown in Figure 26 there were several mediators that discriminated the PMCM co-culture model from PBMCs single model and showed the highest statistical significance including IL-6, LIF (Leukemia Inhibitory Factor) and OPG (Osteoprotegerin). Moreover, data showed higher levels of chemokines from Cys-Cys (C-C) chemokine family including MCP-1 (CCL2), MCP-3 (CCL7), MCP-4 (CCL13), CCL20 (MIP-3a) and from Cys-X-Cys (C-X-C) chemokines family including CXCL1, CXCL5, CXCL6, CXCL8 (IL-8) in PMCM co-culture model compared with PBMCs single model indicating that the interaction between the two cell types alone induces the release of these mediators

3.4.4 Impact of GMMA vaccine formulations on cytokine secretion in PMCM model

Given that both *Shigella* and Ng GMMA-based vaccines, despite the different bacterial origin, induce a similar immune profile evaluated as activation of cellular subsets and production of cytokines/chemokines, in the PBMC model (paragraph 4.1.3), here I tested these GMMA-based vaccines in a more complex model, the PMCM model, to better recapitulate the events occurring at the site of injection following GMMA-based vaccination. Hence, I stimulated both the PBMCs single culture (P) and the PMCM co-culture (P+M) for 22 hours with Alum-adjuvanted and non-adjuvanted *Shigella* and Ng GMMA vaccine formulations, as well as with Alum alone, at a final concentration of 1 µg/ml.

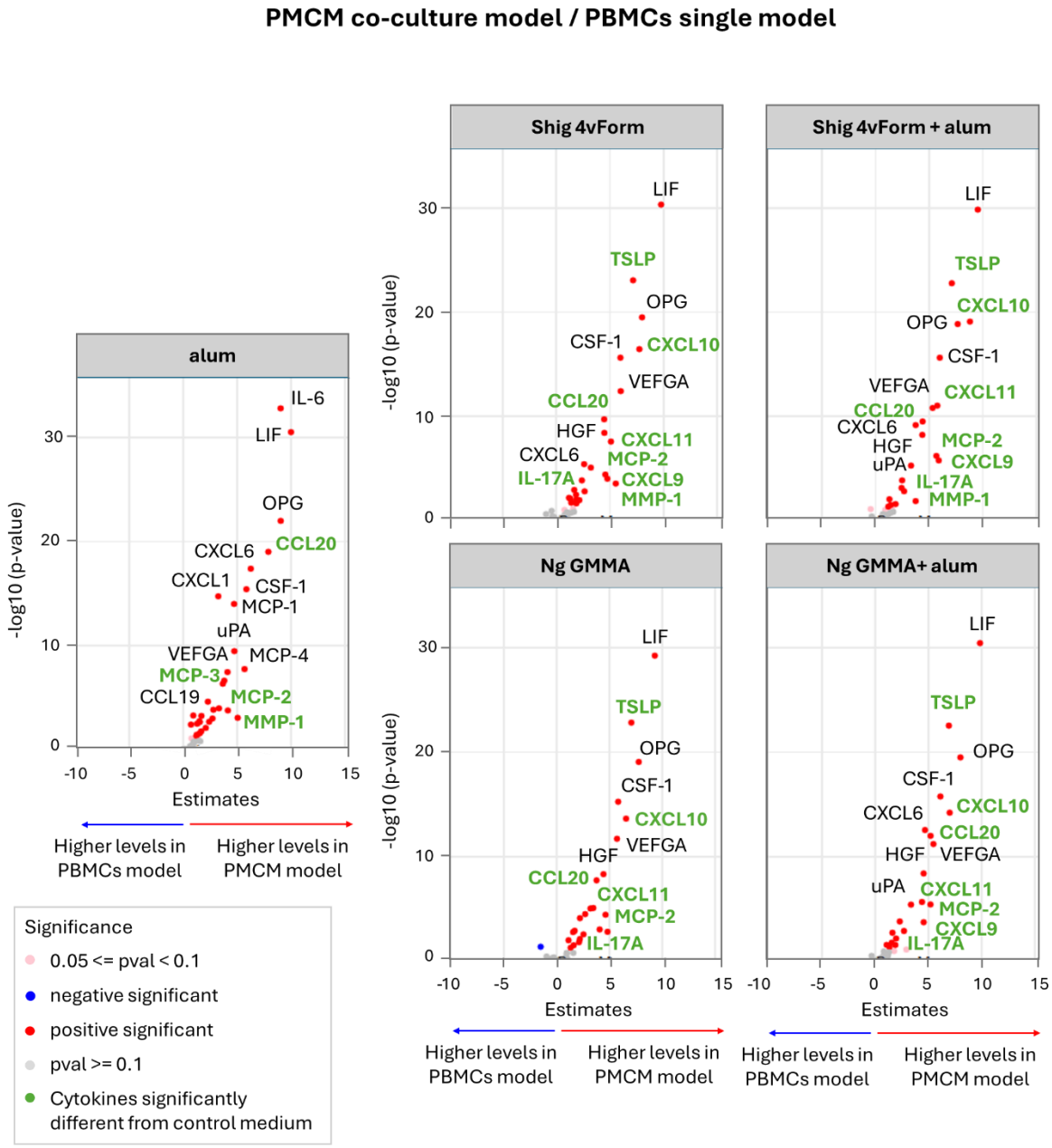

Figure 27. **Differences in Cytokine/chemokine Response to GMMA Vaccine Formulations and Alum in PBMCs/Myotubes co-culture vs PBMCs.** Volcano plots representing the differential cytokine secretion between PBMCs/Myotubes co-culture and PBMCs models following 22 hours-stimulation with alum, Shig 4vForm, Shig4vForm+ alum, Ng GMMA and Ng GMMA+ alum at the concentration of 1 ug/ml; complete medium is used as negative control (Med). X axes represent the estimated reported as the log2 scaled differential Normalized protein expression (NPX) compared to the PBMCs single model (Estimate), while Y axes represent the statistical significance of the modulation (-log10 scaled p-value). Cytokines that are highly secreted in the PBMCs/Myotubes co-cultured model respect to PBMCs single

model are represented as red dots, in the right side, while cytokines that are decreased in PBMCs/Myotubes co-cultured respect to PBMCs single model are reported in blue dots. Cytokines highlighted in green are those that, in each model condition, are statistically different in comparison to the relative negative control (MED).

As shown in **Figure 27** , volcano plot analysis revealed that there were a broad group of cytokines which are significantly upregulated in PMCM co-culture model compared to PBMCs model. These cytokines include TSLP, CXCL10, CXCL11, CXCL9 and IL-17A that were produced following stimulation with alum-adjuvanted and non-adjuvanted *Shigella* and Ng vaccine formulations, but not by alum alone, while molecules like CCL20, MCP-2 and MMP-1 were observed in all samples, including that treated with only alum . In this context, the analysis of their NPX values in the PMCM model, showed that only CCL20 and MMP-1 were significantly higher upon stimulation with both GMMA-based vaccine formulations compared to alum (**Figure 28**).

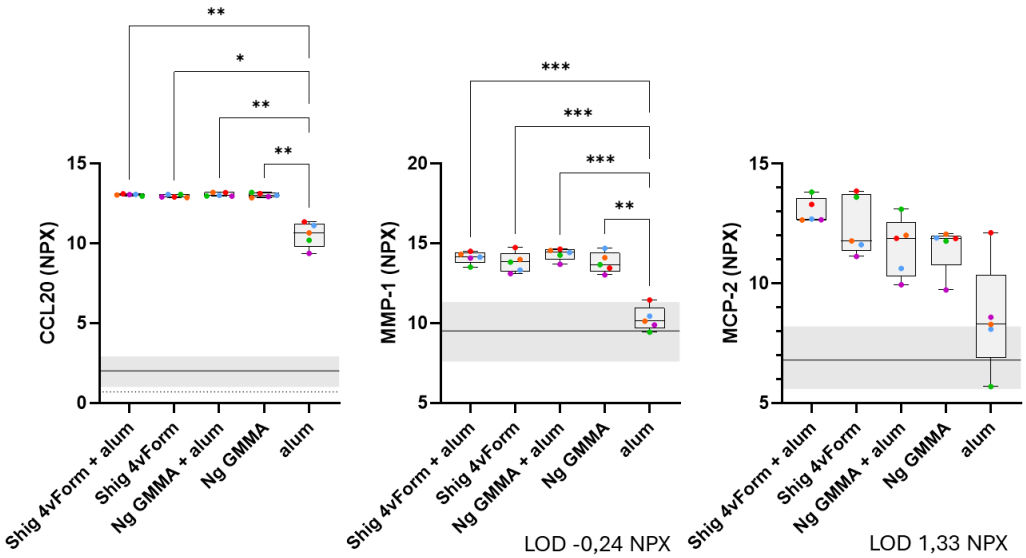

Figure 28**. Cytokine quantification in culture supernatants collected following in vitro stimulation of PMCM co-culture with Shigella and Ng GMMA-based vaccine formulations,**

with and without alum. PBMC/Myotube co-culture was stimulated for 22 hours with Shigella four-component GMMA vaccine adjuvanted with Alum (Shig 4vForm + Alum), non-adjuvanted Shigella GMMA formulation (Shig 4vForm), Neisseria gonorrhoeae GMMA vaccine with Alum (Ng GMMA + Alum), non-adjuvanted Ng GMMA and Alum alone, all at a final concentration of 1 µg/ml. Box plots show cytokine values as Normalized Protein Expression (NPX) units on a log2 scale, representing the minimum, first quartile (25th percentile), median (50th percentile), third quartile (75th percentile), and maximum. Each colored dot corresponds to an individual donor. The unstimulated sample (MED) is reported as mean value (continued black line) with its confidence interval (CI) (grey area). The dotted black line indicates the lower limit of detection (LOD). Significances observed between groups were determined using the RM one-way ANOVA with Geisser-Greenhouse correction (*p-value < 0.05, **p-value<0.005, ***p-value<0.0005, ****p-value<0.00005; ns stands for nonsignificant and are not reported, p-value > 0.05).

These cytokines and chemokines play different immune roles. MCP-2 and MCP3, also known as CCL-7 and CCL-8 respectively, are chemokines secreted by monocytes, endothelial cells, fibroblasts and, under inflammatory stimuli, skeletal muscle cells (158-162). CCL7 and CCL8, alongside CCL2 (or MCP-1), recruit immune cells, specifically monocytes to site of tissue insult (159, 163). CCL20 is also contributing to the recruitment of APCs, in particular DCs and it has been demonstrated that it is secreted by skeletal muscle cells in presence of hPBMCs or pro-inflammatory conditions like IL-17A (154, 164) which is also present in our system. It is secreted by Th17 γδT cells, and ILC3 cells and acts as an inflammatory cytokine capable to dictate tissue inflammation through the induction of pro-inflammatory cytokines (such as IL-6 and TNF), chemokines (such as KC, MCP-1 and MIP-2) and matrix metalloproteases, which mediate tissue infiltration and tissue destruction (165, 166). In particular, our results show the secretion of MMP-1 or collagenase 1 that degrades types I and III collagen facilitating the migration of immune cells

and the remodeling of the extracellular matrix (ECM) (167). CXCL9, CXCL10, and CXCL11 impact on migration, differentiation and activation of immune cells such as effector CD4+ and CD8+ T cells, cytotoxic lymphocytes (CTLs), natural killer (NK) cells, NKT cells, and macrophages and plays a major role in supporting Th1 polarization (168-170).

TSLP acts as an alarmin, being rapidly released by epithelial cells from several tissue such as skin, lungs, gut, and thymus and , under certain conditions, by dendritic cells (171) following several signals which include mechanical injury, microbial ligands such as those recognized by TLR2, TLR3, and NOD2, helminth infection, proteases like trypsin and papain, and pro-inflammatory cytokines such as IL-4, IL-13, TNF, IL-1β (172). TSLP promotes cell maturation, proliferation, survival and recruitment suggesting a pivotal role in immune response regulation (173). TSLP has an impact on a wide range of cells such as neutrophils, mast cells, basophils, eosinophils, ILC2s, NKT cells, smooth muscle cells, tumor cells, B cells and DC cells (174). Moreover, TSLP directly activates DCs and skews towards a Th2 immune response with the production of IL-5, IL-4, IL-13 and TNF (175). Overall, the wide range of actions suggests TSLP as a molecule able to amplify danger signals and inflammatory cascades (176). In addition, evaluating the differential cytokine secretion, these cytokines were low produced (IL-17A, MMP-1, CCL20, MCP-2 and MCP-3) or not produced (CXCL-9, -10, -11 and TSLP) in hPBMCs model upon stimulation with both GMMA-based vaccines (data not shown), suggesting that the PMCM model is a powerful system for investigating cell-to-cell interactions that likely shapes the immune response upon stimulation. Considering the known functional roles of these cytokines, I hypothesize that following vaccination, the skeletal muscle cells may contribute to

enhancing local inflammation by mainly recruiting infiltrating immune cells.

3.4.5 Impact of Alum on cytokine secretion induced by Shigella and Ng GMMA Vaccines in the PMCM model

The data obtained in the comparison between PBMCs and PMCM model indicate that both GMMA-based vaccines induce similar secretion of soluble factors at least in the quality. I therefore investigated the impact of alum on the cytokine response elicited by each vaccine using the PMCM model. The cytokines secretion analysis demonstrated that alum-adjuvanted *Shigella* formulation induced a higher production of CXCL11 respect to non-adjuvanted *Shigella* formulation (**Figure 29A**), while no alum's impact was observed in the case of Ng GMMA vaccine. Moreover, since I also wanted to evaluate the impact of different bacterial origin, comparing *Shigella* and Ng GMMA-based vaccines in PMCM model, CXCL11 together with CXCL10 levels were lower upon stimulation with Ng GMMA vaccine than those elicited by *Shigella* GMMA-based vaccine (**Figure 29B**). These findings highlight that the intrinsic differences among GMMA can induce subtle differences for certain cytokine, although the overall innate response triggered by both vaccines were comparable. Of note, the differential secretion of CXCL10, also known as IP-10, was also detected in Mo-DCs *in vitro* model but not in hPBMCs *in vitro* model, while CXCL11 was not detect in both systems, suggesting the PBMC model could be more useful to characterize the GMMA-based vaccine innate response.

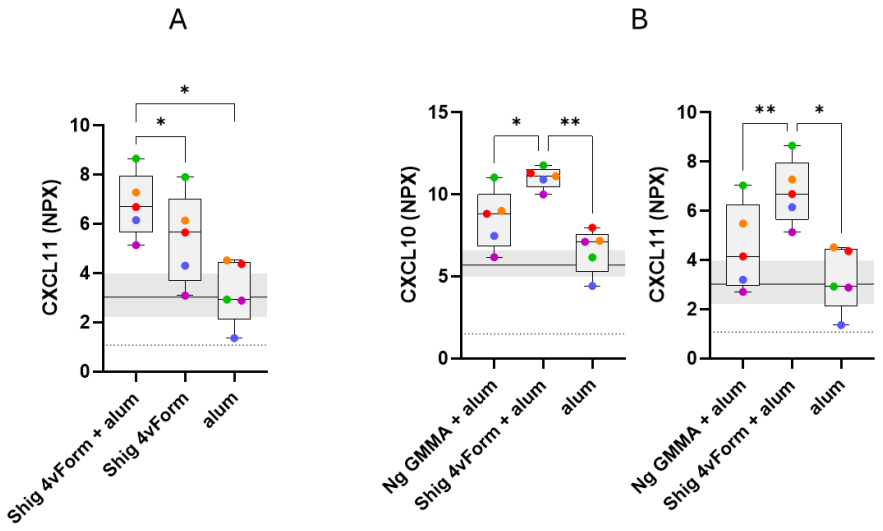

Figure 29. **Cytokine quantification in culture supernatants collected following *in vitro* stimulation of PBMCs/Myotubes co-culture with *Shigella* and Ng GMMA-based vaccine formulations, with and without alum.** PBMC/Myotube co-culture was stimulated for 22 hours with Shigella four-component GMMA vaccine adjuvanted with Alum (Shig 4vForm + Alum), non-adjuvanted Shigella GMMA formulation (Shig 4vForm), Neisseria gonorrhoeae GMMA vaccine with Alum (Ng GMMA + Alum), non-adjuvanted Ng GMMA and Alum alone, all at a final concentration of 1 µg/mL. Box plots show cytokine values as Normalized Protein Expression (NPX) units on a log2 scale, representing the minimum, first quartile (25th percentile), median (50th percentile), third quartile (75th percentile), and maximum. Each colored dot corresponds to an individual donor. The unstimulated sample (MED) is reported as mean value (continued black line) with its confidence interval (CI) (grey area). The dotted black line indicates the lower limit of detection (LOD). In panel A, it is shown the comparison in CXCL11 secretion, among Shig 4vForm + Alum, Shig 4vForm and alum alone; in panel B, it is shown the comparison in CCl19 secretion, among Ng GMMA + Alum, Ng GMMA and alum alone; in panel C, it is shown the comparison in CXCL10 and -11 secretion, among Shig 4vForm + Alum, Ng GMMA+ alum and alum alone. Significances observed between groups were determined using the RM one-way ANOVA with Geisser-Greenhouse correction (*p-value < 0.05, **p-value<0.005, ***p-value<0.0005, ****p-value<0.00005; ns stands for nonsignificant and are not reported, p-value > 0.05).

4. DISCUSSION

Despite the constant scientific research, the spread of drug-resistant pathogens is increasing (3-9), amplifying the urgency for novel therapeutics and prophylactic strategies, where the Outer Membrane Vesicles (OMV) technology represents a promising approach. OMV are nanometric vesicles secreted by gram-negative bacteria that present antigens in their native conformation, offering a strong immunogenicity and self-adjuvanticity (22, 27, 30, 39, 81, 177). To enhance vesicle release and reduce endotoxicity, genetically modified vesicles known as Generalized Modules for Membrane antigens (GMMA) have been developed (22, 39, 49, 58, 59). Currently, GMMA's research based on a classical (55, 85, 105) as well as a multidimensional (67, 68) approach has deeply characterized GMMA-induced innate immune cell response, demonstrating the induction of mainly pro-inflammatory cytokines (e.g. TNFα, IL-6, IL-18, IFN-γ, IL-1β, MIP-1α, GM-CSF) alongside an extensive cellular activation in hPBMCs (monocytes, DC and NK cells) (67).

However, while these studies have provided valuable insights into GMMA–immune cell interactions, a comprehensive understanding of the mode of action of GMMA in vaccine formulations, particularly those derived from *Shigella* and *Neisseria gonorrhoeae, r*emains incomplete.

In this context, our study aimed to dissect the immunological mechanisms triggered by GMMA-based vaccine against *Shigella* and *Neisseria gonorrhoeae*, focusing on innate immune cells response and its capacity to shape *in vitro* the adaptive responses. To achieve this, I employed a well-established multiparametric *in vitro* immune characterization approach on hPBMCs (67), which let to define a comprehensive immune profile of GMMA-based vaccines.

To further investigate the direct cellular targets of GMMA, I focused on Mo-DCs as a simplified *in vitro* system. This choice was based on previous findings identifying DCs and monocytes as primary responders to GMMA stimulation in hPBMCs cultures (67). The use of Mo-DCs enabled us to explore the direct effects of GMMA on APCs, shedding light on their role in shaping the downstream adaptive immune response.

Moreover, I implemented an *in vitro* T cell polarization model to evaluate how the innate signals induced by GMMA influence the differentiation of T helper cell subsets. This model proved to be a valuable tool for understanding the link between innate activation and the induction of specific adaptive immune profiles, particularly in terms of Th1/Th2/Th17 responses.

Finally, to gain insights into the local immunological microenvironment at the site of vaccine administration, I developed an *in vitro* co-culture system involving skeletal muscle cells and immune cells. Given the emerging evidence that the injection site acts as an active immunological niche, this model allowed us to investigate the cellular crosstalk and the potential contribution of non-immune cells to the overall vaccine-induced response. Understanding these interactions is crucial for elucidating the mechanism of action of GMMA-based vaccines and optimizing their design for enhanced immunogenicity and safety.

The multiparametric approach adopted in this study combined the quantification of cytokine and chemokine secretion using classical platforms such as Mesoscale and Luminex, with more sophisticated technologies like Olink, enabling a deeper profiling of the innate immune response. In parallel, flow cytometry was used to assess cellular activation markers. The integration of data from these complementary

methodologies provided a robust and multidimensional characterization of the immune cells' response elicited by GMMA-based vaccines.

The study showed that both *Shigella* and *N. gonorrhoeae* GMMA-based vaccines induced a predominant pro-inflammatory cytokine profile, with a clear production of cytokines like IL-1α, IL-1β, TNF-α, IL-6, IL-8, IFN-γ along with chemokines like MCP-1, and MIP-1α. Interestingly, the anti-inflammatory cytokine IL-10 was also detected, suggesting a potential regulatory mechanism aimed at modulating excessive inflammation within the *in vitro* system (178). These cytokines are most likely produced primarily by professional APCs, such as monocytes and dendritic cells (DCs), which also upregulate CD83 in response to GMMA, as well as by natural killer (NK) cells, where IFN-γ production is accompanied by CD69 upregulation (179, 180). Furthermore, modest activation was also observed for CD4+ T cells with the upregulation of CD69, probably due to a bystander effect. Of note, I demonstrated that GMMA included in *Shigella* GMMA-based vaccine, derived from different *Shigella* serotypes, induce an immune cell activation that was comparable to that elicited by their combination, suggesting that the combination of several serotypes in a single formulation don't affect neither their self-adjuvanticity or show a synergistic effect in inducing the innate response *in vitro*. Building on the observed pro-inflammatory profile induced by GMMA alone, I further investigated the impact of formulation with alum, a widely used adjuvant in human vaccines. Indeed, the study showed that both *Shigella* and *Neisseria gonorrhoeae* GMMA-based vaccines, when adjuvanted with alum, elicited a markedly stronger immune cells response compared to their non-adjuvanted counterparts. This enhancement was evident in the increased secretion of cytokines such as

IL-1α, IL-1β, IL-6, TNF-α, and IFN-γ in both hPBMCs and Mo-DCs, as well as IL-12, IL-13, and IL-15 specifically in Mo-DCs. A parallel increase in cellular activation was observed in monocytes, DCs, and Mo-DCs. Nevertheless, alum administered alone didn't induce any response, suggesting that it acted in synergy with GMMA in the formulation and not as independent enhancer. This synergy may be attributed to alum's physicochemical properties: its positively charged, micrometric crystalline particles can efficiently adsorb acidic antigens and interact with negatively charged immune cells, while remaining within a size range suitable for phagocytosis (181). These features likely facilitate enhanced antigen uptake and presentation by antigen-presenting cells at the site of injection (182). Indeed, it has been demonstrated, both *in vitro* and *in vivo*, that $AlOH_3$ enhances the antigen uptake and processing which correlates with activation and maturation of APCs (182-186). Therefore, I hypothesize that the adsorption of GMMA on alum allows the presentation of GMMA in particulate form which can be more antigenic and effectively phagocytosed. However, this hypothesis requires further experimental validation. Confocal microscopy studies could provide direct evidence of GMMA-alum interactions and their uptake by immune cells, helping to clarify the physical and functional dynamics of this synergistic mechanism. A key indicator of this synergistic effect was the significant increase in IL-1β production that I observed following stimulation with alum-adjuvanted GMMA formulations, compared to the non-adjuvanted formulations. This finding aligns with established mechanisms of alum adjuvanticity, including activation of the NLRP3 inflammasome, complement pathways, and release of DAMPs such as uric acid and host DNA, all of which contribute to IL-1β secretion (187). In particular, *in vivo*

and *in vitro* studies showed that NLRP3 activation leads to IL-1β secretion (188-192), a pro-inflammatory cytokine that supports adaptive immunity and Th2 polarization (190, 192, 193). In contrast to cytokine profile induced by alum-adjuvanted formulations including IL-1β, IL-18, this study revealed that alum-adjuvanted GMMA formulations also triggered significant production of other cytokines, such as IL-6, IFN-γ, TNF-α, and IL-12. These pro-inflammatory mediators are known to be involved in innate immune responses and are typically secreted upon activation of TLRs pathway strongly engaged by GMMA (56). Overall, these findings suggest that there is a synergism between alum and GMMA components mechanisms of action, resulting in a stronger innate immune cells response.

Another important aspect I aimed to dissect was how the bacterial origin of GMMA influences the immune response. Notably, despite the different bacterial origin, both *Shigella* and Ng GMMA-based vaccines induced a similar quality of innate immune cell response, mainly characterized by the production of pro-inflammatory cytokines by both hPBMCs and Mo-DCs. Nevertheless, I observed differences in the magnitude of specific cytokines such as IFN-γ, IL-10, IL-1α, IL-6, and TNF-α, highlighting distinct patterns of immune modulation between the two GMMA formulations. While these variations are evident *in vitro*, it remains challenging to directly extrapolate their impact *in vivo*. What emerges clearly, however, is that both GMMA constructs activate a comparable innate immune signature, supporting the concept of GMMA as a versatile and consistent vaccine platform. As described above, to further explore the cellular mechanisms underlying GMMA-induced innate immunity, I focused on Mo-DCs, a widely used *in vitro model* for studying DCs function and their role in

shaping adaptive immune responses (194, 195). APCs, through PRRs like TLRs, detect pathogens or vaccines and, by shaping the cytokine environment, direct naïve $CD4^+$ T-helper cells toward protective subsets, thereby orchestrating effective adaptive immunity (155, 200, 201). I demonstrated that Mo-DCs were activated after GMMA-based vaccines stimulation and efficiently internalized GMMA, a process that is crucial for the maturation and subsequent antigen presentation functions. As DCs underwent maturation influenced by GMMA uptake, they shaped the surrounding cytokine milieu characterized by both pro-inflammatory cytokines and chemokines. Notably, among these cytokines, there was IL-12, which strictly polarizes the T helper cell towards a Th1 phenotype and also were IL-6 and IL-1β that may contribute to drive a Th17 phenotype (196). Indeed, the naive CD4+ T helper cells polarization *in vitro* established in this research, showed that supernatants derived from both *Shigella* and Ng GMMA vaccine- treated Mo-DCs skewed naive CD4+ T helper cells towards Th1 phenotype. Th1 cells, defined by IFN-γ secretion and T-bet expression, are important for protective immune response against intracellular pathogens, fungi and protozoa (196). Particularly, Th1 cells, activate macrophages enhancing phagocytic killing and supporting the development of cytotoxic $CD8^+$ T cells which are critical for intracellular bacteria elimination (197, 198). Th1 cells also help B cells in producing opsonizing and complement-fixing antibodies which also contribute to intracellular bacteria clearance, critical for protective efficacy (199). The ability of GMMA-based vaccines to induce Th1 differentiation suggests its advantage in supporting robust T cell-mediated immunity which, alongside the antibody generation, is fundamental for an effective vaccine protection (200). Therefore, the optimized T cell

polarization *in vitro* model is a suitable tool for comprehensively understanding how the innate immune cells response induced by the GMMA vaccine can influence the induction of specific T helper cell–mediated adaptive immune responses.

To gain deeper insights into the mechanism of action of GMMA-based vaccines beyond immune cell activation, I investigated the local microenvironment at the injection site. This niche, composed of both immune and non-immune cells, plays a crucial role in shaping the early phases of the immune response through cellular crosstalk and localized signaling events (75). Given that GMMA-based vaccines are administrated intramuscularly, I focused on skeletal muscle cells and their crosstalk with immune cells following GMMA vaccination. Recent evidence indicates that skeletal muscle cells can produce a range of cytokines, called specifically “myokines“ including IL-6, IL-8, IL-1β and CCL2, CCL3, CXCL10, in response to pro-inflammatory stimuli (e.g., IFN-γ and TLR ligands such as LPS, CpG) (74). In line with these findings, I demonstrated that human skeletal muscle myoblasts, and *in vitro* differentiated myotubes secrete cytokines such as interleukin-6 (IL-6), IL-8, as well as chemokines like CCL-20, CXCL1, CXCL5 and CXCL6 upon stimulation with GMMA-based vaccines. These myokines are involved in several processes including, inflammatory responses, and the recruitment of several immune cells such as dendritic cells (DCs), neutrophils, monocytes and Th17/Tfh (162, 201-205), thus underlining the immunocompetency of muscle cells. This activation may be mediated by TLRs since they are expressed on skeletal muscle cells (154, 206). Furthermore, confocal microscopy revealed that myotubes interacted with and internalized GMMA, implying that muscle cells can contribute to

immune response not only modulating the cytokine environment but also acting as non-professional APC, potentially offering a substrate for antigen presentation. This finding is preliminary evidence. Indeed, the complete antigen presentation cascade including antigen uptake, processing, peptide-MHC complex formation, and subsequent T-cell activation need to be investigated through additional experiments. Nonetheless, there are some important features that may be considered to understand the internalization mechanism. Skeletal muscle cells have a unique membrane architecture characterized by a rich caveolae's composition maintained by the caveolin–cavin system (207, 208), providing a lipid raft-rich platform that ideally support the capture of nanoscale vesicles. This process is further refined by accessory receptors such as CD36, basally expressed in differentiated myotubes and scavenger receptors including SREC-I/SCARF1. The receptor CD36 binds LPS and lipoproteins, cooperating with CD14/TLR4, whereas SRECI/SCARF1 recruits TLR4 into cholesterol-rich microdomains to facilitate- co-internalization (209-211). Moreover, TLR2, which is strongly inducible in myotubes, may be a co-sensor since the high lipoprotein's presence in GMMA' composition. Indeed, CD36 may also partner with TLR2 for lipoprotein recognition (211). Despite these interactions suggest that GMMA' internalization may be mediated through multiple entry routes, this hypothesis needs to be explored experimentally. However, since it has been demonstrated that both professional APCs, such as Mo-DCs, and non-professional APCs, such as muscle cells, can internalize GMMA, it is reasonable to hypothesize the induction of a specific CD4+ and CD8+ T-cell response. From an experimental perspective, *in vitro* antigen presentation models could be developed based on the co-culture

of autologous T cells and Mo-DCs. T-cell responses could be evaluated through multiple parameters, including activation (upregulation of markers such as CD25, CD69, OX40, ICOS, and CD40L); proliferation using assays such as CFSE dilution or cytokine production (IFN-γ, TNF-α, IL-2, IL-4, IL-13, IL-17A, and Granzyme B) through intracellular cytokine staining (212). Although I demonstrated that myotubes actively interacted with GMMA-based vaccine, to better mimic the *in vivo* microenvironment at the site of vaccine injection, I employed the primary muscle cell model (PMCM) comprising a co-culture of myotubes and PBMCs. In this system, PBMCs serve as the immune compartment that initiates local inflammation and directs the subsequent adaptive response. The PMCM thus provides a more physiologically relevant *in vitro* model for studying the mode of action and immunogenicity of GMMA-based vaccines compared with PBMC or myotubes single cultures. To better interpret the complexity of the immune response across different culture conditions, I performed a PCA, which allowed us to reduce data dimensionality and identify global patterns of variation. The PCA comparing the PMCM co-culture, myotube monoculture, and PBMC monoculture revealed statistically significant differences among the three groups. Notably, cytokines such as IL-6, CSF-1, and CCL20, associated with inflammation, muscle activation and immune cell recruitment (202, 203, 213), were significantly secreted in the PMCM co-culture respect to individual cultures. This evidence gives an insight on how the crosstalk between immune cells and muscle cells, without any external stimulus, can define a different immunological environment, absent in the monocultures, which can influence the vaccine response. Interestingly, the myotube culture showed minimal cytokine secretion, while most cytokines

associated with the co-culture were either absent or produced at lower levels in PBMC monocultures. These findings highlight the importance of synergistic interactions between muscle and immune cells in establishing the unique local milieu at the injection site. In the PMCM co-culture model, I observed a distinct cytokine and chemokine profile that reflects the complexity of the local immune microenvironment at the injection site. Several mediators, including leukemia inhibitory factor (LIF), osteoprotegerin (OPG), hepatocyte growth factor (HGF) and leukocytes chemo-attractants including CCL2, CCL7, CCL20, CXCL1, CXCL5, CXCL6 and CXCL8, were highly basally expressed in PMCM system. These molecules are involved in inflammation, tissue repair, and immune cell recruitment, highlighting the immunocompetency of muscle cells and their active role in shaping the early immune response. IL-6, as previous mentioned is produced by both myotubes and immune cells being crucial both in muscle function and cellular crosstalk leading DC maturation and regulation of Tfh/IL-21 programs (202, 214, 215). LIF, a cytokine belonging to IL-6 family is important in inflammation as well as tissue repair processes and OPG, alongside HGF, are crucial in regulating the balance between inflammation and tissue repair which is finely tuned during the early vaccine- induce immune activation (216-218). This synergism was particularly evident upon stimulation with GMMA-based vaccine which induced the predominant secretion of C-C chemokine family members (CCL7, CCL8, CCL20), already mentioned, and C-X-C chemokine family members (CXCL9, CXCL10 and CXCL11) which regulate the migration and activation of effector T cells, NK cells, and macrophages, thus promoting a Th1-polarized response (168-170). Moreover, the metalloprotease MMP-1, implicated in extracellular matrix remodeling (167), was significantly

elevated, indicating that beyond recruiting immune cells, the muscle cells can also contribute to their localization. Furthermore, GMMA-based vaccine stimulation of PMCM co-culture resulted in marked production of IL-17A and Thymic Stromal Lymphopoietin (TSLP) which further potentiate the local inflammatory response. IL-17A can induce proinflammatory cytokines (such as IL-6 and TNF), chemokines (such as MCP-1 and MIP-2)(164) while TSLP, secreted in response to injury and/or microbial signals, amplifies inflammation by activating dendritic cells. Moreover, it is reported that TSLP drives the response toward a Th2 profile through the induction of IL-4, IL-5, IL-13, and TNF(175, 176). Therefore, it is important to fully elucidate how the immunological environment triggered at the site of injection, influence the final Th cells response.

Interestingly, as observed in the hPBMCs and Mo-DCs *in vitro* system, the quality of innate immune responses generated by alum-adjuvanted and non-adjuvanted formulation was similar with a differential secretion, in this context, only observed for the chemokine CXCL11 upon stimulation with alum-adjuvanted *Shigella* GMMA- based vaccine, while no alum's impact was observed following N. *gonorrhoeae* GMMA formulations. This evidence advises that, at least in the context of *Shigella* GMMA-based vaccine stimulation *in vitro*, alum can enhance lymphocyte chemotaxis to favor a Th1 type response as CXCL11 is a chemokine implicated into Th cell recall in situ. Moreover, as demonstrated in hPBMCs and Mo-DCs *in vitro* models, *Shigella* and Ng GMMA-based vaccines showed to induce a similar innate immune response with some differences in the magnitude. Specifically in this model, differences were observed for chemokines CXCL10 and CXCL11, which were higher upon *Shigella* GMMA-based vaccine compared to *N. gonorrhoeae* GMMA-based vaccines. Therefore,

GMMA-based vaccines activate a comparable innate immune signature though with subtle differences for certain cytokines which likely relate to the intrinsic features linked to the bacterial origin of GMMA.

Altogether, these data demonstrate that the PMCM model not only mimics key aspects of *in vivo* immune activation but also provides a physiologically relevant tool to study cell–cell interactions at the injection site. In this model, I hypothesize that GMMA-based vaccines trigger a dual response: PBMCs produce pro-inflammatory cytokines and chemokines (e.g., IL-6, TNF, IL-1, CCL2), while myotubes secrete myokines (e.g., IL-6, CCL20) that are crucial for DCs recruitment and T cell activation (55, 66). The IL-17A–driven environment further amplifies CCL20 production, enhancing DC recruitment. This signaling cascade promotes the secretion of MCP-2 and MCP-3 (CCL8 and CCL7), which provide monocyte recruitment and their subsequent differentiation into DCs (67, 68). This integrated signaling also induces interferon-inducible chemokines (CXCL9, CXCL10, CXCL11), recruiting effector CD4+ and CD8+ T cells, NK cells, and macrophages to support Th1 polarization. Additionally, TSLP release acts as an alarmin, enhancing DCs maturation and promoting a potential Th2 bias. Consequently, the overall T cell response is likely regulated by the balance between Th1-inducing cytokines and Th2-associated signals that need to be fully elucidated through further experimental investigation. Moreover, the increased production of MMP-1 could provide an insight of what can happen in a tissue context, where this metalloproteinase can help in cellular repositioning. Overall, these data suggest that the microenvironment shaped by the crosstalk between muscle and immune cells is crucial for the early steps of GMMA vaccine-induced immune responses. The PMCM model represents a valuable

platform for dissecting these mechanisms and advancing our understanding of GMMA-based vaccines immunogenicity as well as other vaccines formulations.

In summary, this study suggests that GMMA- based vaccine are likely to activate innate immunity at the site of injection not only through classical immune cells such as monocytes, dendritic cells, and NK cells, but also by engaging non-immune cells like skeletal muscle cells, which contribute to shaping the local environment via cytokine and chemokine production. This highlights the intrinsic self-adjuvanticity of GMMA and its capacity to initiate a multifaceted immune response. Notably, I demonstrated that alum enhances the GMMA immunostimulatory properties through a synergistic mechanism, likely involving amplification of pro-inflammatory signaling and modulation of antigen presentation due to final vaccine particles size. These findings support the strategic use of adjuvants to fine-tune vaccine formulations and improve immunogenicity. Although GMMA derived from different bacterial sources such as *Shigella* and *Neisseria gonorrhoeae,* a qualitatively similar pro-inflammatory profile, subtle differences in cytokine magnitude suggest that pathogen-specific components may influence the immune response. Moreover, this study showed the critical role of the injection site as an active immunological niche. The PMCM model lets us dissect the cellular crosstalk that occurs locally, evidencing how muscle cells contribute to immune cell recruitment, activation, and polarization. This model provides a physiologically relevant platform to study early vaccine-induced events and could be used to investigate other vaccine platforms. These findings have important implications for the rational design of next-generation vaccines. Understanding how GMMA interact with both

immune and non-immune cells, and how adjuvants modulate these interactions, can lead the development of formulations that optimize both safety and efficacy. Moreover, the identification of key cytokines and chemokines involved in early immune activation provides potential biomarkers for evaluating vaccine potency and predicting immunogenicity. Overall, this study emphasizes the potential of GMMA as a versatile and effective vaccine platform and provides a base for further exploration into the cellular and molecular mechanisms that drive vaccine-induced immunity.

5. FUNDING & TRANSPARENCY STATEMENT

This work was sponsored by GlaxoSmithKline Biologicals SA. Mariateresa Marrocco is a PhD student at University of Siena and participated in a postgraduate studentship program at GSK.

6. REFERENCES

1. Zahid A, Ismail H, Wilson JC, Grice ID. Bioengineering Outer-Membrane Vesicles for Vaccine Development: Strategies, Advances, and Perspectives. Vaccines. 2025;13(7):767.
2. Bloom DE, Black S, Salisbury D, Rappuoli R. Antimicrobial resistance and the role of vaccines. Proceedings of the National Academy of Sciences. 2018;115(51):12868-71.
3. Akhondi H, Goldin J, Simonsen KA. Bacterial Diarrhea. StatPearls. Treasure Island (FL): StatPearls Publishing

4. Global burden of 369 diseases and injuries in 204 countries and territories, 1990-2019: a systematic analysis for the Global Burden of Disease Study 2019. Lancet. 2020;396(10258):1204-22.
5. (WHO) WHO. Global priority list of antibiotic-resistant bacteria to guide research, discovery, and development of new antibiotics 2024 [This WHO document reports a list of antibiotic-resistant bacteria to help in prioritizing research and development investments for new and effective interventions]. Available from: https://www.who.int/news/item/17-05-2024-who-updates-list-of-drug-resistant-bacteria-most-threatening-to-human-health#:~:text=The%20World%20Health%20Organization%20%28WHO%29%20today%20released%20its,into%20critical%2C%20high%20and%20medium%20categories%20for%20prioritization.
6. (WHO) WHO. Urgent call for better use of existing vaccines and development of new vaccines to tackle AMR 2022 [This document reports the pipeline of the vaccines currently in development to prevent infections caused by antimicrobial-resistant (AMR) bacterial pathogens]. Available from: https://www.who.int/news/item/12-07-2022-urgent-call-for-better-use-of-existing-vaccines-and-development-of-new-vaccines-to-tackle-amr.
7. prevention CfDca. New CDC analysis shows steep and sustained increases in STDs in recent years 2018 [updated 28 August 2018. Available from: https://archive.cdc.gov/#/details?url=https://www.cdc.gov/media/releases/2018/p0828-increases-in-stds.html.
8. Diseases ECfDPaCSAoI. Surveillance atlas of infectious diseases 2017 [updated 28 April 2023. Available from: https://www.ecdc.europa.eu/en/surveillance-atlas-infectious-diseases.
9. Hendriksen RS, Munk P, Njage P, van Bunnik B, McNally L, Lukjancenko O, et al. Global monitoring of antimicrobial resistance based on metagenomics analyses of urban sewage. Nature Communications. 2019;10(1):1124.
10. Micoli F, Bagnoli F, Rappuoli R, Serruto D. The role of vaccines in combatting antimicrobial resistance. Nat Rev Microbiol. 2021;19(5):287-302.
11. Baker SJ, Payne DJ, Rappuoli R, De Gregorio E. Technologies to address antimicrobial resistance. Proceedings of the National Academy of Sciences. 2018;115(51):12887-95.

12. Costanzo V, Roviello GN. The Potential Role of Vaccines in Preventing Antimicrobial Resistance (AMR): An Update and Future Perspectives. Vaccines (Basel). 2023;11(2).
13. Clift C, Salisbury DM. Enhancing the role of vaccines in combatting antimicrobial resistance. Vaccine. 2017;35(48 Pt B):6591-3.
14. Bagnoli F, Payne DJ. Reaction: Alternative Modalities to Address Antibiotic-Resistant Pathogens. Chem. 2017;3(3):369-72.
15. James SL, Abate D, Abate KH, Abay SM, Abbafati C, Abbasi N, et al. Global, regional, and national incidence, prevalence, and years lived with disability for 354 diseases and injuries for 195 countries and territories, 1990–2017: a systematic analysis for the Global Burden of Disease Study 2017. The lancet. 2018;392(10159):1789-858.
16. Ghattas M, Dwivedi G, Lavertu M, Alameh M-G. Vaccine Technologies and Platforms for Infectious Diseases: Current Progress, Challenges, and Opportunities. Vaccines. 2021;9(12):1490.
17. Mba IE, Sharndama HC, Anyaegbunam ZKG, Anekpo CC, Amadi BC, Morumda D, et al. Vaccine development for bacterial pathogens: Advances, challenges and prospects. Tropical Medicine & International Health. 2023;28(4):275-99.
18. Minor PD. Live attenuated vaccines: Historical successes and current challenges. Virology. 2015;479:379-92.
19. Gupta S, Pellett S. Recent developments in vaccine design: from live vaccines to recombinant toxin vaccines. Toxins. 2023;15(9):563.
20. Gote V, Bolla PK, Kommineni N, Butreddy A, Nukala PK, Palakurthi SS, et al. A comprehensive review of mRNA vaccines. International journal of molecular sciences. 2023;24(3):2700.
21. Antonelli G, Cappelli L, Cinelli P, Cuffaro R, Manca B, Nicchi S, et al. Strategies to Tackle Antimicrobial Resistance: The Example of Escherichia coli and Pseudomonas aeruginosa. International Journal of Molecular Sciences. 2021;22(9):4943.
22. van der Pol L, Stork M, van der Ley P. Outer membrane vesicles as platform vaccine technology. Biotechnology Journal. 2015;10(11):1689-706.
23. Li R, Liu Q. Engineered bacterial outer membrane vesicles as multifunctional delivery platforms. Frontiers in Materials. 2020;7:202.
24. Furuyama N, Sircili MP. Outer Membrane Vesicles (OMVs) Produced by Gram-Negative Bacteria: Structure, Functions, Biogenesis, and Vaccine Application. Biomed Res Int. 2021;2021:1490732.
25. Lieberman LA. Outer membrane vesicles: A bacterial-derived vaccination system. Front Microbiol. 2022;13:1029146.
26. Schwechheimer C, Kuehn MJ. Outer-membrane vesicles from Gram-negative bacteria: biogenesis and functions. Nat Rev Microbiol. 2015;13(10):605-19.
27. Ellis TN, Kuehn MJ. Virulence and immunomodulatory roles of bacterial outer membrane vesicles. Microbiol Mol Biol Rev. 2010;74(1):81-94.
28. Schooling SR, Beveridge TJ. Membrane vesicles: an overlooked component of the matrices of biofilms. Journal of bacteriology. 2006;188(16):5945-57.
29. Micoli F, MacLennan CA. Outer membrane vesicle vaccines. Semin Immunol. 2020;50:101433.

30. Kulkarni HM, Jagannadham MV. Biogenesis and multifaceted roles of outer membrane vesicles from Gram-negative bacteria. Microbiology. 2014;160(10):2109-21.
31. Kulp A, Kuehn MJ. Biological functions and biogenesis of secreted bacterial outer membrane vesicles. Annual review of microbiology. 2010;64(1):163-84.
32. Lee EY, Choi DS, Kim KP, Gho YS. Proteomics in gram-negative bacterial outer membrane vesicles. Mass spectrometry reviews. 2008;27(6):535-55.
33. van der Ley P, van den Dobbelsteen G. Next-generation outer membrane vesicle vaccines against Neisseria meningitidis based on nontoxic LPS mutants. Human Vaccines. 2011;7(8):886-90.
34. Georgieva M, Buckee CO, Lipsitch M. Models of immune selection for multi-locus antigenic diversity of pathogens. Nat Rev Immunol. 2019;19(1):55-62.
35. Kuehn MJ, Kesty NC. Bacterial outer membrane vesicles and the host-pathogen interaction. Genes Dev. 2005;19(22):2645-55.
36. Mashburn-Warren LM, Whiteley M. Special delivery: vesicle trafficking in prokaryotes. Mol Microbiol. 2006;61(4):839-46.
37. Bonnington KE, Kuehn MJ. Protein selection and export via outer membrane vesicles. Biochim Biophys Acta. 2014;1843(8):1612-9.
38. Ellis TN, Leiman SA, Kuehn MJ. Naturally produced outer membrane vesicles from Pseudomonas aeruginosa elicit a potent innate immune response via combined sensing of both lipopolysaccharide and protein components. Infect Immun. 2010;78(9):3822-31.
39. Mancini F, Rossi O, Necchi F, Micoli F. OMV Vaccines and the Role of TLR Agonists in Immune Response. Int J Mol Sci. 2020;21(12).
40. Dowling DJ, Sanders H, Cheng WK, Joshi S, Brightman S, Bergelson I, et al. A meningococcal outer membrane vesicle vaccine incorporating genetically attenuated endotoxin dissociates inflammation from immunogenicity. Frontiers in immunology. 2016;7:562.
41. Gerritzen MJ. Production of bioengineered outer membrane vesicles as a vaccine platform: Wageningen University and Research; 2019.
42. Arigita C, Jiskoot W, Westdijk J, van Ingen C, Hennink WE, Crommelin DJ, et al. Stability of mono- and trivalent meningococcal outer membrane vesicle vaccines. Vaccine. 2004;22(5-6):629-42.
43. Kis Z, Shattock R, Shah N, Kontoravdi C. Emerging Technologies for Low-Cost, Rapid Vaccine Manufacture. Biotechnol J. 2019;14(7):1-2.
44. Berlanda Scorza F, Colucci AM, Maggiore L, Sanzone S, Rossi O, Ferlenghi I, et al. High yield production process for Shigella outer membrane particles. PLoS One. 2012;7(6):e35616.
45. Rappuoli R, Black S, Bloom DE. Vaccines and global health: In search of a sustainable model for vaccine development and delivery. Sci Transl Med. 2019;11(497).
46. Piccioli D, Bartolini E, Micoli F. GMMA as a 'plug and play' technology to tackle infectious disease to improve global health: context and perspectives for the future. Expert Rev Vaccines. 2022;21(2):163-72.
47. Li R, Liu Q. Engineered Bacterial Outer Membrane Vesicles as Multifunctional Delivery Platforms. Frontiers in Materials. 2020;Volume 7 - 2020.

48. Micoli F, Adamo R, Nakakana U. Outer Membrane Vesicle Vaccine Platforms. BioDrugs. 2024;38(1):47-59.
49. Gnopo YMD, Watkins HC, Stevenson TC, DeLisa MP, Putnam D. Designer outer membrane vesicles as immunomodulatory systems - Reprogramming bacteria for vaccine delivery. Adv Drug Deliv Rev. 2017;114:132-42.
50. Balhuizen MD, Veldhuizen EJ, Haagsman HP. Outer membrane vesicle induction and isolation for vaccine development. Frontiers in Microbiology. 2021;12:629090.
51. Turner L, Praszkier J, Hutton ML, Steer D, Ramm G, Kaparakis-Liaskos M, et al. Increased outer membrane vesicle formation in a Helicobacter pylori tolB mutant. Helicobacter. 2015;20(4):269-83.
52. Bernadac A, Gavioli M, Lazzaroni J-C, Raina S, Lloubès R. Escherichia coli tol-pal mutants form outer membrane vesicles. Journal of bacteriology. 1998;180(18):4872-8.
53. Mitra S, Sinha R, Mitobe J, Koley H. Development of a cost-effective vaccine candidate with outer membrane vesicles of a tolA-disrupted Shigella boydii strain. Vaccine. 2016;34(15):1839-46.
54. Gerke C, Colucci AM, Giannelli C, Sanzone S, Vitali CG, Sollai L, et al. Production of a Shigella sonnei Vaccine Based on Generalized Modules for Membrane Antigens (GMMA), 1790GAHB. PLoS One. 2015;10(8):e0134478.
55. Rossi O, Pesce I, Giannelli C, Aprea S, Caboni M, Citiulo F, et al. Modulation of endotoxicity of Shigella generalized modules for membrane antigens (GMMA) by genetic lipid A modifications: relative activation of TLR4 and TLR2 pathways in different mutants. J Biol Chem. 2014;289(36):24922-35.
56. Rossi O, Caboni M, Negrea A, Necchi F, Alfini R, Micoli F, et al. Toll-Like Receptor Activation by Generalized Modules for Membrane Antigens from Lipid A Mutants of Salmonella enterica Serovars Typhimurium and Enteritidis. Clin Vaccine Immunol. 2016;23(4):304-14.
57. Keiser PB, Biggs-Cicatelli S, Moran EE, Schmiel DH, Pinto VB, Burden RE, et al. A phase 1 study of a meningococcal native outer membrane vesicle vaccine made from a group B strain with deleted lpxL1 and synX, over-expressed factor H binding protein, two PorAs and stabilized OpcA expression. Vaccine. 2011;29(7):1413-20.
58. Schromm AB, Brandenburg K, Loppnow H, Moran AP, Koch MH, Rietschel ET, et al. Biological activities of lipopolysaccharides are determined by the shape of their lipid A portion. Eur J Biochem. 2000;267(7):2008-13.
59. Pfalzgraff A, Correa W, Heinbockel L, Schromm AB, Lübow C, Gisch N, et al. LPS-neutralizing peptides reduce outer membrane vesicle-induced inflammatory responses. Biochim Biophys Acta Mol Cell Biol Lipids. 2019;1864(10):1503-13.
60. Micoli F, Alfini R, Di Benedetto R, Necchi F, Schiavo F, Mancini F, et al. GMMA is a versatile platform to design effective multivalent combination vaccines. Vaccines. 2020;8(3):540.
61. Micoli F, Alfini R, Di Benedetto R, Necchi F, Schiavo F, Mancini F, et al. GMMA Is a Versatile Platform to Design Effective Multivalent Combination Vaccines. Vaccines (Basel). 2020;8(3).
62. Zhao T, Cai Y, Jiang Y, He X, Wei Y, Yu Y, et al. Vaccine adjuvants: mechanisms and platforms. Signal Transduction and Targeted Therapy. 2023;8(1):283.

63. Kang JY, Nan X, Jin MS, Youn S-J, Ryu YH, Mah S, et al. Recognition of lipopeptide patterns by Toll-like receptor 2-Toll-like receptor 6 heterodimer. Immunity. 2009;31(6):873-84.
64. Tavano R, Franzoso S, Cecchini P, Cartocci E, Oriente F, Aricò B, et al. The membrane expression of Neisseria meningitidis adhesin A (NadA) increases the proimmune effects of MenB OMVs on human macrophages, compared with NadA–OMVs, without further stimulating their proinflammatory activity on circulating monocytes. Journal of leukocyte biology. 2009;86(1):143-53.
65. Winter J, Letley D, Rhead J, Atherton J, Robinson K. Helicobacter pylori membrane vesicles stimulate innate pro-and anti-inflammatory responses and induce apoptosis in Jurkat T cells. Infection and immunity. 2014;82(4):1372-81.
66. Mancini F, Alfini R, Caradonna V, Monaci V, Carducci M, Gasperini G, et al. Exploring the Role of GMMA Components in the Immunogenicity of a 4-Valent Vaccine against Shigella. Int J Mol Sci. 2023;24(3).
67. Tondi S, Clemente B, Esposito C, Sammicheli C, Tavarini S, Martin LB, et al. Dissecting in Vitro the Activation of Human Immune Response Induced by Shigella sonnei GMMA. Front Cell Infect Microbiol. 2022;12:767153.
68. Tondi S, Siena E, Essaghir A, Bozzetti B, Bechtold V, Scaillet A, et al. Molecular Signature of Monocytes Shaped by the Shigella sonnei 1790-Generalized Modules for Membrane Antigens Vaccine. Int J Mol Sci. 2024;25(2).
69. Mancini F, Micoli F, Necchi F, Pizza M, Berlanda Scorza F, Rossi O. GMMA-Based Vaccines: The Known and The Unknown. Frontiers in Immunology. 2021;Volume 12 - 2021.
70. Chatterjee D, Chaudhuri K. Vibrio cholerae O395 outer membrane vesicles modulate intestinal epithelial cells in a NOD1 protein-dependent manner and induce dendritic cell-mediated Th2/Th17 cell responses. Journal of Biological Chemistry. 2013;288(6):4299-309.
71. Alaniz RC, Deatherage BL, Lara JC, Cookson BT. Membrane vesicles are immunogenic facsimiles of Salmonella typhimurium that potently activate dendritic cells, prime B and T cell responses, and stimulate protective immunity in vivo. The Journal of Immunology. 2007;179(11):7692-701.
72. Schetters STT, Jong WSP, Horrevorts SK, Kruijssen LJW, Engels S, Stolk D, et al. Outer membrane vesicles engineered to express membrane-bound antigen program dendritic cells for cross-presentation to CD8+ T cells. Acta Biomaterialia. 2019;91:248-57.
73. Prior JT, Davitt C, Kurtz J, Gellings P, McLachlan JB, Morici LA. Bacterial-derived outer membrane vesicles are potent adjuvants that drive humoral and cellular immune responses. Pharmaceutics. 2021;13(2):131.
74. Wiendl H, Hohlfeld R, Kieseier BC. Immunobiology of muscle: advances in understanding an immunological microenvironment. Trends Immunol. 2005;26(7):373-80.
75. Liang F, Lore K. Local innate immune responses in the vaccine adjuvant-injected muscle. Clin Transl Immunology. 2016;5(4):e74.
76. Laera D, HogenEsch H, O'Hagan DT. Aluminum Adjuvants—'Back to the Future'. Pharmaceutics. 2023;15(7):1884.

77. Ghimire TR, Benson RA, Garside P, Brewer JM. Alum increases antigen uptake, reduces antigen degradation and sustains antigen presentation by DCs in vitro. Immunol Lett. 2012;147(1-2):55-62.
78. Rosenqvist E, Høiby EA, Bjune G, Aase A, Halstensen A, Lehmann AK, et al. Effect of aluminium hydroxide and meningococcal serogroup C capsular polysaccharide on the immunogenicity and reactogenicity of a group B Neisseria meningitidis outer membrane vesicle vaccine. Dev Biol Stand. 1998;92:323-33.
79. Holst J, Martin D, Arnold R, Huergo CC, Oster P, O'Hallahan J, et al. Properties and clinical performance of vaccines containing outer membrane vesicles from Neisseria meningitidis. Vaccine. 2009;27:B3-B12.
80. Moyer TJ, Zmolek AC, Irvine DJ. Beyond antigens and adjuvants: formulating future vaccines. J Clin Invest. 2016;126(3):799-808.
81. Bachmann MF, Jennings GT. Vaccine delivery: a matter of size, geometry, kinetics and molecular patterns. Nature Reviews Immunology. 2010;10(11):787-96.
82. Schager AE, Dominguez-Medina CC, Necchi F, Micoli F, Goh YS, Goodall M, et al. IgG Responses to Porins and Lipopolysaccharide within an Outer Membrane-Based Vaccine against Nontyphoidal Salmonella Develop at Discordant Rates. mBio. 2018;9(2):10.1128/mbio.02379-17.
83. Micoli F, Rondini S, Alfini R, Lanzilao L, Necchi F, Negrea A, et al. Comparative immunogenicity and efficacy of equivalent outer membrane vesicle and glycoconjugate vaccines against nontyphoidal Salmonella. Proceedings of the National Academy of Sciences. 2018;115(41):10428-33.
84. Fiorino F, Pettini E, Koeberling O, Ciabattini A, Pozzi G, Martin LB, et al. Long-Term Anti-Bacterial Immunity against Systemic Infection by Salmonella enterica Serovar Typhimurium Elicited by a GMMA-Based Vaccine. Vaccines. 2021;9(5):495.
85. Spinsanti M, Monaci E, Romagnoli G, Buffi G, Manetti AGO, Carboni F, et al. A novel GMMA-based gonococcal vaccine demonstrates functional immune responses in mice. npj Vaccines. 2025;10(1):146.
86. Oftung F, Korsvold GE, Aase A, Næss LM. Cellular Immune Responses in Humans Induced by Two Serogroup B Meningococcal Outer Membrane Vesicle Vaccines Given Separately and in Combination. Clin Vaccine Immunol. 2016;23(4):353-62.
87. Raso MM, Arato V, Gasperini G, Micoli F. Toward a Shigella Vaccine: Opportunities and Challenges to Fight an Antimicrobial-Resistant Pathogen. Int J Mol Sci. 2023;24(5).
88. Kotloff KL, Riddle MS, Platts-Mills JA, Pavlinac P, Zaidi AKM. Shigellosis. The Lancet. 2018;391(10122):801-12.
89. Khalil IA, Troeger C, Blacker BF, Rao PC, Brown A, Atherly DE, et al. Morbidity and mortality due to shigella and enterotoxigenic Escherichia coli diarrhoea: the Global Burden of Disease Study 1990–2016. The Lancet Infectious Diseases. 2018;18(11):1229-40.
90. Estimates of the global, regional, and national morbidity, mortality, and aetiologies of diarrhoea in 195 countries: a systematic analysis for the Global Burden of Disease Study 2016. Lancet Infect Dis. 2018;18(11):1211-28.
91. Kotloff KL, Nasrin D, Blackwelder WC, Wu Y, Farag T, Panchalingham S, et al. The incidence, aetiology, and adverse clinical consequences of less severe diarrhoeal episodes among infants and children residing in low-income and middle-income

countries: a 12-month case-control study as a follow-on to the Global Enteric Multicenter Study (GEMS). Lancet Glob Health. 2019;7(5):e568-e84.
92. Livio S, Strockbine NA, Panchalingam S, Tennant SM, Barry EM, Marohn ME, et al. Shigella isolates from the global enteric multicenter study inform vaccine development. Clin Infect Dis. 2014;59(7):933-41.
93. Shad AA, Shad WA. Shigella sonnei: virulence and antibiotic resistance. Arch Microbiol. 2021;203(1):45-58.
94. Muthuirulandi Sethuvel DP, Devanga Ragupathi NK, Anandan S, Veeraraghavan B. Update on: Shigella new serogroups/serotypes and their antimicrobial resistance. Lett Appl Microbiol. 2017;64(1):8-18.
95. MacLennan CA, Grow S, Ma L-f, Steele AD. The Shigella Vaccines Pipeline. Vaccines. 2022;10(9):1376.
96. Cohen D, Meron-Sudai S, Bialik A, Asato V, Goren S, Ariel-Cohen O, et al. Serum IgG antibodies to Shigella lipopolysaccharide antigens–a correlate of protection against shigellosis. Human vaccines & immunotherapeutics. 2019;15(6):1401-8.
97. Cohen D, Block C, Green M, Lowell G, Ofek I. Immunoglobulin M, A, and G antibody response to lipopolysaccharide O antigen in symptomatic and asymptomatic Shigella infections. Journal of clinical microbiology. 1989;27(1):162-7.
98. Robin G, Cohen D, Orr N, Markus I, Slepon R, Ashkenazi S, et al. Characterization and quantitative analysis of serum IgG class and subclass response to Shigella sonnei and Shigella flexneri 2a lipopolysaccharide following natural Shigella infection. Journal of Infectious Diseases. 1997;175(5):1128-33.
99. Levine MM, Kotloff KL, Barry EM, Pasetti MF, Sztein MB. Clinical trials of Shigella vaccines: two steps forward and one step back on a long, hard road. Nature Reviews Microbiology. 2007;5(7):540-53.
100. Mani S, Wierzba T, Walker RI. Status of vaccine research and development for Shigella. Vaccine. 2016;34(26):2887-94.
101. Micoli F, Nakakana UN, Berlanda Scorza F. Towards a Four-Component GMMA-Based Vaccine against Shigella. Vaccines (Basel). 2022;10(2).
102. Rossi O, Citiulo F, Giannelli C, Cappelletti E, Gasperini G, Mancini F, et al. A next-generation GMMA-based vaccine candidate to fight shigellosis. NPJ Vaccines. 2023;8(1):130.
103. Valentini S, Santoro G, Baffetta F, Franceschi S, Paludi M, Brandini E, et al. Monocyte-activation test to reliably measure the pyrogenic content of a vaccine: An in vitro pyrogen test to overcome in vivo limitations. Vaccine. 2019;37(29):3754-60.
104. Micoli F, Nakakana UN, Berlanda Scorza F. Towards a Four-Component GMMA-Based Vaccine against Shigella. 2022;10(2):328.
105. Mancini F, Gasperini G, Rossi O, Aruta MG, Raso MM, Alfini R, et al. Dissecting the contribution of O-Antigen and proteins to the immunogenicity of Shigella sonnei generalized modules for membrane antigens (GMMA). Sci Rep. 2021;11(1):906.
106. Launay O, Ndiaye AG, Conti V, Loulergue P, Scire AS, Landre AM, et al. Booster vaccination with GVGH Shigella sonnei 1790GAHB GMMA vaccine compared to single vaccination in unvaccinated healthy European adults: results from a phase 1 clinical trial. Frontiers in immunology. 2019;10:335.
107. Obiero CW, Ndiaye AGW, Sciré AS, Kaunyangi BM, Marchetti E, Gone AM, et al. A Phase 2a Randomized Study to Evaluate the Safety and Immunogenicity of the

1790GAHB Generalized Modules for Membrane Antigen Vaccine against Shigella sonnei Administered Intramuscularly to Adults from a Shigellosis-Endemic Country. Front Immunol. 2017;8:1884.
108. Launay O, Lewis DJ, Anemona A, Loulergue P, Leahy J, Scire AS, et al. Safety profile and immunologic responses of a novel vaccine against Shigella sonnei administered intramuscularly, intradermally and intranasally: results from two parallel randomized phase 1 clinical studies in healthy adult volunteers in Europe. EBioMedicine. 2017;22:164-72.
109. Frenck RW, Jr., Conti V, Ferruzzi P, Ndiaye AGW, Parker S, McNeal MM, et al. Efficacy, safety, and immunogenicity of the Shigella sonnei 1790GAHB GMMA candidate vaccine: Results from a phase 2b randomized, placebo-controlled challenge study in adults. eClinicalMedicine. 2021;39.
110. Citiulo F, Necchi F, Mancini F, Rossi O, Aruta MG, Gasperini G, et al. Rationalizing the design of a broad coverage Shigella vaccine based on evaluation of immunological cross-reactivity among S. flexneri serotypes. PLoS Negl Trop Dis. 2021;15(10):e0009826.
111. Gerke C, Colucci AM, Giannelli C, Sanzone S, Vitali CG, Sollai L, et al. Production of a Shigella sonnei vaccine based on generalized modules for membrane antigens (GMMA), 1790GAHB. PloS one. 2015;10(8):e0134478.
112. Leroux-Roels I, Maes C, Mancini F, Jacobs B, Sarakinou E, Alhatemi A, et al. Safety and Immunogenicity of a 4-Component Generalized Modules for Membrane Antigens Shigella Vaccine in Healthy European Adults: Randomized, Phase 1/2 Study. The Journal of Infectious Diseases. 2024;230(4):e971-e84.
113. De Ryck I, Sarakinou E, Nakakana U, Cilio GL, Ndiaye A, Vella V, et al. GMMA Technology for the Development of Safe Vaccines: Meta-Analysis of Individual Patient Data to Assess the Safety Profile of Shigella sonnei 1790GAHB Vaccine in Healthy Adults, with Special Focus on Neutropenia. Infectious Diseases and Therapy. 2022;11(2):757-70.
114. Rowley J, Vander Hoorn S, Korenromp E, Low N, Unemo M, Abu-Raddad LJ, et al. Chlamydia, gonorrhoea, trichomoniasis and syphilis: global prevalence and incidence estimates, 2016. Bull World Health Organ. 2019;97(8):548-62p.
115. Unemo M, Seifert HS, Hook EW, Hawkes S, Ndowa F, Dillon J-AR. Gonorrhoea. Nature Reviews Disease Primers. 2019;5(1):79.
116. Rice PA, Shafer WM, Ram S, Jerse AE. Neisseria gonorrhoeae: Drug Resistance, Mouse Models, and Vaccine Development. Annu Rev Microbiol. 2017;71:665-86.
117. Cohen MS, Hoffman IF, Royce RA, Kazembe P, Dyer JR, Daly CC, et al. Reduction of concentration of HIV-1 in semen after treatment of urethritis: implications for prevention of sexual transmission of HIV-1. AIDSCAP Malawi Research Group. Lancet. 1997;349(9069):1868-73.
118. Prevention CfDCa. Gonorrhea 2017 [updated 31 January 2025. Available from: https://www.cdc.gov/gonorrhea/about/index.html.
119. Abara WE, Jerse AE, Hariri S, Kirkcaldy RD. Planning for a Gonococcal Vaccine: A Narrative Review of Vaccine Development and Public Health Implications. Sex Transm Dis. 2021;48(7):453-7.
120. Petousis-Harris H, Paynter J, Morgan J, Saxton P, McArdle B, Goodyear-Smith F, et al. Effectiveness of a group B outer membrane vesicle meningococcal vaccine

against gonorrhoea in New Zealand: a retrospective case-control study. The Lancet. 2017;390(10102):1603-10.
121. Escobar A, Rodas PI, Acuña-Castillo C. Macrophage-Neisseria gonorrhoeae Interactions: A Better Understanding of Pathogen Mechanisms of Immunomodulation. Front Immunol. 2018;9:3044.
122. Criss AK, Seifert HS. A bacterial siren song: intimate interactions between Neisseria and neutrophils. Nat Rev Microbiol. 2012;10(3):178-90.
123. Shaughnessy J, Ram S, Rice PA. Biology of the Gonococcus: Disease and Pathogenesis. Methods Mol Biol. 2019;1997:1-27.
124. Higashi DL, Lee SW, Snyder A, Weyand NJ, Bakke A, So M. Dynamics of Neisseria gonorrhoeae attachment: microcolony development, cortical plaque formation, and cytoprotection. Infect Immun. 2007;75(10):4743-53.
125. Rotman E, Seifert HS. The genetics of Neisseria species. Annu Rev Genet. 2014;48:405-31.
126. Massari P, Ram S, Macleod H, Wetzler LM. The role of porins in neisserial pathogenesis and immunity. Trends in Microbiology. 2003;11(2):87-93.
127. Edwards JL, Jennings MP, Apicella MA, Seib KL. Is gonococcal disease preventable? The importance of understanding immunity and pathogenesis in vaccine development. Critical reviews in microbiology. 2016;42(6):928-41.
128. Zhu W, Thomas C, Sparling P. DNA immunization of mice with a plasmid encoding Neisseria gonorrhea PorB protein by intramuscular injection and epidermal particle bombardment. Vaccine. 2004;22(5-6):660-9.
129. Zhu W, Thomas CE, Chen C-j, Van Dam CN, Johnston RE, Davis NL, et al. Comparison of immune responses to gonococcal PorB delivered as outer membrane vesicles, recombinant protein, or Venezuelan equine encephalitis virus replicon particles. Infection and immunity. 2005;73(11):7558-68.
130. Wetzler L, Blake M, Barry K, Gotschlich E. Gonococcal porin vaccine evaluation: comparison of Por proteosomes, liposomes, and blebs isolated from rmp deletion mutants. Journal of Infectious Diseases. 1992;166(3):551-5.
131. Greenberg L. Field trials of a gonococcal vaccine. The Journal of reproductive medicine. 1975;14(1):34-6.
132. Brinton C, Wood S, Brown A, Labik A, Bryan J, Lee S, et al., editors. Seminars in Infectious Diseases. Seminars in infectious disease; 1982: Thieme-Stratton New York, NY.
133. Rice PA, Shafer WM, Ram S, Jerse AE. Neisseria gonorrhoeae: drug resistance, mouse models, and vaccine development. Annual review of microbiology. 2017;71(1):665-86.
134. Whelan J, Kløvstad H, Haugen IL, van Beest MR-DR, Storsaeter J. Ecologic study of meningococcal B vaccine and Neisseria gonorrhoeae infection, Norway. Emerging infectious diseases. 2016;22(6):1137.
135. Azze RFO. A meningococcal B vaccine induces cross-protection against gonorrhea. Clinical and experimental vaccine research. 2019;8(2):110-5.
136. Wang B, Giles L, Andraweera P, McMillan M, Almond S, Beazley R, et al. Effectiveness and impact of the 4CMenB vaccine against invasive serogroup B meningococcal disease and gonorrhoea in an infant, child, and adolescent programme: an observational cohort and case-control study. The Lancet Infectious Diseases. 2022;22(7):1011-20.

137. Bruxvoort KJ, Lewnard JA, Chen LH, Tseng HF, Chang J, Veltman J, et al. Prevention of Neisseria gonorrhoeae with meningococcal B vaccine: a matched cohort study in Southern California. Clinical Infectious Diseases. 2023;76(3):e1341-e9.
138. Ruiz García Y, Sohn W-Y, Seib KL, Taha M-K, Vázquez JA, de Lemos APS, et al. Looking beyond meningococcal B with the 4CMenB vaccine: the Neisseria effect. npj Vaccines. 2021;6(1):130.
139. Marjuki H, Topaz N, Joseph SJ, Gernert KM, Kersh EN, Group A-RNgW, et al. Genetic similarity of gonococcal homologs to meningococcal outer membrane proteins of serogroup B vaccine. MBio. 2019;10(5):10.1128/mbio. 01668-19.
140. Semchenko EA, Tan A, Borrow R, Seib KL. The serogroup B meningococcal vaccine Bexsero elicits antibodies to Neisseria gonorrhoeae. Clinical Infectious Diseases. 2019;69(7):1101-11.
141. Williams E, Seib KL, Fairley CK, Pollock GL, Hocking JS, McCarthy JS, et al. Neisseria gonorrhoeae vaccines: a contemporary overview. Clin Microbiol Rev. 2024;37(1):e0009423.
142. Liu Y, Hammer LA, Daamen J, Stork M, Egilmez NK, Russell MW. Microencapsulated IL-12 drives genital tract immune responses to intranasal gonococcal outer membrane vesicle vaccine and induces resistance to vaginal infection with diverse strains of Neisseria gonorrhoeae. Msphere. 2023;8(1):e00388-22.
143. MacLennan C, Ram S, Freixero P, Rollier C, Kaminski R, Delany-Moretlwe S. Advancing a native outer membrane vesicle vaccine against gonorrhoea towards clinical development: University of Birmingham Birmingham; 2023.
144. Rice PA, Vayo HE, Tam MR, Blake MS. Immunoglobulin G antibodies directed against protein III block killing of serum-resistant Neisseria gonorrhoeae by immune serum. Journal of experimental medicine. 1986;164(5):1735-48.
145. Ellis CD, Lindner B, Khan CMA, Zähringer U, De Hormaeche RD. The Neisseria gonorrhoeae lpxLII gene encodes for a late-functioning lauroyl acyl transferase, and a null mutation within the gene has a significant effect on the induction of acute inflammatory responses. Molecular Microbiology. 2001;42(1):167-81.
146. Densen P, McRill CM, Ross SC. Assembly of the membrane attack complex promotes decay of the alternative pathway C3 convertase on Neisseria gonorrhoeae. Journal of immunology (Baltimore, Md: 1950). 1988;141(11):3902-9.
147. Schmidt KA, Schneider H, Lindstrom JA, Boslego JW, Warren RA, Van De Verg L, et al. Experimental gonococcal urethritis and reinfection with homologous gonococci in male volunteers. Sexually transmitted diseases. 2001;28(10):555-64.
148. Kleinewietfeld M, Manzel A, Titze J, Kvakan H, Yosef N, Linker RA, et al. Sodium chloride drives autoimmune disease by the induction of pathogenic TH17 cells. Nature. 2013;496(7446):518-22.
149. Gilmour BC, Corthay A, Øynebråten I. High production of IL-12 by human dendritic cells stimulated with combinations of pattern-recognition receptor agonists. npj Vaccines. 2024;9(1):83.
150. Hilligan KL, Ronchese F. Antigen presentation by dendritic cells and their instruction of CD4+ T helper cell responses. Cell Mol Immunol. 2020;17(6):587-99.
151. Annunziato F, Maggi L. Strategies for T Helper Cell Subset Differentiation from Naïve Precursors. Methods Mol Biol. 2017;1514:127-37.

152. Marino M, Scuderi F, Provenzano C, Bartoccioni E. Skeletal muscle cells: from local inflammatory response to active immunity. Gene Ther. 2011;18(2):109-16.
153. Chal J, Pourquié O. Making muscle: skeletal myogenesis in vivo and in vitro. Development. 2017;144(12):2104-22.
154. Schreiner B, Voss J, Wischhusen J, Dombrowski Y, Steinle A, Lochmuller H, et al. Expression of toll-like receptors by human muscle cells in vitro and in vivo: TLR3 is highly expressed in inflammatory and HIV myopathies, mediates IL-8 release and up-regulation of NKG2D-ligands. FASEB J. 2006;20(1):118-20.
155. Zuckerman JN. The importance of injecting vaccines into muscle. Different patients need different needle sizes. Bmj. 2000;321(7271):1237-8.
156. Keller CW, Fokken C, Turville SG, Lünemann A, Jens, Schmidt, et al., editors. TNF-alpha induces macroautophagy and regulates MHC class II expression in human skeletal muscle cells2018.
157. Ding M, Huang T, Zhu R, Gu R, Shi D, Xiao J, et al. Immunological Behavior Analysis of Muscle Cells under IFN-γ Stimulation in Vitro and in Vivo. The Anatomical Record. 2018;301(9):1551-63.
158. Raschke S, Eckardt K, Bjørklund Holven K, Jensen J, Eckel J. Identification and Validation of Novel Contraction-Regulated Myokines Released from Primary Human Skeletal Muscle Cells. PLOS ONE. 2013;8(4):e62008.
159. Mosca F, Tritto E, Muzzi A, Monaci E, Bagnoli F, Iavarone C, et al. Molecular and cellular signatures of human vaccine adjuvants. Proceedings of the National Academy of Sciences. 2008;105(30):10501-6.
160. Win Z, Weiner 3rd J, Listanco A, Patel N, Sharma R, Greenwood A, et al. Systematic Evaluation of Kinetics and Distribution of Muscle and Lymph Node Activation Measured by 18F-FDG- and 11C-PBR28-PET/CT Imaging, and Whole Blood and Muscle Transcriptomics After Immunization of Healthy Humans With Adjuvanted and Unadjuvanted Vaccines. Frontiers in Immunology. 2021;Volume 11 - 2020.
161. Henningsen J, Pedersen BK, Kratchmarova I. Quantitative analysis of the secretion of the MCP family of chemokines by muscle cells. Molecular BioSystems. 2011;7(2):311-21.
162. De Rossi M, Bernasconi P, Baggi F, de Waal Malefyt R, Mantegazza R. Cytokines and chemokines are both expressed by human myoblasts: possible relevance for the immune pathogenesis of muscle inflammation. International Immunology. 2000;12(9):1329-35.
163. Seubert A, Monaci E, Pizza M, O'Hagan DT, Wack A. The adjuvants aluminum hydroxide and MF59 induce monocyte and granulocyte chemoattractants and enhance monocyte differentiation toward dendritic cells. J Immunol. 2008;180(8):5402-12.
164. Beringer A, Gouriou Y, Lavocat F, Ovize M, Miossec P. Blockade of Store-Operated Calcium Entry Reduces IL-17/TNF Cytokine-Induced Inflammatory Response in Human Myoblasts. Frontiers in Immunology. 2019;Volume 9 - 2018.
165. Kolls JK, Lindén A. Interleukin-17 Family Members and Inflammation. Immunity. 2004;21(4):467-76.
166. Bettelli E, Oukka M, Kuchroo VK. T(H)-17 cells in the circle of immunity and autoimmunity. Nat Immunol. 2007;8(4):345-50.

167. Parks WC, Wilson CL, López-Boado YS. Matrix metalloproteinases as modulators of inflammation and innate immunity. Nat Rev Immunol. 2004;4(8):617-29.
168. Schoenborn JR, Wilson CB. Regulation of interferon-gamma during innate and adaptive immune responses. Adv Immunol. 2007;96:41-101.
169. Groom JR, Luster AD. CXCR3 in T cell function. Experimental Cell Research. 2011;317(5):620-31.
170. Tokunaga R, Zhang W, Naseem M, Puccini A, Berger MD, Soni S, et al. CXCL9, CXCL10, CXCL11/CXCR3 axis for immune activation - A target for novel cancer therapy. Cancer Treat Rev. 2018;63:40-7.
171. Ziegler SF, Artis D. Sensing the outside world: TSLP regulates barrier immunity. Nature Immunology. 2010;11(4):289-93.
172. Takai T. TSLP expression: cellular sources, triggers, and regulatory mechanisms. Allergol Int. 2012;61(1):3-17.
173. Rochman Y, Leonard WJ. Thymic stromal lymphopoietin: a new cytokine in asthma. Curr Opin Pharmacol. 2008;8(3):249-54.
174. Licona-Limón P, Kim LK, Palm NW, Flavell RA. TH2, allergy and group 2 innate lymphoid cells. Nat Immunol. 2013;14(6):536-42.
175. Soumelis V, Liu YJ. Human thymic stromal lymphopoietin: a novel epithelial cell-derived cytokine and a potential key player in the induction of allergic inflammation. Springer Semin Immunopathol. 2004;25(3-4):325-33.
176. Ying S, O'Connor B, Ratoff J, Meng Q, Mallett K, Cousins D, et al. Thymic stromal lymphopoietin expression is increased in asthmatic airways and correlates with expression of Th2-attracting chemokines and disease severity. J Immunol. 2005;174(12):8183-90.
177. Tan K, Li R, Huang X, Liu Q. Outer Membrane Vesicles: Current Status and Future Direction of These Novel Vaccine Adjuvants. Front Microbiol. 2018;9:783.
178. Sabat R, Grütz G, Warszawska K, Kirsch S, Witte E, Wolk K, et al. Biology of interleukin-10. Cytokine Growth Factor Rev. 2010;21(5):331-44.
179. Caux C, Vanbervliet B, Massacrier C, Azuma M, Okumura K, Lanier LL, et al. B70/B7-2 is identical to CD86 and is the major functional ligand for CD28 expressed on human dendritic cells. J Exp Med. 1994;180(5):1841-7.
180. Zhou LJ, Tedder TF. CD14+ blood monocytes can differentiate into functionally mature CD83+ dendritic cells. Proceedings of the National Academy of Sciences. 1996;93(6):2588-92.
181. Hogenesch H. Mechanism of immunopotentiation and safety of aluminum adjuvants. Front Immunol. 2012;3:406.
182. Kooijman S, Vrieling H, Verhagen L, de Ridder J, de Haan A, van Riet E, et al. Aluminum Hydroxide And Aluminum Phosphate Adjuvants Elicit A Different Innate Immune Response. Journal of Pharmaceutical Sciences. 2022;111(4):982-90.
183. Verdier F, Burnett R, Michelet-Habchi C, Moretto P, Fievet-Groyne F, Sauzeat E. Aluminium assay and evaluation of the local reaction at several time points after intramuscular administration of aluminium containing vaccines in the Cynomolgus monkey. Vaccine. 2005;23(11):1359-67.
184. Seubert A, Monaci E, Pizza M, O'Hagan DT, Wack A. The adjuvants aluminum hydroxide and MF59 induce monocyte and granulocyte chemoattractants and

enhance monocyte differentiation toward dendritic cells1. Journal of Immunology. 2008;180(8):5402-12.
185. Mannhalter JW, Neychev HO, Zlabinger GJ, Ahmad R, Eibl MM. Modulation of the human immune response by the non-toxic and non-pyrogenic adjuvant aluminium hydroxide: effect on antigen uptake and antigen presentation. Clin Exp Immunol. 1985;61(1):143-51.
186. Ulanova M, Tarkowski A, Hahn-Zoric M, Hanson LÅ. The Common Vaccine Adjuvant Aluminum Hydroxide Up-Regulates Accessory Properties of Human Monocytes via an Interleukin-4-Dependent Mechanism. Infection and Immunity. 2001;69(2):1151-9.
187. He P, Zou Y, Hu Z. Advances in aluminum hydroxide-based adjuvant research and its mechanism. Human Vaccines & Immunotherapeutics. 2015;11(2):477-88.
188. Eisenbarth SC, Colegio OR, O'Connor W, Sutterwala FS, Flavell RA. Crucial role for the Nalp3 inflammasome in the immunostimulatory properties of aluminium adjuvants. Nature. 2008;453(7198):1122-6.
189. He P, Zou Y, Hu Z. Advances in aluminum hydroxide-based adjuvant research and its mechanism. Human Vaccines and Immunotherapeutics. 2015;11(2):477-88.
190. Kool M, Soullié T, Van Nimwegen M, Willart MAM, Muskens F, Jung S, et al. Alum adjuvant boosts adaptive immunity by inducing uric acid and activating inflammatory dendritic cells. Journal of Experimental Medicine. 2008;205(4):869-82.
191. Li H, Willingham SB, Ting JP-Y, Re F. Cutting edge: inflammasome activation by alum and alum's adjuvant effect are mediated by NLRP3. The Journal of Immunology. 2008;181(1):17-21.
192. Kool M, Pétrilli V, De Smedt T, Rolaz A, Hammad H, Van Nimwegen M, et al. Cutting edge: Alum adjuvant stimulates inflammatory dendritic cells through activation of the NALP3 inflammasome. Journal of Immunology. 2008;181(6):3755-9.
193. Kooijman S, Brummelman J, van Els CACM, Marino F, Heck AJR, Mommen GPM, et al. Novel identified aluminum hydroxide-induced pathways prove monocyte activation and pro-inflammatory preparedness. Journal of Proteomics. 2018;175:144-55.
194. Cunha P, Gilbert FB, Bodin J, Godry L, Germon P, Holbert S, et al. Simplified Approaches for the Production of Monocyte-Derived Dendritic Cells and Study of Antigen Presentation in Bovine. Frontiers in Veterinary Science. 2022;Volume 9 - 2022.
195. Vandebriel R, Hoefnagel MM. Dendritic cell-based in vitro assays for vaccine immunogenicity. Hum Vaccin Immunother. 2012;8(9):1323-5.
196. Annunziato F, Romagnani S. Heterogeneity of human effector CD4+ T cells. Arthritis Res Ther. 2009;11(6):257.
197. Swain SL, McKinstry KK, Strutt TM. Expanding roles for CD4+ T cells in immunity to viruses. Nature Reviews Immunology. 2012;12(2):136-48.
198. Zhu J, Yamane H, Paul WE. Differentiation of effector CD4 T cell populations (*). Annu Rev Immunol. 2010;28:445-89.
199. Sallusto F, Lanzavecchia A, Araki K, Ahmed R. From Vaccines to Memory and Back. Immunity. 2010;33(4):451-63.
200. Seder RA, Hill AVS. Vaccines against intracellular infections requiring cellular immunity. Nature. 2000;406(6797):793-8.

201. Peake JM, Della Gatta P, Suzuki K, Nieman DC. Cytokine expression and secretion by skeletal muscle cells: regulatory mechanisms and exercise effects. Exerc Immunol Rev. 2015;21:8-25.
202. Pedersen BK, Febbraio MA. Muscle as an endocrine organ: focus on muscle-derived interleukin-6. Physiol Rev. 2008;88(4):1379-406.
203. Schutyser E, Struyf S, Van Damme J. The CC chemokine CCL20 and its receptor CCR6. Cytokine & Growth Factor Reviews. 2003;14(5):409-26.
204. Deyhle MR, Hafen PS, Parmley J, Preece CN, Robison M, Sorensen JR, et al. CXCL10 increases in human skeletal muscle following damage but is not necessary for muscle regeneration. Physiol Rep. 2018;6(8):e13689.
205. Lee J, Yoon YJ, Kim JH, Dinh NTH, Go G, Tae S, et al. Outer Membrane Vesicles Derived From Escherichia coli Regulate Neutrophil Migration by Induction of Endothelial IL-8. Front Microbiol. 2018;9:2268.
206. Tingstad RH, Norheim F, Haugen F, Feng YZ, Tunsjø HS, Thoresen GH, et al. The effect of toll-like receptor ligands on energy metabolism and myokine expression and secretion in cultured human skeletal muscle cells. Sci Rep. 2021;11(1):24219.
207. Lo HP, Hall TE, Parton RG. Mechanoprotection by skeletal muscle caveolae. BioArchitecture. 2016;6(1):22-7.
208. Lo HP, Nixon SJ, Hall TE, Cowling BS, Ferguson C, Morgan GP, et al. The caveolin–cavin system plays a conserved and critical role in mechanoprotection of skeletal muscle. Journal of Cell Biology. 2015;210(5):833-49.
209. Biedron R, Perun A, Jozefowski S. CD36 Differently Regulates Macrophage Responses to Smooth and Rough Lipopolysaccharide. PLoS One. 2016;11(4):e0153558.
210. Murshid A, Gong J, Prince T, Borges TJ, Calderwood SK. Scavenger receptor SREC-I mediated entry of TLR4 into lipid microdomains and triggered inflammatory cytokine release in RAW 264.7 cells upon LPS activation. PLoS One. 2015;10(4):e0122529.
211. Passey SL, Bozinovski S, Vlahos R, Anderson GP, Hansen MJ. Serum Amyloid A Induces Toll-Like Receptor 2-Dependent Inflammatory Cytokine Expression and Atrophy in C2C12 Skeletal Muscle Myotubes. PLoS One. 2016;11(1):e0146882.
212. Cossarizza A, Chang HD, Radbruch A, Abrignani S, Addo R, Akdis M, et al. Guidelines for the use of flow cytometry and cell sorting in immunological studies (third edition). Eur J Immunol. 2021;51(12):2708-3145.
213. Sehgal A, Irvine KM, Hume DA. Functions of macrophage colony-stimulating factor (CSF1) in development, homeostasis, and tissue repair. Seminars in Immunology. 2021;54:101509.
214. Scheler M, Irmler M, Lehr S, Hartwig S, Staiger H, Al-Hasani H, et al. Cytokine response of primary human myotubes in an in vitro exercise model. American Journal of Physiology-Cell Physiology. 2013;305(8):C877-C86.
215. Yang J, Sakai J, Siddiqui S, Lee RC, Ireland DDC, Verthelyi D, et al. IL-6 Impairs Vaccine Responses in Neonatal Mice. Frontiers in Immunology. 2018;Volume 9 - 2018.
216. Marcadet L, Bouredji Z, Argaw A, Frenette J. The Roles of RANK/RANKL/OPG in Cardiac, Skeletal, and Smooth Muscles in Health and Disease. Frontiers in Cell and Developmental Biology. 2022;Volume 10 - 2022.

217. Sheehan SM, Tatsumi R, Temm-Grove CJ, Allen RE. HGF is an autocrine growth factor for skeletal muscle satellite cells in vitro. Muscle Nerve. 2000;23(2):239-45.
218. Broholm C, Laye MJ, Brandt C, Vadalasetty R, Pilegaard H, Pedersen BK, et al. LIF is a contraction-induced myokine stimulating human myocyte proliferation. J Appl Physiol (1985). 2011;111(1):251-9.